Preliminary Reports, Memoranda and Technical Notes of the Materials Research Council Summer Conference

La Jolla, California

Volume I
Rapid Solidification Technology

July 1981

Sponsored by
Defense Advanced Research Projects Agency
ARPA Order No. 4000

Department of Materials and Metallurgical Engineering

PRELIMINARY REPORTS, MEMORANDA AND TECHNICAL NOTES

of the

MATERIALS RESEARCH COUNCIL SUMMER CONFERENCE

La Jolla, California

July 1981

VOLUME I

RAPID SOLIDIFICATION TECHNOLOGY

DARPA Order Number: 4000
Program Code Number: P1D10
Contractor: The Regents of The University of Michigan
Effective Date of Contract: 10 June 81
Amount of Contract: $349,980
Contract Number: MDA903-80-C-0505
Principal Investigator: Professor Maurice J. Sinnott
Department of Chemical Engineering
The University of Michigan
Ann Arbor, Michigan 48109
(313)764-4314

TABLE OF CONTENTS

Foreword

This collection of papers does not constitute a formal reporting of the activities of the DARPA Materials Research Council Summer Conference. Each report, memoranda or technical note is a draft of the author or authors and is their work alone. The Steering Committee, in conjunction with the authors, will decide how this material can best be presented as a formal report to DARPA.

Steering Committee

Professor Henry Ehrenreich
Secretary of the Steering Committee
Pierce Hall
Harvard University
Cambridge, MA 02138

Professor Robert L. Coble
Materials Science Department
Massachusetts Institute of Technology
Cambridge, MA 02139

Dean Daniel C. Drucker
College of Engineering
University of Illinois
Urbana, IL 61801

Professor Anthony G. Evans
University of California
Lawrence Berkeley Laboratories
1 Cyclotron Road
Berkeley, CA 94720

Professor Paul L. Richards
Department of Physics
University of California
Berkeley, CA 94720

Professor Amnon Yariv
Electrical Engineering Department
California Institute of Technology
Pasadena, CA 91125

Project Director

Professor Maurice J. Sinnott
Department of Chemical Engineering
The University of Michgigan
Ann Arbor, MI 48109

Members

Professor Nico Bloembergen
Div. of Eng. & Appl. Physics
231 Pierce Hall
Harvard University
Cambridge, MA 02138

Professor Bernard Budiansky
Division of Applied Sciences
Pierce Hall
Harvard University
Cambridge, MA 02139

Professor Roland M. Cannon
Materials Science Department
Room 13-4026
Massachusetts Institute of Technology
Cambridge, MA 02139

Professor Brice Carnahan
Department of Chemical Engineering
The University of Michigan
Ann Arbor, MI 48109

Professor Morris Cohen
Dept. of Mat. Sci. & Engineering
Room 13-5046
Massachusetts Institute of Technology
Cambridge, MA 02139

Professor Leslie E. Cross
Electrical Engineering
Pennsylvania State University
251A Materials Research Labs.
University Park, PA 16801

Professor Anthony H. Francis
Department of Chemistry
3028 Chemistry Building
University of Michigan
Ann Arbor, MI 48109

Dr. John J. Gilman
Manager, Corp. Res.
Standard Oil Company (Indiana)
AMOCO Research Center
P.O. Box 400
Naperville, IL 60540

Professor Robert Gomer
James Franck Institute
University of Chicago
Chicago, IL 60637

Professor Robert E. Green
Materials Science Engineering
Johns Hopkins University
Baltimore, MD 21218

Professor Alan J. Heeger
Department of Physics/El
University of Pennsylvania
Philadelphia, PA 19104

Professor John P. Hirth
Metallurgical Engineering Dept.
Ohio State University
Columbus, OH 43201

Professor Edward E. Hucke
Materials & Metallurgical Engineering Dept.
The University of Michigan
Ann Arbor, MI 48109

Professor John W. Hutchinson
Div. of Applied Sciences
316 Pierce Hall
Harvard University
Cambridge, MA 02138

Professor Gordon S. Kino
Ginzton Laboratory
Stanford University
Stanford, CA 94305

Professor Walter Kohn
Institute for Theoretical Physics
University of California
Santa Barbara, CA 93106

Professor James A. Krumhansl
Department of Physics
Clark Hall
Cornell University
Ithaca, NY 14850

John L. Margrave, Vice President
Rice University
316 Lovett Hall
Houston, TX 77001

Dr. Robert Mehrabian
National Bureau of Standards
Washington, DC 20234

Professor Frank A. McClintock
Dept. of Mechanical Engineering
Room 1-304
Massachusetts Institute of Technology
Cambridge, MA 02139

Professor Thomas C. McGill
M.S. 116-81
California Institute of Technology
Pasadena, CA 91125

Professor Elliott W. Montroll
Institute for Physical Science
and Technology
University of Maryland
College Park, MD 20740

Professor Howard Reiss
Department of Chemistry
University of California
Los Angeles, CA 90024

Professor James R. Rice
Division of Applied Science
Room 224, Pierce Hall
Harvard University
Cambridge, MA 02138

Professor Frans Spaepen
Division of Applied Science
207A Pierce Hall
Harvard University
Cambridge, MA 02138

Dr. C. Martin Stickley
BDM Corporation
7915 Jones Branch Drive
McLean, VA 22102

Dr. Robb M. Thomson
National Bureau of Standards
Center for Materials Science
Washington, DC 20234

Dr. George H. Vineyard
Brookhaven National Laboratory
Upton, Long Island, NY 11973

Professor J. C. Williams
Metallurgy & Materials Science
Carnegie-Mellon University
Pittsburgh, PA 15213

Professor Mark S. Wrighton
Department of Chemistry
Room 6-335
Massachusetts Institute of Technology
Cambridge, MA 02139

REPORT ON THE DARPA-MRC MEETING ON RAPID SOLIDIFICATION TECHNOLOGY

M. Cohen, J. P. Hirth, L. Jacobson, and R. Mehrabian

INTRODUCTION

A three day conference on Rapid Solidification Technology was held on 7-9 July as a portion of the 1981 MRC meeting. The program and attendees are appended as Section V of this report. The results of the conference are presented in three sections of the following report. Section II presents key issues that emerged in the discussions, Section III contains summaries of the different sessions, and Section IV is a series of individual contributions. The latter contributions include summaries of presentations, prepared discussions and discussions engendered at the meeting.

KEY ISSUES

At the meeting, lists of areas of needed research and questions for guided discussion were generated. Together with spontaneous discussion, these led to the elucidation of some key issues representing research needs, points of progress in understanding, or technological requirements. An outline of these key issues now follows. Many of the points are discussed in somewhat greater detail in Sections III and IV and many references to that section are provided.

The Interaction of Supercooling and Heat Extraction Rate in Influencing Nucleation

It became clear during the meeting that cooling rate, or, more properly, heat extraction rate, had been perhaps overemphasized as the factor governing the attainment of microcrystalline, segregation free solids by RST. Through their influence on nucleation rate, both heat extraction rate and the attainable degree of supercooling are important. The supercooling achievable depends on heterogenities, the limiting homogeneous nucleation rate and in turn surface energy. Thus, considerations of nucleation theory are important. Specific factors are:

1. The interplay of heat extraction rate and nucleation rate in determining the maximum supercooling can be conveniently represented on an enthalpy-temperature diagram (Mehrabian). The sequence of structures, from isothermal solidification structures (planar, cellular, dendritic) to segregated microcrystalline to hypercooled microcrystallites with minimal segregation, can be understood in terms of increased supercooling.

2. Several discussions (see Fraser) are consistent with the view that microcrystallites nucleate at substantial undercoolings, and that the segregation that appears near the grain boundaries arises after recalescence has raised the temperature back to the liquidus. However, there is no direct observation of this sequence. Metallographic studies of dispersed droplets

* Names in parentheses refer to individual contributions.

transformed isothermally and other studies of the origin of the microcrystallite structure are important and needed.

3. The standard form of nucleation theory appears adequate for the application to RST, even though large gradients in temperature and composition may be present (Reiss).

4. The role of alloy additions in influencing heterogeneous nucleation is important. A general classification in terms of nucleation potency is needed. Additions for one purpose, such as to provide second-phase particles to maintain a fine grain size, may enhance heterogeneous nucleation in a way deleterious to powder structure (Cohen).

5. Somewhat related to item 2 above, research is needed on the change in mode of growth in the course of recalescence. The heat and mass balances lead to different distributions than in steady-state growth. Calculations are becoming available, while experimental work is required (Mehrabian).

Growth Morphology

Growth rates are of interest through the control they exert on interface stability. The corresponding growth morphologies can influence properties by establishing both the size scale of microstructural features and the degree of segregation. Specific issues are:

1. The details of the transient build up of solute at the growing interface in a powder droplet under complex surface cooling-interface heating conditions and the consequences for interface stability need to be considered in detail.

2. For the finest cellular and dendritic structures, produced at large heat extraction rates, the curvatures of the interface features may become so large that the relevant surface energies can become curvature dependent.

3. Short wave length perturbations at high interface velocities are stabilized due to capillary forces. If the thermal field is stabilizing, the interface velocity for absolute stability is a function of the solute content and is independent of the temperature gradient in the liquid (Mehrabian).

4. Departures from local equilibrium at the solid-liquid interface tend to have a stabilizing influence on the interface. However, the exact form or magnitude of these departures are not known (Mehrabian) and should be studied.

5. In undercooled melts, the temperature gradient in the solid plays an important role in interface stability (Mehrabian). No models are available for growth of an alloy into a highly undercooled melt.

6. In most rapid solidification experiments, interface velocity varies with undercooling and the changing thermal fields. Thus, the assumption of constant interface velocity has seriously limited the design of conclusive experiments to test the theory (Mehrabian).

7. At very high interface velocities, the solute enriched layer approaches atomic dimensions and the macroscopic transport equations used to derive the stability criterion are no longer valid. For example, with liquid diffusivities of $\sim 10^{-9}$ m^2/s and

growth rates of 1 to 10 m/s, the characteristic diffusion boundary layer ahead of the interface is 1 to 10Å (Mehrabian).

8. Metastable structures, for example, extended solid solubility, cannot always be adequately explained when interface equilibrium is invoked. Experiments with systems containing a retrograde solidus have shown that over a very large range of compositions enhanced solubility must be caused by a solute trapping mechanism rather than by second phase nucleation avoidance (Mehrabian).

9. Controlled experiments, perhaps with directed high energy sources, are needed to test the absolute stability region predicted by the morphological stability theory.

10. The T_o curve delineates the locus of all the points on a phase diagram where the free energy of a single phase solid and liquid of the same composition have the same value. To the left and below the T_o curve partitionless solidification of a liquid to a single phase metastable solid of the same composition is permitted. At temperatures or compositions above the T_o curve the crystalline solid that forms must be multiphase (Mehrabian).

Formation and Stability of Amorphous Structures

1. Changes in viscosity at the glass transition temperature as a fraction of the cooling rate at which an amorphous alloy is formed and changes in the heat of crystallization show that there are different configurations and properties in the amorphous state.

2. Amorphous alloy formation should be carefully investigated as an alternative pathway to the formation of a crystalline structure.

3. In connection with item 2, a comparison of properties should be performed on an alloy of the same composition formed by alternative methods. One would be the divitrification of an amorphous alloy while the other would be direct microcrystalline solidification by the spinning disc method.

4. Amorphous solidification can be obtained in some eutectic and off-eutectic alloy compositions even in the presence of the crystalline phase. That is, crystalline solidification is growth limited (Mehrabian).

5. In a region of the phase diagram where partitionless solidification of a single phase is thermodynamically forbidden, to the right and above the T_o curve, diffusion processes are required to sort out the constituents into two or more phase mixtures of different compositions. In this region crystallization velocities typically will not exceed 5 cm/s, making glass formation very probable during solidification (Mehrabian).

Microstructural Properties of RSR Alloys

1. Second phase particles have been found to be quite important in pinning grain boundaries and maintaining a fine grain size (Cohen). Work is needed on the role of cooling rate and composition of powders prior to and after their solidification on the kinetics of formation of the second phase particles and

their microstructural form; on metastable phase formation; and on coherent-incoherent interface transitions.

2. The role of coherency and particle size on pinning of grain boundaries needs to be defined (γ' in Ni-base alloys, Al_3Zr in Al-base alloys).

3. Instability in the form of discontinuous coarsening of γ' in Ni-base RST alloys has been observed by H. Lipsitt and co-workers. The instability has been observed to initiate only at grain boundaries. The mechanism of initiation of the reaction is not understood and needs to be defined.

4. The kinetics of grain coarsening in alloys containing pinning particles are associated with Ostwald ripening of the pinning particles (Cohen). Theory is available for ripening of particles in stable structures but not for particles associated with bowed out or moving interfaces. A coupled theory is needed.

5. Thermodynamic data for solubility products, important in estimating the stability of second phase particles, which are important in controlling grain size, are needed. Such data is sparse for Fe-based systems and essentially lacking for Al-base, Ni-base and Ti-base systems. Research to provide such data, which seems to have been out of favor with funding agencies for the past decade, is needed.

6. Work is required to delineate the influence and relative importance of powder production method and consolidation method on the above phenomena. New, low temperature consolidation

methods may be promising. For example with low temperature dynamic compaction of Ni-base alloys, a fine enough γ' precipitate may be formed to permit low temperature direct recrystallization and improved structure (Fraser, Rath).

7. Submicron powders provide a suitable tool for fundamental rapid solidification studies. In addition to having the potential to achieve substantial undercoolings prior to nucleation, these powders are electron-transparent and permit microstructural examination of the complete solidification structure of a small casting without thinning (Mehrabian).

8. Some new theoretical developments have already been qualitatively verified on extremely fine powders of aluminum alloys (Mehrabian). For example, interface breakdown from planar to cellular in the middle of the powders is clearly delineated. More work is required to couple this type of microstructural observations to thermodynamic, kinetic and heat flow concepts to elucidate the thermal history and solidification mode of rapidly solidified powders and their effect on microstructure.

Physical and Mechanical Properties of RST Alloys

1. The RST melt spinning method has produced Ni-base particles with catalytic activities greatly enhanced compared to standard materials (Adam).

2. With refined microstructures and higher strength alloy produced by RST, guidelines are needed for mechanical properties

such as fracture toughness. A discussion of such guidelines is presented by Drucker in Section IV.

3. Work on wrought alloys suggests that for a given alloys system a "critical" particle size-stress combination exists above which the particles decohere or crack and diminish ductility and fracture toughness but below which they do not. Experiment and theory are needed as a guideline for alloy design of microstructures in RST.

4. RST Al-alloys inhibit enhanced resistance to crack initiation in fatigue of smooth bar specimens but decreased resistance to stable crack propagation (da/dN vs. K_I), (Williams). It is plausible that the behavior is related to enhanced multiple slip induced by fine second-phase particles, but experimental verification of the role of dislocation structure is needed.

5. Improved oxidation and corrosion resistance have been observed for several RST alloys compared to conventional alloys. While chemical homogeneity undoubtedly contributes to these effects, they also occur when second-phase particles are present. Work is needed to define the specific mechanism of the property enhancement.

6. Work is needed on single-variable experiments. Studies of the effects of cooling rate, for example, have been done on powder lots of different sizes where there may be other effects of particle size.

7. Work is needed on the effects of consolidation, in particular the new low-temperature, dynamic compaction techniques.

8. In view of the success in making improved catalysts by RST, other possibilities for improved physical properties, suggested in the Reports of the DARPA Materials Research Council for 1975, 1976 and 1978 should be investigated. These suggestions were outgrowths of earlier RST meetings.

Methods of Production and Consolidation

1. Melt spun ribbon, consisting of microcrystals, which is subsequently broken into fine particles should be studied as an alternative to the droplet solidification methods for forming particulate. Advantages would be uniform cooling history, a solidification structure independent of particle size, ease of process control (ribbon size material), and perhaps less contamination in post-solidification handling. Possible disadvantages would be reduced packing density compared to spherical powders and contamination from the chill cylinder or wheel.

2. The mechanism of adherence, important in achieving rapid cooling in melt spinning, is not understood and needs further study.

3. Work is needed on comparisons of structure and properties of spherical powders produced by the different methods of atomization.

4. Somewhat connected with item 3, work is needed to establish whether, for a given alloy, there exists a critical

cooling rate-supercooling combination which produces a substantial improvement in ultimate properties.

5. Further work is needed in the area of surface melting by high energy methods to establish possible property improvements.

6. The effects of processing variables on properties needs further work. These include effects of atomization method, inert handling of particulate (particularly for Al alloys where data is sparce), consolidation method (mentioned previously) and of heat treatment (particularly optimization).

Other Factors

1. Many of the RST alloys represent incremental changes of conventional wrought or cast alloys. More attention might be given to radical departures in alloy design. Some guidelines for the design of "ideal" microstructures are available (Drucker, Battelle Conference on Alloy Design, 1977, Report of the DARPA Materials Research Council, 1975).

2. In the area of non-destructive evaluation, problems remain in resolving finer potential flaws in the high-strength alloys and in developing methods for on-line control of parameter during rapid solidification and subsequent consolidation (Mehrabian), and in developing inspection methods for near net shapes.

3. There is a strong need for experiments on the welding of RST alloys. Surface melting studies give some indication of

problems (microstructure coarsening) but are not representative of final welded structures.

4. Predictive models need to be developed that relate alloy composition and process variables to structure and properties of rapidly solidified alloys. These models would require coupling of phase diagram information to realistic heat flow models and emerging theories of rapid solidification processing (Mehrabian).

5. Computer-base phase stability data compilation coupled to predictive models for phase diagrams (Mehrabian) are needed for the development of new alloys specifically designed to exploit the beneficial effects of rapid solidification processes on microstructure.

6. Heat flow models have recently been developed for rapid solidification of ribbons, surface layers and atomized droplets (Mehrabian). These models, coupled with available experimental data, predict strict limitations in achieveable cooling rates in these processes imposed by attainable heat transfer coefficients and/or useful melt thickness and powder size.

7. In general, definition of rapid solidification processes in terms of just high cooling rates has led to confusion. A measure of rapid solidification processes could be the cooling rate of an alloy at its liquidus temperature since this rate influences the "incubation period" available for nucleation. On the other hand, fineness of microstructure is usually correlated to average cooling rate during solidification or time available

for coarsening. Finally, many structural manifestations of rapid solidification are not correlated to solid-liquid interface velocity (Mehrabian).

SUMMARY OF SESSION I - R. Mehrabian

Recent advances in our understanding of the fundamental aspects of rapid solidification were discussed by Mehrabian. He described these advances in the areas of; phase diagrams, heat flow, interface stability, glass formation, microstructural observations and nondestructive testing.

He pointed out that in the phase diagram area advances have been made in thermodynamic optimization and the development of computer-base phase stability data (both equilibrium and metastable) for binary and some ternary alloy systems. Interesting new thermodynamic features, useful to rapid solidification, emanating from this work include calculation of T_o curves and prediction of retrograde points on metastable solidus curves. The T_o curve is important in that below this curve liquid can transform to solid without change in composition (a partitionless solidification). Whereas, above this curve the crystalline solid that forms must be multiphase. The existance of retrogrades in metastable solidus curves is important in that it shows that over large range of compositions enhanced solubility must be caused by solute trapping rather than second phase avoidance.

Mehrabian continued by describing the heat flow models that are now available for splat cooling, surface melting and atomization. These can be used to both describe limitations in achievable cooling rates in various processes, as well as help in the development of predictive models for rapid solidification

when they are combined with emerging thermodynamic and kinetic theories. An important contribution of the work presented was a new model for solidification of undercooled droplets that utilizes a dimensionless enthalpy-temperature representation of the thermal history. Findings from this work included the conclusion that external cooling has little effect in extending interface recalescence and hence, metastable effects associated with initial undercooling.

In this area of solid-liquid interface stability, he described the details of extending the morphological stability theory to high interface velocities. He pointed out that plane front solidification, which would avoid microsegregation, becomes increasingly stable with increasing interface velocity during rapid solidification. On the other hand, work is needed, he noted, in establishing the exact effects of departures from equilibrium at the interface on stability, and extension of the theory to account for variation in interface velocity encountered in practice. It was suggested that critical laboratory experiments to verify predictions of interface stability theory need to be carried out.

In the field of glass formation, the T_o curve was emphasized with its significance in establishing regions of a phase diagram where crystallization velocities are limited by the necessary diffusional sorting of the constituents into a multiphase product. He gave examples of sudden changes from cystalline to amorphous solidification as the growth interface was

accelerated. It was agreed that this field remains ripe for further study.

Microstructural manifestations of undercooled and rapidly solidified materials were described by Mehrabian using direct TEM observations on submicron droplets. He gave examples of extended solid solubility, solid-liquid interface breakdown and segregation and coupled them to thermodynamic, kinetic and heat flow concepts to elucidate the thermal history and solidification of the droplets. He noted that fundamental studies of undercooling and nucleation, formation of metastable structures and growth morphologies are being pursued on fine alloy droplets. Finally, Mehrabian stated that fundamental studies have been initiated aimed at coupling rapid solidification processing to nondestructive testing.

Patterson described work with centrifugal atomization to produce amorphous powders. The amorphous alloys, he noted, present a useful tool in establishing the capabilities and limitations of the process in achieving the necessary cooling rates to produce metallic glass powders. The efforts described included studies on the thermal stability of the powders.

Cohen gave a comprehensive presentation on the role of second-phase dispersions obtained by rapid solidification of ferrous alloys. He emphasized that second phase particles are important in pinning grain boundaries at austenitizing temperatures, and could thus play an important role in achieving a combination of strength and toughness. He associated the

kinetics of grain coarsening in alloys containing pinning particles with Oswald ripening of the particles. Cohen also noted that the product of diffusion coefficient and concentration of a rate controlling account is the important parameter in precipitate coarsening. Thus, thermodynamic data for solubility products are needed for estimating the stability of second phase particles.

Cohen pointed out that the principles outlined can be equally applied to other alloy systems and that precipitation of stable distribution of fine precipitates need not be limited to the pinning of grain boundaries. For example, large volume fractions of fine precipitates could be equally effective for dispersion strengthening. He concluded that work is needed to establish the relationships between alloy composition and process variables on the formation and stability of second phase particles.

Fraser described the various analytical electron microscopy tools and techniques available to study rapidly solidified structures. He emphasized the advantages and limitations of the various techniques in terms of resolution and specimen size and geometry requirements. He gave examples of dendritic and microcrystalline structures found in atomized nickel alloy powders. He also showed some preliminary calculations of nucleation events using a homogeneous nucleation model and the heat flow model previously described by Mehrabian. He stated that fine submicron droplets, in addition to their advantages, previously

noted by Mehrabian, lend themselves to in situ remelting and resolidification in the TEM. He concluded with examples of fine Y_2O_3 dispersoid obtained in titanium alloys by surface melting.

VanderSande then initiated the discussion by pointing out the possibility of precipitation hardening austenitic steels with fine dispersions of TiC. He also reemphasized Cohen's discussion on the need to make selective additions to a melt to produce durable grain boundary pinning phases. He concluded by stating that increased emphasis should be placed on research in the area of consolidation

Lipsitt followed with a discussion of the instability of rapidly solidified and consolidated nickel base alloys. He described discontinuous coarsening of γ' at the grain boundaries of a number of nickel-base alloys. He concluded by noting that the mechanism of initiation of this reaction is not yet understood and needs to be defined.

SUMMARY OF SESSION II - J. P. Hirth

Williams led off by introducing and discussing microstructural effects in RST alloys. He pointed out two mechanics problems pertinent to alloy design and application: the need for a prediction of expected K_{IC} values for the high-strength-fine microstructure combinations expected for RST alloys; and the apparent inconsistency between a threshold ΔK value for sustained crack growth under cyclic loading and the observation of a continally decreasing stress to failure at high cycles in smooth bar tests (the so-called short crack problem). He also pointed out the problem with microstructural instabilities in RST alloys, e.g. Ni-base alloys aged at 1000°C for 100H, which show discontinuous coarsening initiating at grain boundaries. Lipsitt later elaborated on this instability and mentioned the possibility of abnormal grain growth in some RST Ni-base alloys. Williams continued by noting that RST alloys had improved smooth bar fatigue properties but poorer da/dN-ΔK properties compared to conventional materials; this was reinforced in the discussion by Lawley. For Al-base alloys, Williams also noted that in ductile fracture, voids initiated at large dispersed particles but not at small ones, that the voids linked up by shear instabilities, and that the properties depended on processing variables. For Ti-base alloys, so far comparative yield strengths were improved but low-cycle fatigue properties were diminished, with cracks initiating at β-flecks associated with transition metals (W, Fe).

Palmer mainly discussed Al-2 to 3 Li-X RST alloys intended to increase modulus, specific modulus and strength. He noted that oxide could cause problems, but that an improved oxide dispersion was obtained after extrusion. On this point, several discussers suggested that property improvements could be expected if all-inert processing were to replace air atomizing and processing. The RST alloys with transition metal dispersoids exhibited increased strength, particularly at 450-650°F. A promising alloy to meet the goals mentioned above was Al-3Cu-2Li-1Mg-0 to 0.2Zr. Palmer mentioned that Al_3Zr was a coherent precipitate that appeared to pin grain boundaries and restrict grain growth. In the discussion, it was noted that a study of the mechanism of this pinning would be interesting because there would be little decrease in grain boundary energy for a grain boundary at such a particle (the usual pinning mechanism) so that a local impediment to motion of the boundary through the particle would be required.

Apelian urged the consideration of alternate atomization processes for forming RST alloys. Lawley and Lipsitt presented discussions as already mentioned.

Hirth then led a discussion to focus on fundamental research needs. Specific ideas which evolved were: a Johnson-Mehl type analysis of the nucleation and growth of dispersed size powder aggregates (such analyses have been performed for aerosol formation); effects of T and concentration gradient or nucleation rate in droplet solidification; the critical particle

size-stress combination for decohesion of second-phase particles under strain; comparison of properties of otherwise identical powders formed at different cooling rates; studies on the abnormal resistance of RST FeAl to grain growth; the initiation mechanism for discontinuous cellular coarsening of precipitates; whether the tendency for enhanced multiple slip accounted for the decreased resistance to stable crack propagation (da/dN) for RST alloys; effects of reheating RS powder in thermal and thermomechanical processing; effects of cooling rate of powders in the solid state; optimized heat treatments for RST alloys; solute versus particle pinning of grain boundaries; need for thermal properties of engineering alloys; the origin and growth of the microcrystalline structure; interface stability during growth from fine liquid droplets; the short-crack problem, K_{Ic} prediction and the mechanism of grain boundary pinning by coherent particles already mentioned. Later, after some reflection, Cahn suggested the following topics with respect to phase change kinetics: anisotropies, as they influence interface stability, produced by diffusion and heat conduction in low-symmetry crystals, surface free energy at low growth velocity, diffusion kinetics at intermediate velocities, and partitioning anisotropy at non-equilibrium, intermediate velocities; devitrification kinetics and resulting morphologies; relaxations and structural changes in the glassy state; nucleation of crystals from the melt and from glass; glass formation and transition (does glass always form if crystallization is avoided?); twin

nucleation during crystallization or recrystallization; Ll_2 phase formation and metastability in Al-Li and Al-Mn alloys; efficient strategies for finding multicomponent glass-forming alloys; wetting studies for the melt spinning process; and discontinuous or cellular coarsening. Many of the research suggestions are discussed further in Section II.

SUMMARY OF SESSION III - M. Cohen

L. Jacobson of DARPA highlighted various R&D programs involving rapid solidification: theory and experiments on high-velocity liquid/solid interfaces (NBS), production of very fine powders by electrohydrodynamics (Phrasor, Inc.), production of crystalline alloys via the amorphous state (Marko Materials, Inc.), dynamic consolidation (United Technologies), planning for use of RST in DoD systems (IDA), survey of present facilities for rapid solidification and consolidation processing (NMAB), development of Al-Li alloys (MIT and Lockheed), plasma deposition for jet-engine combustors (GE), superalloys for jet-engine blades and vanes (PWA, AFML, NRL, Carnegie-Mellon U., U. of Pittsburgh, United Technologies), dual alloy radial turbine engine design (Kongberg, Norway).

C. Adam of PWA emphasized the distinction between cooling rate and solidification rate. If heterogeneous nucleation can be minimized, the resulting undercooling can lead to a rapid solidification rate even with a relatively slow cooling rate. Moreover, variations in solidification rate within a given droplet due to the latent heat being evolved can cause a change in mode of solidification from microcrystalline (segregationless) to dendritic or cellular (with microsegregation). The former mode in an Al 12Cr 8Fe 10Mn alloy, being developed for high-temperature properties, yields a highly supersaturated metastable phase which then precipitates a very fine dispersion of stable-compound particles. In Al-Mg alloys, 30% Mg can be

retained in supersaturated solution, with noteworthy increases in strength and rate of strain hardening. One of the objectives of this aluminum-alloy research is to develop high specific strength and stiffness, commensurate with the attractive properties characteristic of titanium alloys.

There were many questions concerning the weldability of rapidly solidified alloys in general and aluminum alloys in particular. More attention should be given to this aspect of RST.

The catalytic effectiveness of Raney nickel can be improved significantly by rapid solidification before leaching out the contained aluminum. This has been shown in the synthesis of methanol from natural gas and in other reactions of commercial interest. Such work is underway at United Technologies.

R. Ray of Marko Materials described the preparation, structure, and properties of many Fe-base and Ni-base crystalline alloys derived via devitrification from the amorphous state, the latter being obtained by melt spinning. One general range of compositions is: $(Fe, Ni, Co)_{bal}\ Cr_{5-30}Mo_{0-20}B_{8-10}$, with possible additions of carbon and phosphorus. On devitrification, the metallic-phase grain size is ~0.1-0.3 μm and the borides are about the same size but do not form a continuous network. This ribbon material can be chopped and pulverized by hammer milling (100% under 80 mesh) and then consolidated by hot isostatic pressing or hot extrusion. Good structural stability and retention of strength at elevated temperatures are observed. The alloy Fe 5Cr 7MO 8W 1V 1.8B 0.4C also responds to heat treatment, as needed for die and tool applications.

There was some discussion concerning the merits of passing through the amorphous state in order to achieve a microcrystalline structure. Thusfar, this route appears to generate a finer grain size than obtained directly by rapid solidification. On the other hand, the compositional ranges are then limited to those which can avoid crystallization under the available cooling rates from the liquid state.

L. Davis of Allied Corporation pointed out the contrast between the federally supported research on rapidly solidified crystalline alloys (mostly powder making by atomization processes) and the industrially supported research on rapidly solidified glassy alloys (mostly ribbon or strip making by melt spinning). The former has been directed to "structural" applications where mechanical and chemical properties are important, while the latter has been directed to electrical and device applications where magnetic properties are important. He showed the large reduction in core energy losses that can be realized by using glassy alloy laminations (instead of the more conventional silicon and grain oriented steels) in power transformers, but the utility industry does not have the investment capital to make the changeover. In his opinion, this is another technological advance that will be captured by Japanese industry unless sufficient help is forthcoming from the U.S. government. Another economic barrier at the present time is the raw material cost of the amorphous alloys, particularly the contained boron.

Accordingly, further research on cost-reduction in the commercial production of boron and ferroboron was suggested.

In connection with crystalline alloys derived from the melt-spun amorphous state, Allied Corporation has announced a new wear and temperature resistant die alloy: 53Ni 36.1Mo 9Fe 1.7B.

T. F. Kearns of IDA presented a detailed analysis of the lead times required to adopt RST materials for DoD systems, e.g., a military aircraft. In order for a component design to be based on RST, the latter would have to be ready and validated some ten years before the production start-up of the subject aircraft. On the other hand, due to design changes and other problems along the way, improved materials may be required later (even if more expensive), and so further opportunities for the application of RST can arise during testing or production of the aircraft.

E. J. Dulis of Colt Industries reminded us that RST has been in operation on a commercial scale for many years--in the form of gasatomized high speed steel and other alloy steel powders which are then HIPed into appropriate shapes. Rene alloy powders made in this way are observed to have dendritic arm spacings comparable to those found in centrifugally atomized powders. HIPing variables have been studied; raising the consolidation temperature appears to improve the fatigue properties. In the atomizing step, helium gas gives a finer size distribution of the solidified particles than does the regularly

used nitrogen. It was also pointed out that a new wear resistant ferrous alloy containing high carbon and vanadium would not have been feasible because of extreme brittleness if it were not for rapid solidification processing.

P. Domalavage of MIT described ultrasonic gas atomizing by a shock tube device. Cooling rates of 10^4-10^5 K/s are achieved, and there is no hydride problem with aluminum alloys. Increasing the gas pressure leads to a finer particle size distribution. Research is underway to strengthen aluminum-base alloys by employing rapid solidification to obtain supersaturated solid solutions and fine dispersions of precipated phases.

J. B. Moore of PWA concluded the session with an impressive list of potential RST applications for jet engines. In particular, the 150-200°F improvement in high temperature capability for superalloys has far-reaching implications.

SUMMARY OF SESSION IV - L. Jacobson

Dulis, Davis, Jacobson and Mehrabian reported to the group on the results of the 1-2 July workshops sponsored by COMAT. There were three workshops in which industrial and university attendees were asked to respond to questions compiled by the panel moderators and COMAT steering group. Three separate workshops in areas of Light Alloys, Superalloys, and Ferrous and Specialty Materials were conducted and reports were given to the group in reverse order.

Ferrous and Specialty Materials

In Rapid Solidification of ferrous alloys, several principles and guidelines have emerged; in particular, the need to consider the thermodynamic stability of various compounds in alloy design. The difficulty of obtaining adequate amounts of rapidly solidified material for study was highlighted.

Needs for further research were identified regarding the various steps from rapid solidification, consolidation, characterization and application. Areas receiving strong emphasis were the powder forming process and the consolidation process. In addition to better fundamental understanding of these processes, their influence on final properties needs to be clarified.

Prospects for engineering application of RST to typical ferrous products were discussed, and high speed tool steels were identified as the best opportunity. Cost and quality control considerations may pose roadblocks.

The workshops concluded that prospects were good for the scale-up of RST techniques for cost-effective production, based on current techniques. Melt-spinning to ribbon and then comminuting the ribbon to powder was described as having potential cost benefits over existing processes. The recent NMAB report on amorphous and microcrystalline materials was considered inadequate guidance for national policy on RS amorphous alloys technology development. Reasons given ranged from its being dated, to its over-concern with structural applications and inadequate treatment of potential magnetic applications in transformers.

The economic and other driving forces and barriers for application of amorphous alloys were examined with specific reference to soft ferromagnetic iron-based ribbon. Numerous barriers were identified, some obvious, and some not so obvious (cost of high purity boron). Application driving force is the dollar savings due to lower transformer core power losses, estimated to be two billion dollars per year over the next fifteen years, including the cost of generating facilities which would not be needed. Concern was expressed over possible competition from Japan, based on strong Japanese government support for low-loss transformers.

Surface treatments by rapid solidification methods were examined for ferrous and amorphous materials. Use of such techniques for surface composition modification appeared to have the

best prospects, while directed energy beam characterization and control issues posed the strongest barriers to application.

The possibility of developing bulk rapidly solidified materials using the amorphous state as a means to achieving microcrystalline structures was discussed, and several advantages were stated.

Superalloys

The superalloy workshop concluded that because of its emphasis on disk applications the recent NMAB report was not adequate as a quideline for establishing national policy for rapidly solidified superalloy development. Report recommendations do need to be prioritized, a suggestion which may be helpful to future studies.

More work on structure-property relationships and heat treatment effects on stability in RS superalloys is clearly needed. While maintaining an exploratory attitude regarding new opportunities for microstructure development, care should be exercised in using the best available analytical tools for microstructure characterization. Consolidation and processing effects on structure/property relationships should be determined for specific component parts. The nature of initiation and propagation of short cracks should be given greater emphasis.

The lack of suitable techniques for detection and separation of non-metallic and other foreign inclusions from superalloy powder was considered to be a serious matter, but not a major roadblock to application. The severity of the problem

depends on the type of consolidation and subsequent processing, and the specific application environment. Correction of the problem may lie in achieving better control of processing steps. Master melt contamination may be more important than contamination arising from the powder process, for instance.

Assistance needed by producers, users and designers to develop higher confidence in RST superalloy technology was discussed. The most significant recommendation was that application programs should focus on less critical parts in order to gain experience with, and confidence in the new technology.

Gas turbine engines for aircraft, ground transport and power generation were identified as the market sector which will benefit most over the next ten years from RST superalloys. Energy conversion and oil well tooling applications were also cited. Investments are needed in advanced forming concepts and ceramic-less melting.

Important commercial applications could result from surface processing of superalloys, but more support and cost/benefit analysis are needed. In addition to component forming applications, such processes could make important contributions to superalloy rework and repair.

It was agreed that there is a need for sources of high quality, research quantity, rapidly solidified particulate, and possibility of establishing such a capability at NBS was endorsed. The proposed government-wide program in RST should stimulate strong university/industry involvement and industry

investment, but several recommendations for additional actions were made.

Additional questions raised from the workshop floor were discussed. Main points were: the need for common tests to compare RST materials with single crystals and mechanically alloyed materials; the need for improvement of credibility regarding the impact of RST on critical/strategic materials issues; and the need to maintain vigilance in comparing the effects of consolidation processes on unique rapidly solidified microstructures.

Light Alloys Workshop

The workshop concluded that the recent NMAB study on RS aluminum alloys did contain adequate guidelines for establishing national policy, and that the current national program was addressing the needs identified by the study. However, more RST materials need to be made available for evaluation, more work is needed on alloy development, and more work is needed on processing effects on properties.

Aerospace applications of RS aluminum alloys will be driven generally by requirements for higher strength and stiffness, lower density and better durability, and non-aerospace applications will also be possible. Cost considerations compared to ingot processing will be the limiting factor, both in the short and the long range.

It was agreed that in the production of large quantities of RS particulate there is no problem in the short range with air atomization of 7090, 7091, but more R and D needs to be done

on other methods, and Al-Li alloys pose special problems. Production of billets, sheet and plate will be difficult to scale up, and this is probably the most critical aspect of the short range problem in commercialization of RS aluminum alloy products.

Existing processing technology is adequate for 7090, 7091 alloys, for the near term. But long term technical considerations for more unusual alloy compositions suggest that unconventional consolidation processes and thermomechanical treatments may be needed to achieve full density and to control metastability.

It was agreed that industrial facilities are capable of providing research quantities of rapidly solidified aluminum alloy particulate, and therefore a government source is not needed. More government support, in the short range, is needed for component demonstration programs, and for the long range, more sponsorship is needed in microstructure control and thermomechanical processing.

Other topics covered in the afternoon session included an update on the Titanium Aluminide program and the new Iron Aluminide effort by Harry Lipsitt, a discussion by Bhakta Rath of RST opportunities in high damping alloys and surface modification (hardening). Other short presentations were made by Tom Tietz, on his in-progress NMAB study of powder making and consolidation processes, Ernie Bloore on ARRADCOM programs related to RST, and Roland Cannon, on issues concerning grain boundary mobility.

ADVANCES IN OUR UNDERSTANDING OF RAPID SOLIDIFICATION

Robert Mehrabian

It is generally agreed that while significant advances have recently been made in the engineering aspects of rapid solidification, our understanding of the basic phenomena at play in this field is still in its embryonic state. Yet, in the long run, the full potential and limitations of this evolving technology can only be realized through the incisive explanations offered by the underlying science. An enhanced understanding of the fundamentals will permit development of predictive models elucidating the interrelationships between "rapid solidification" processing/structure/property and performance. This paper reviews both recent advances in our understanding of the fundamental aspects of rapid solidification, and outlines future directions for investigation.

The two major ways in which rapid solidification processing provides improved structures and hence improved properties are:

Production of refined structures and more homogeneous materials

For example, through the production of fine dendrites, eutectics and other microdiscontinuities, or through the reduction and elimination of intercellular and interdendritic alloy segregation.

Production of new alloy compositions, microstructures and phases

For example, through extended solid solubility, new

phase reaction sequences, and formation of metallic glass microstructures.

In the past few years, generic programs first at the University of Illinois and more recently at the National Bureau of Standards* have focussed on the development of the necessary science base, data and measurement techniques for rapid solidification. A major objective of the work has been the development of guidelines based on kinetic and thermodynamic solidification theory for alloy design, and prediction and control of rapid solidification processes and structures. In particular, heat flow limitations, segregation effects and rules governing the formation of equilibrium and non-equilibrium phases, including metallic glasses were investigated. The work which was both theoretical and experimental is continuing and will be expanded to include application of advanced nondestructive techniques to measure and control transformation kinetics during and subsequent to rapid solidification.

The results, the guidelines that have been developed and future directions in these investigations are described below under the following headings:

A. Phase Diagrams
B. Heat Flow
C. Interface Stability
D. Glass Formation
E. Microstructural Observations
F. Nondestructive Testing

*The program at the University of Illinois was carried out during the period 1977 to 1979 under DARPA sponsorship. The investigations at NBS initiated in 1979 are partially funded by DARPA.

PHASE DIAGRAMS

Advances in the development of predictive models for phase diagrams are essentiaal in the development of new alloys specifically designed to exploit the beneficial effects of rapid solidification processes on microstructure. Improved predictive techniques have recently been employed, including computer graphics display of phase stability information to estimate rapid solidification effects. This effort is part of a broader joint program between the National Bureau of Standards and the American Society for Metals aimed at developing a critically evaluated phase diagram data bank and on-line computer graphic system.

The computer-based phase stability data compilation program has four basic and interrelated components. These include compilation and evaluation, development of computerized bibliographic files, thermodynamic optimization and development of computer software. In addition to data on the equilibrium phase boundaries, non-equilibrium structures and transformations are also considered. The aim is to provide a complete description of the phase relations (both equilibrium and metastable) of tne alloy system.

Figure 1 shows the Ag-Cu phase diagram from this study[1]. The diagram includes metastable extensions of two-phase equilibria, solid lines; spinoidal curves, dashed lines; T_o curve for partitionless solidification, short-long dashed lines; and metastable liquid miscibility gap, dotted line. Experimental

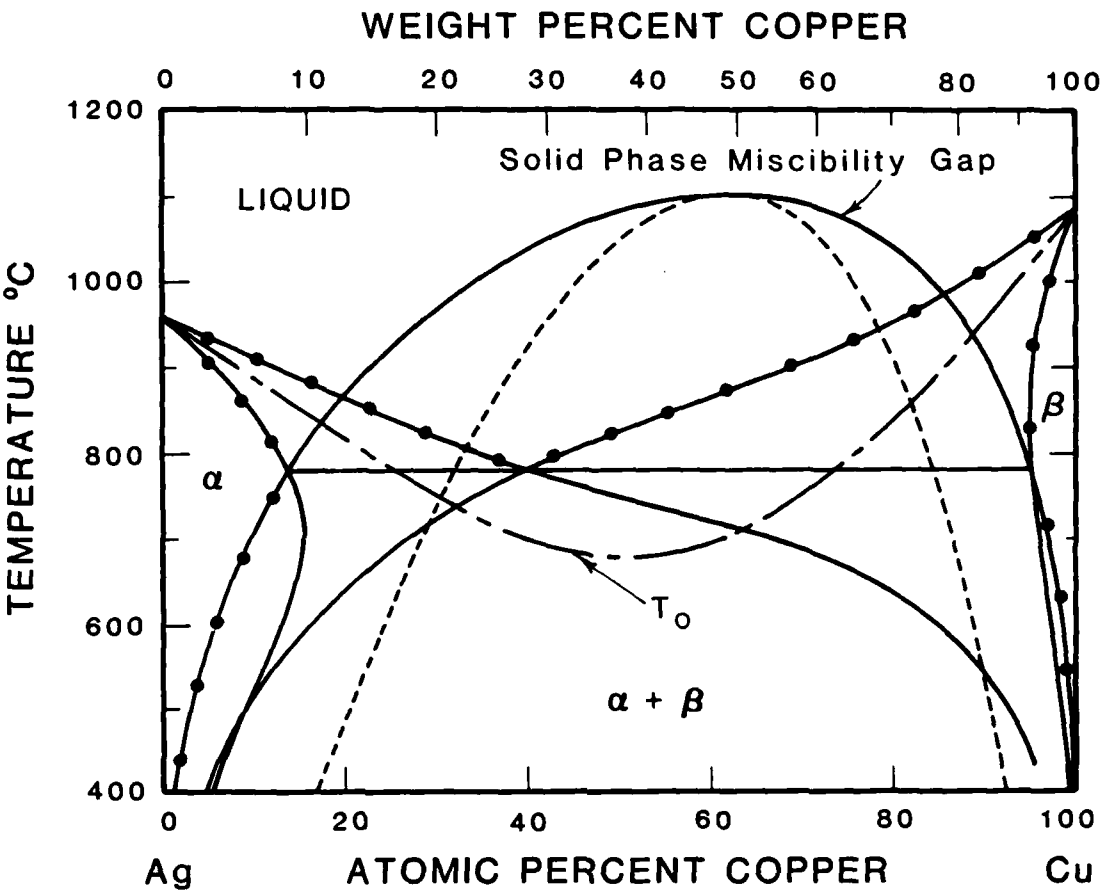

Figure 1. The Ag-Cu phase diagram[1].

data, dots, are also included. The Ag-Cu alloy system contains several interesting features for the study of rapid solidification. Both equilibrium and metastable phase boundaries as well as additional phase diagram features have been calculated from free energy functions for the liquid and solid phases. These free energy functions were determined by fitting the equilibrium regions of the phase diagram for which excellent experimental data exist. Implicit in this approach is the assumption that, while phases may fail to nucleate or equilibrium at interfaces may break down, phases have well behaved free energies represented by the thermodynamic state variables. For example, the short-long dashed curve is the T_o curve for the transition from liquid to crystalline solid. At temperatures below this curve liquid can transform from liquid to solid without change in composition (partitionless solidification). In Ag-Cu, this curve is only about 100°C below the liquidus and so it is not surprising that by rapid solidification a complete series of FCC solid solutions has been obtained previously by Duwez and coworkers[2].

A second interesting feature of the metastable diagram is the existence of retrograde solidus curves for both the Ag rich and Cu rich phases. The retrogrades are points on the metastable solvi with infinite slope. The existence of these retrogrades are important for they show that over a very large range of compositions, enhanced solubility must be caused by a solute trapping mechanism rather than by second phase nucleation avoidance.

HEAT FLOW

The development of predictive models for rapid solidification processes requires the coupling of realistic heat flow models to the emerging theories for rapid solidification processing. Heat flow models are now available for splat cooling, surface melting with directed high energy sources and solidification of atomized liquid droplets. There are limitations in attainable cooling rate in these processes imposed by attainable heat transfer coefficients and/or useful melt thickness and powder size. These limitations are discussed herein along with a short summary of the various heat flow models developed in the past few years.

It is generally agreed that the term Rapid Solidification Processing is equally applicable to the formation of both crystalline and non-crystalline solid phases by quenching of a material from an initial liquid state. On the other hand, a cursory review of the published literature on the subject shows that there is some confusion when rapid solidification is defined in terms of high cooling rates. For example, it is possible to obtain rapidly solidified structures during recalescence of significantly undersooled melts. In general, achievable undercooling is a function of available sights for heterogeneous nucleation and time-"incubation period". The latter is inversely proportional to cooling rate in the liquid as a specimen is rapidly cooled from above to below its melting temperature. Therefore, clearly a measure of rapid solidification

processing could be the cooling rate of an alloy at its liquidus temperature. On the other hand, the crystalline microstructure (e.g., segregate spacing, size of second phase particles, etc.) can usually be correlated to average cooling rate during solidification or time available for coarsening. Thus, a clear distinction must be made between cooling rates in the liquid (or during non-crystalline solidification) and during crystalline solidification - the latter is significantly lower at equivalent rates of external heat extraction due to the heat of fusion. Finally, many structural manifestations of rapid solidification are best correlated to solid-liquid interface velocity. Examples include formation of amorphous structures in the presence of a crystalline substrate and solute trapping at high interface velocities.

Heat Flow During Solidification Against a Metal Substrate

In the recent past a large number of innovative batch and continuous techniques for production of rapidly solidified material against a metal substrate have been developed. Determination of exact cooling rates during solidification of crystalline and non-crystalline structures in these processes have required estimates of heat transfer coefficients between the melt and the substrate. Two measurements of heat transfer coefficient in splat cooling have been reported[3,4]. Table I shows these values along with measured heat transfer coefficients for the case of a pressurized (13,000 psi) 89.7 MN/m^2 aluminum casting against a steel mold[5] and liquid aluminum die cast against a steel mold at 55 m/s metal flow velocity[6]. It

TABLE I

MEASURED HEAT TRANSFER COEFFICIENTS FOR SOLIDIFICATION OF ALUMINUM AGAINST A METAL SUBSTRATE

TECHNIQUE	THICKNESS OF CASTING	h, $W/m^2 .K$
Splat on Ni Substrate (from Ref. 3)	1 μm	1.1×10^5 to 2.8×10^5
Drop Smash on Fe (from Ref. 4)	150 μm	1.7×10^4 - 1.8×10^5
Pressure Cast in Steel Mold (from Ref. 5)	10^4 μm	No Pressure 3.1×10^3 89.7 MPa 3.3×10^4
Die Cast in Steel Mold (from Ref. 6)	1.6×10^3 μm	7.94×10^4 Metal flow velocity 55 m/s Pressure 175 MPa

appears that an upper limit exists for practically achievable heat transfer coefficients between liquid metals and substrates. It is probably in the range of $h = 10^5$ to 10^6 W/m^2 K.

Computer heat flow calculations carried out to estimate cooling rates in a pure aluminum melt are shown in Fig. 2. The data is presented in terms of the dimensionless variables

$$Bi = \frac{hL}{k_L} \text{ and } Fo = \frac{\alpha_L t}{L^2} \qquad (1)$$

where L is casting thickness, k_L is melt conductivity, t is time and α_L is thermal diffusivity of the melt. Bi is the Biot number and Fo is the Fourier number.

As expected, for small Biot numbers temperature gradients in the melt are negligible, the linear portion of the curve in Fig. 2. At Biot numbers larger than ~10 resistance to heat flow is primarily within the aluminum melt (cooling is essentially ideal) and dimensionless average cooling rate is independent of Biot number - actual average cooling rate $(\partial T/\partial t)_{avg}$ is inversely proportional to the square of melt thickness. Thus, for Biot numbers in the Newtonian and ideal cooling ranges the actual average cooling rate in the liquid increases by one and two orders of magnitude, respectively, as the melt thickness is decreased by one order of magnitude. Thus, the most effective way to increase cooling rate is to decrease melt thickness.

Similar calculations have been reported for crystalline solidification of iron splats against a copper substrate[7]. It

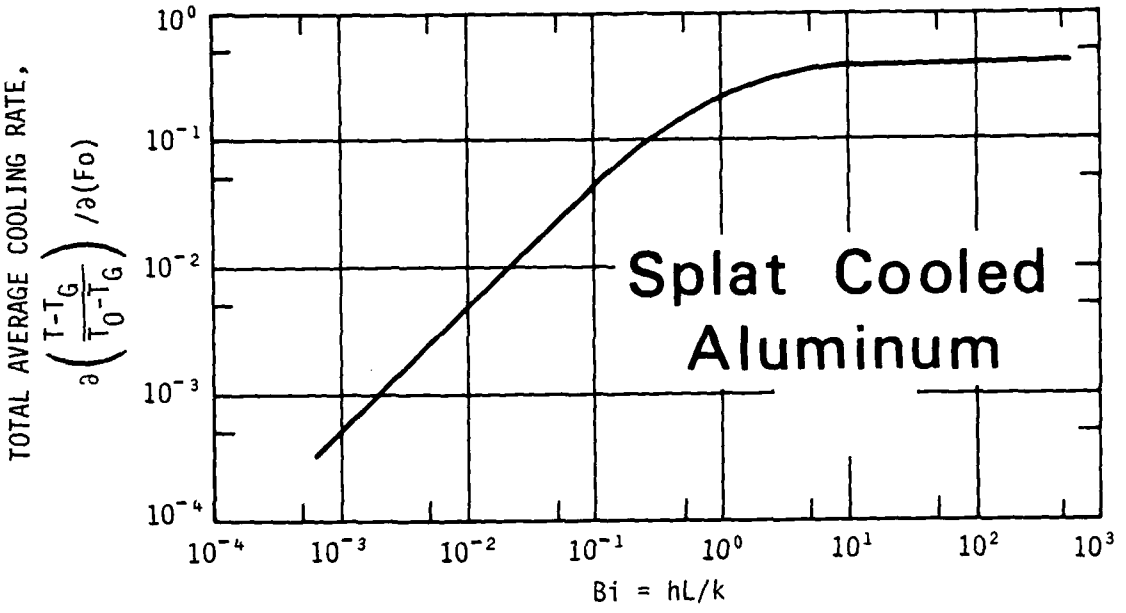

Figure 2. Dimensionless cooling rate averaged over melt thickness and time for temperature to reach half the melting point for an aluminum melt against a copper substrate. T_o and T_g are initial melt and substrate temperatures, respectively.

was found that for Biot numbers less than ~0.015 and more than ~30, cooling was Newtonian and ideal, respectively.

Analytical expressions are available for the solid-liquid interface velocity during plane front solidification of a melt against a substrate for the cases of Newtonian and ideal cooling, Eqs. (2) and (3), respectively.

$$R = \frac{h}{\rho_S \Delta H_M} (T-T_g) \tag{2}$$

$$R = \frac{2\gamma^2 \alpha_S}{S} \tag{3}$$

where R = solid-liquid interface velocity

α_S = thermal diffusivity of the solid forming

ρ_S = density of the solid forming

S = distance solidified

γ = argument of the error function solution of the temperature distribution; it is determined from a characteristic equation which contains metal and substrate thermal constants.

Approximate analytical solutions are available for Biot numbers between these two extremes. However, numerical solutions such as those described above can be readily employed.

Several attempts have been made to predict critical cooling rates in the liquid during rapid solidification for the formation of non-crystalline structures[8-10]. Heat flow calculations are usually combined with theories of nucleation, growth and transformation kinetics. This area, as well as, rapid

solidification of undercooled crystalline structures remains fertile for future investigations.

Heat Flow During Melting and Solidification of a Surface Layer

The recent availability of high power directed energy sources such as the electron beam and the different types of lasers has led to the development of rapid melting and solidification techniques in which a bulk (semi-finite) substrate in intimate contact with a molten layer acts as the quenching medium. Results of recent one and two-dimensional computer heat flow analyses for stationary and moving heat sources[10-14] carried out to investigate the effect of high intensity radiation on the important surface layer melting and subsequent solidification variables are summarized below.

The problem considered was the rapid melting and subsequent solidification of the surface layer of semi-infinite solid pure metals[11-12] and alloys[14], initially at room temperature, subjected to a high intensity stationary heat flux over a circular region on its bounding surface. Since the melt and the substrate are in intimate contact, heat transfer coefficient between the two tends to infinity. Thus, one important limitation on rapid rate of heat extraction encountered in atomization and splat cooling types of processes has been removed. However, surface melting via directed energy sources has its own inherent limitation on maximum achievable cooling rate which is again a function of the thickness of the molten surface region.

In general, the absorbed heat flux distribution can be

both a function of position within the circular region as well as time. The generalized, two-dimensional heat flow model and numerical solution techniques developed in stationary and moving oblate spheroidal coordinate systems[12-14] can readily take into consideration both the space and the time variation of the absorbed heat flux. In what follows, we will first consider the one and two-dimensional stationary heat flow problem and then give an example of the temperature distributions when the heat source is moved with respect to the substrate.

Two important criteria were deduced, from the computer heat flow calculations[12-14], for the surface melting of a semi-infinite pure or alloy substrate subjected to a uniform heat flux q over a circular region of radius a on its bounding surface. First, it was shown that the product qa should exceed specific values if surface melting is to be initiated and the center of the circular region is to reach a given temperature up to the vaporization temperature of the substrate. The second important criterion was that for large values of the product qa isotherms in the substrate are planar in shape and one-dimensional heat flow conditions prevail - lateral heat flow in the substrate can be ignored. As an example, for an aluminum substrate, when $qa > 1.4 \times 10^6$ W/m heat flow is essentially in one-dimension.

Results from one-dimensional heat flow analysis, when the second criterion noted above is applicable, are shown in Fig. 3. These are the calculated melt depths versus total time

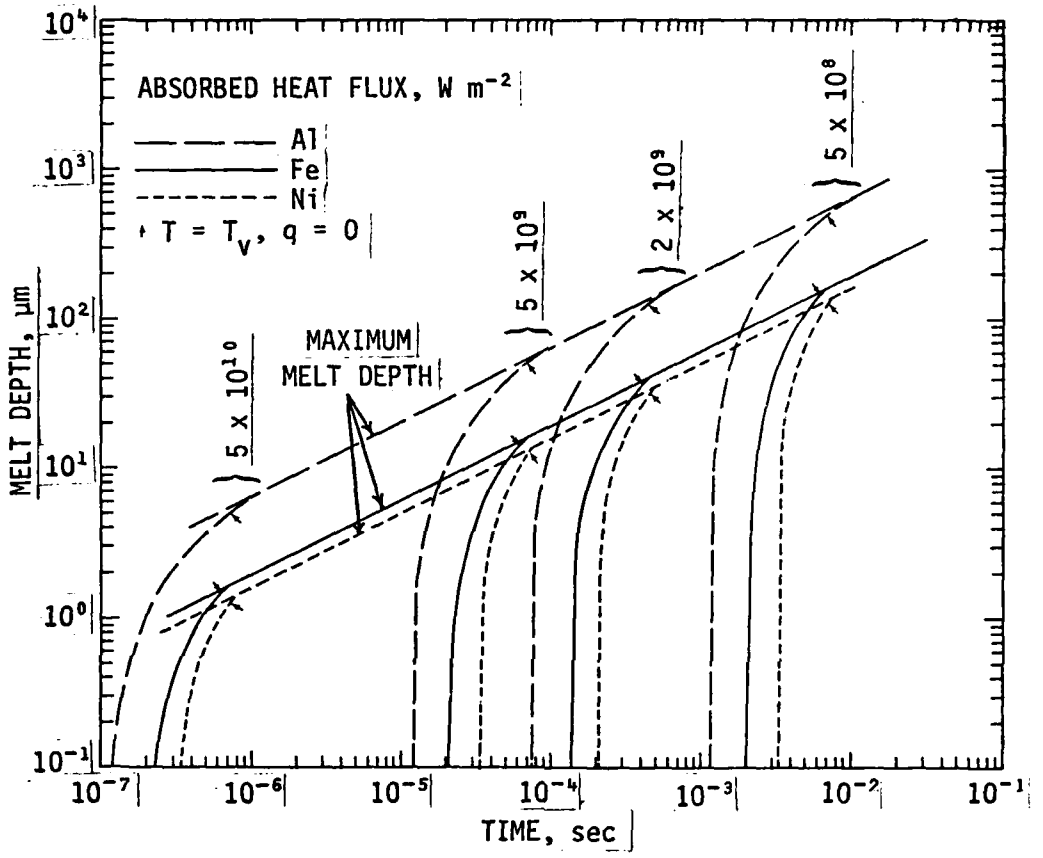

Figure 3. Melt depth versus total time for different uniform absorbed heat fluxes obtained via a numerical technique. Arrows indicate times at which a surface reaches its vaporization temperature and heat flux is removed.

for several uniform absorbed heat fluxes. The arrows in the figure denote times at which the surface of each material reaches its vaporization temperature T_v, and the heat flux, $\underline{q}$, is removed. Melting continues a while longer until a maximum melt depth, z_{max}, is reached. Note that for an aluminum substrate subjected to uniform absorbed heat fluxes of 5×10^8 W/m^2 and 5×10^{10} W/m^2 the criterion for one-dimensional heat flow would be met if the radii of the circular regions exceed 2800 μm and 28 μm, respectively. The corresponding maximum melt depths, z_{max}, from Fig. 3 are ~650 μm and 6.5 μm, respectively.

The general trends established in these one-dimensional computer calculations[11] are summarized in Table II. They show that temperature gradients in the liquid and solid phases and interface velocities are directly proportional to the absorbed heat flux, whereas melt depth is inversely proportional to the absorbed heat flux. Average cooling rates comparable to and exceeding those predicted for splat cooling can be achieved by increasing the heat flux and reducing the dwell time of the incident radiation. An order of magnitude increase in the absorbed heat flux results in a corresponding two orders of magnitude increase in average cooling rates in the liquid during solidification of crystalline and non-crystalline structures.

Examples of results from the two-dimensional heat flow calculations[12-14] for a stationary absorbed heat flux $\underline{q}$ over a circular region of radius $\underline{a}$ on the bounding surface of semi-infinite pure aluminum and Al 4.5 wt% Cu alloy substrates are

TABLE II

ONE-DIMENSIONAL HEAT FLOW
THE EFFECT OF CHANGE IN ABSORBED HEAT FLUX ON OTHER VARIABLES

Order of Magnitude increase in q results in the following changes:

q	Time	Melt Depth	R	G_L	$G_L \cdot R$	G_L/R
$10\uparrow$	$10^2\downarrow$	$10\downarrow$	$10\uparrow$	$10\uparrow$	$10^2\uparrow$	$\leftrightarrow$

$\uparrow$ increase

$\downarrow$ decrease

$\leftrightarrow$ no change

shown in Figs. 4 and 5, respectively. An important finding from this work is that for a given value of T(0,0) at the center of the circular region the dimensionless temperature distributions in the substrate materials during melting and solidification are identical for any combination q and a as long as qa = constant. Figure 4 shows the effect of increasing the product qa on the geometry and the location of the liquid-solid interface. The curve for qa = 1.9×10^6 W/m is in the range where heat flow can be assumed to be essentially one-dimensional and the shape of the isotherm verifies this fact. On the other hand, with decreasing values of qa, laterial heat flow becomes significant and the liquid-solid interfaces assume increasingly more convex geometries.

Figure 5 shows the dimensionless plots of the locations and shapes of the liquidus and eutectic isotherms for qa = 4.76×10^5 W/m during melting and subsequent solidification of an Al 4.5 wt% Cu substrate. In this similation, the heat flux was removed when the center of the circular region reached the vaporization temperature. Melting of the substrate continues until heat flux in the "mushy" zone and the solid at the solidus isotherm (821K) become equal -the solidus isotherm velocity approaches zero. Decreasing values of a $2\sqrt{\alpha_s t}$, increasing time, denote successive position and shape of the "mushy" zone during the melting and the solidification sequence.

Most experiments with a directed energy source, such as the continuous CO_2 laser, involve scanning of the source over

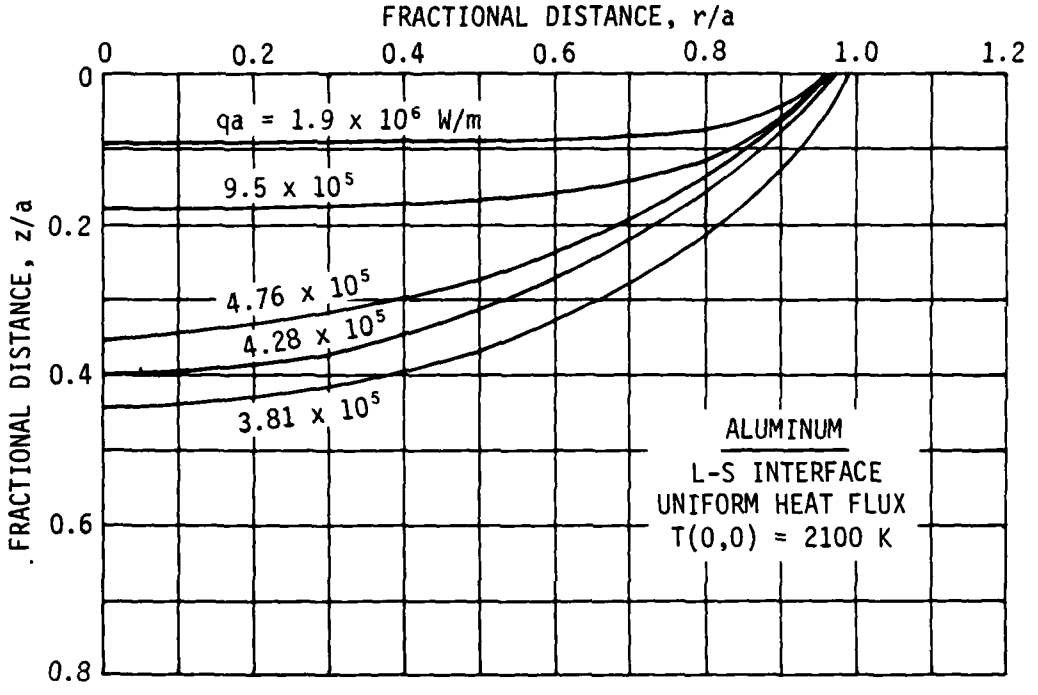

Figure 4. Liquid-solid interfaces during melting of an aluminum substrate subjected to a uniform heat flux q over a circular region of radius a. The interfaces for each constant qa are shown at the instant the center of the circular region reaches the vaporization temperature.

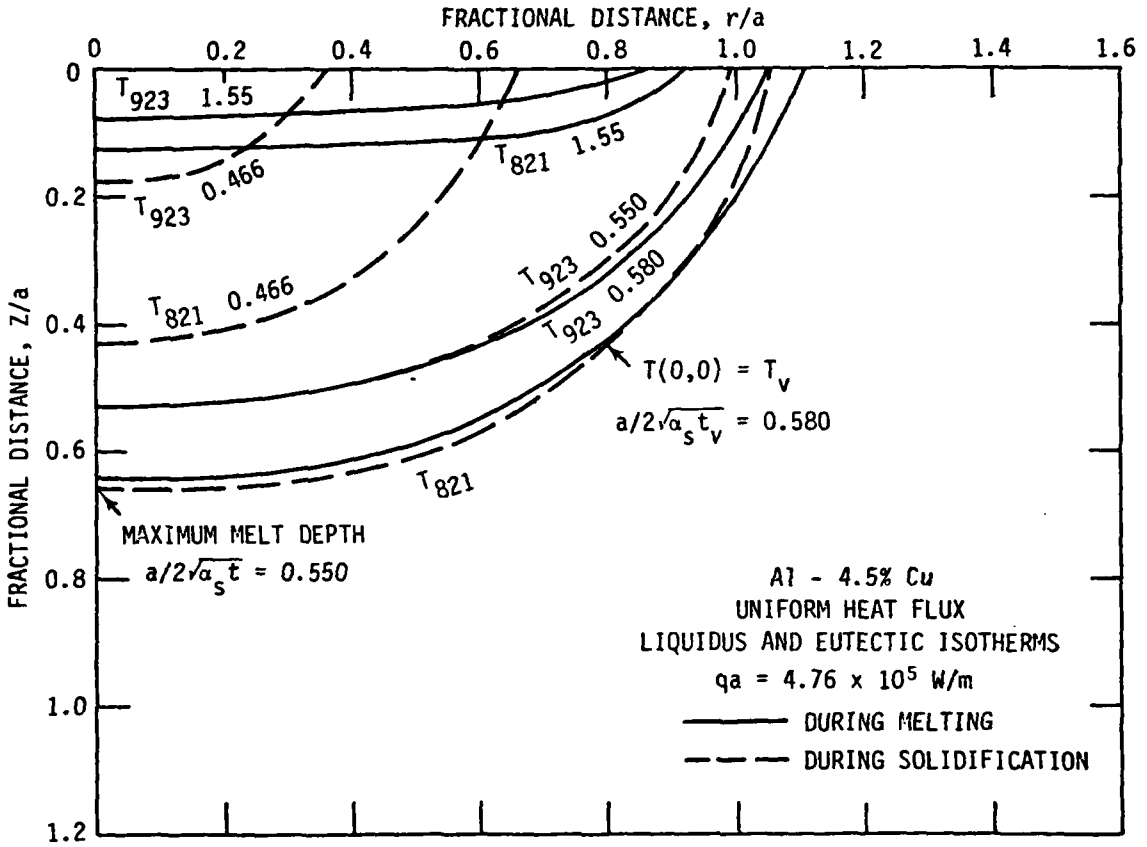

Figure 5. Liquidus and solidus (eutectic) interfaces during melting and subsequent solidification of an Al-4.5% Cu alloy substrate subjected to a uniform absorbed heat flux q over a circular region of radius a. The curve marked T(0,0) = Tv shows the location of the interface at which time the heat flux was removed.

the surface of the substrate. In a recent paper[13], we considered the rapid melting and solidification of a semi-infinite substrate subjected to a high intensity heat flux over a circular region on its bounding surface moving with a constant velocity, U, in the positive y-direction in cartesian coordinate system, Fig. 6. An important finding of the investigation was that the three variables, absorbed heat flux q, the radius of the circular region a and the velocity of the moving heat flux U, could be combined into two independent variables. That is, the dimensionless temperature distribution in the liquid metal pool and the solid substrate remain the same as long as the products qa and Ua or U/q are kept constant while the individual values of the three variables are varied.

Examples of the shape and location of several isotherms, including the liquid-solid interface, for given values of the products qa and Ua/2a are shown in Fig. 7. This figure shows composite top and side views of the isotherms at steady state for a stationary and a moving heat source.

The dimensionless velocity $Ua/2\alpha = 0.75$ would, for example, translate into actual velocities of 0.1 m/s and 1 m/s for radii of the circular region of ~1260 μm and ~126 μm, respectively. Figure 7 shows significant shifts in the geometry of the isotherms to the trailing end of the moving heat source.

It is interesting to note that due to the high conductivity of the aluminum substrate the distortions in the isotherms are not nearly as pronounced as those expected in lower

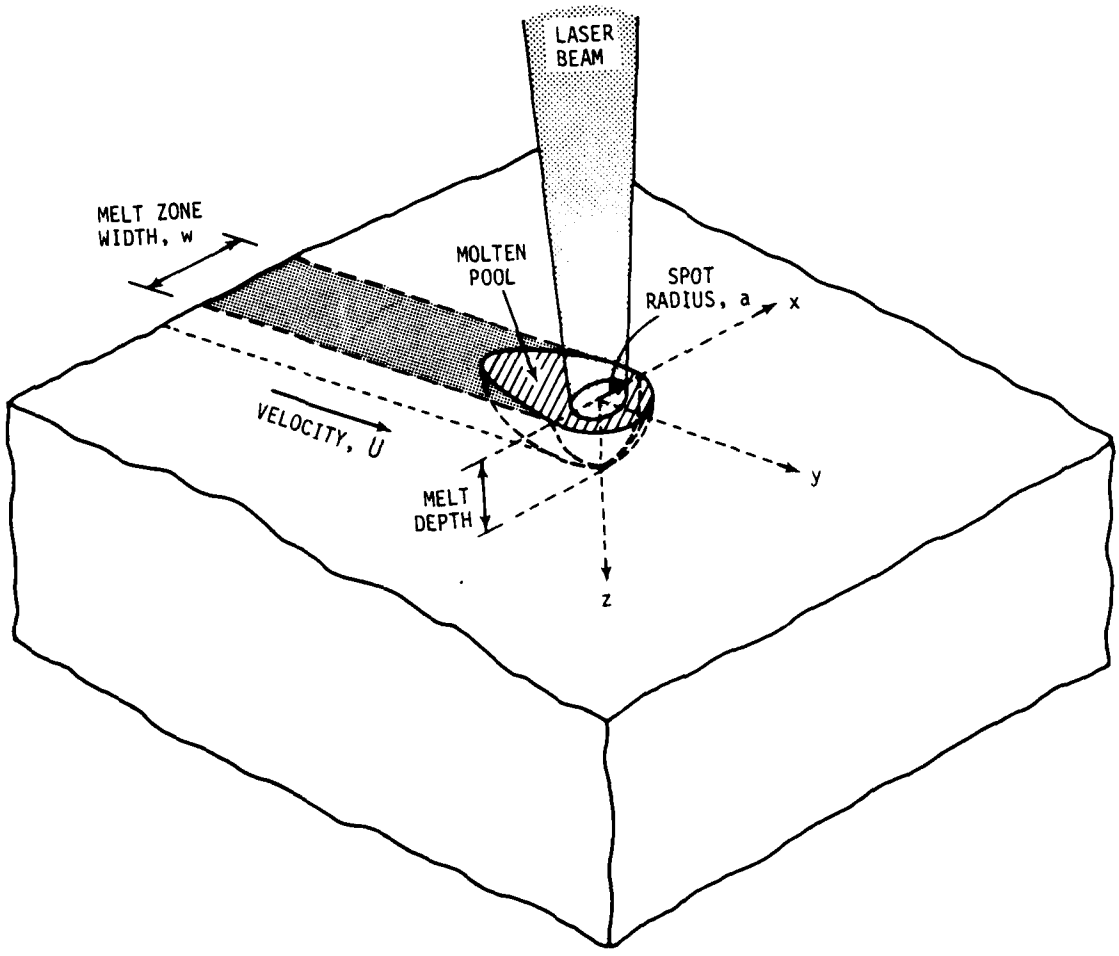

Figure 6. Schematic illustration of laser beam-substrate geometry during rapid surface melting and solidification.

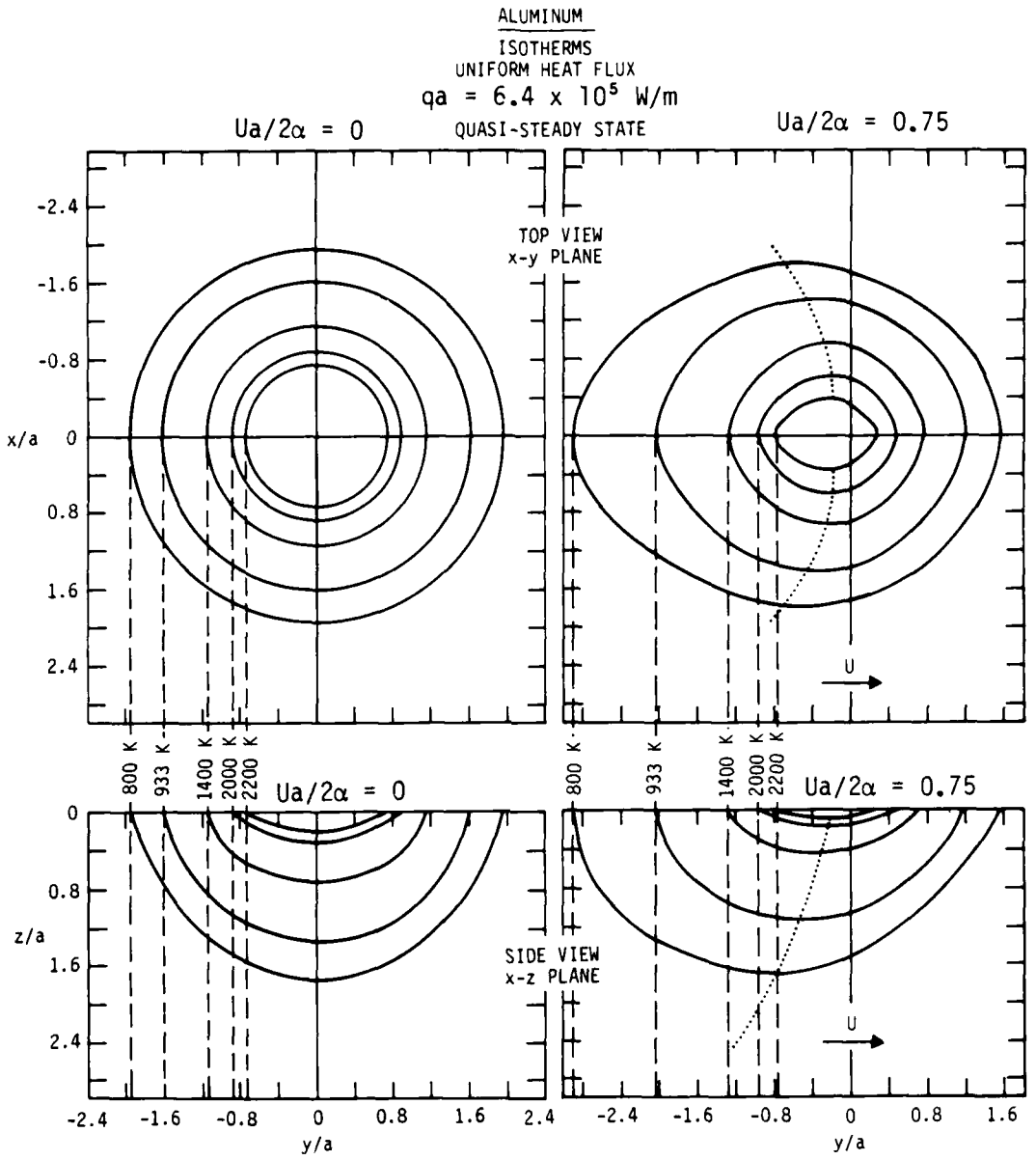

Figure 7. Composite side and top views of the isotherms in an aluminum substrate subjected to stationary and moving uniform absorbed heat fluxes over a circular region on its boundary surface. The n-n curve connects the points of maximum temperature farthest from the y-axis.

conductivity materials such as iron or nickel. This point was clearly demonstrated in the moving point source calculations of Rosenthal[15].

In summary then, the rapid surface melting and solidification technique, via directed high energy sources, has its own limitation on specimen size and thickness, even though the melt is in intimate contact with its own substrate. High cooling rates during solidification are only achieved at the expense of high absorbed heat fluxes, reduced heat affected zones and melt depths.

Heat Flow During Atomization

Since atomization is more limited than surface melting or splat cooling in the achievable rates of heat extraction, it is desirable to reach substantial under-coolings prior to nucleation in order to enhance the rapid solidification effects. Experimental evidence from several investigations[16-21] has shown that large metastable effects can indeed be obtained under slow cooling conditions by suppressing the onset of nucleation. On the other hand, it has been contended that the external cooling during some atomization processes may be sufficiently high to partially offset the recalescence of the droplet and extend the regime of rapid solidification.

The solidification of undercooled spherical droplets with a discrete melting temperature was recently analyzed[22] using both a Newtonian and a non-Newtonian (Enthalpy) model. Relationships were established between atomization parameters, the

growth kinetics, the interface velocity and undercooling, and other important solidification variables. A summary of the findings from this study is given below. The important process parameters in the solidification model are the initial undercooling, the particle size, the combined convective and radiative heat transfer coefficient, h, and a kinetic relationship between undercooling and interface velocity. Droplet diameters from 0.1 to 1000 μm were considered to cover the typical range of most current laboratory and commercial atomization techniques.

The heat transfer coefficient, h, during atomization may vary between 10 $W/m^{-2}\ K^{-1}$ for the pure radiation case to less than 10^6 $W/m^{-2}\ K^{-1}$ for convection under the most favorable experimental conditions[23]. The limitations on h translate into Biot numbers lower than 1 for most metals and particle sizes of interest. For example, 500 μm droplets of Al, Fe and Ni result in Biot numbers of 0.28, 0.62 and 0.64 for a high heat transfer coefficient of 10^5 $W/m^{-2}\ K^{-1}$ [23]. The third major parameter is the kinetic relationship between the interface undercooling and velocity. Both exponential and linear relationships between interface velocity and undercooling were employed[23]. It was shown that thermal history can best be described in terms of the ratio of a kinetic coefficient K to the Biot number:

$$(K/Bi) = 2 \times 10^7\ (\beta/h) \qquad (4)$$

where β is a factor which was incorporated in the continuous

growth model by Cahn et al.[24]. Kinetic considerations generally limit β within 1 and 10^2. With the limitation on the heat transfer coefficients during atomization noted above the parameter K/Bi can vary from about $\sim 10^2$ to $\sim 10^8$.

The thermal history of powder solidification can be readily described on the enthalpy-temperature diagram shown in Fig. 8. This diagram represents graphically the following equation:

$$(H-H_{SM}) = [\Delta H_M + C_L(T-T_M)](1-g) + C_S(T-T_M)g \qquad (5)$$

where H is the enthalpy of the system at temperature T and fraction solid g, and H_{SM} is the enthalpy of the solid at the melting temperature. Alternatively, Fig. 8 can be plotted in terms of dimensionless enthalpy ϕ and temperature θ:

where

$$\phi = [H-H_{SM})/\Delta H_M \qquad (6)$$

$$\theta = C_L(T-T_M)/\Delta H_M \qquad (7)$$

For a solid volume (g = 1) the dimensionless nodal enthaply ϕ is always negative or zero since $\theta \leq 0$, whereas for a volume of superheated liquid (g = 0, $\theta > 0$) ϕ is larger than unity.

The system can conceivably follow any "path" of decreasing enthalpy in the supercooled region ($\phi < 1$) starting at the nucleation temperature ($\theta_N < 0$) on the liquid line, and ending at some point on the solid line. A vertical "path" represents isothermal solidification, of which a limiting case is the no-undercooling situation ("path" 1 in Fig. 8). A horizontal

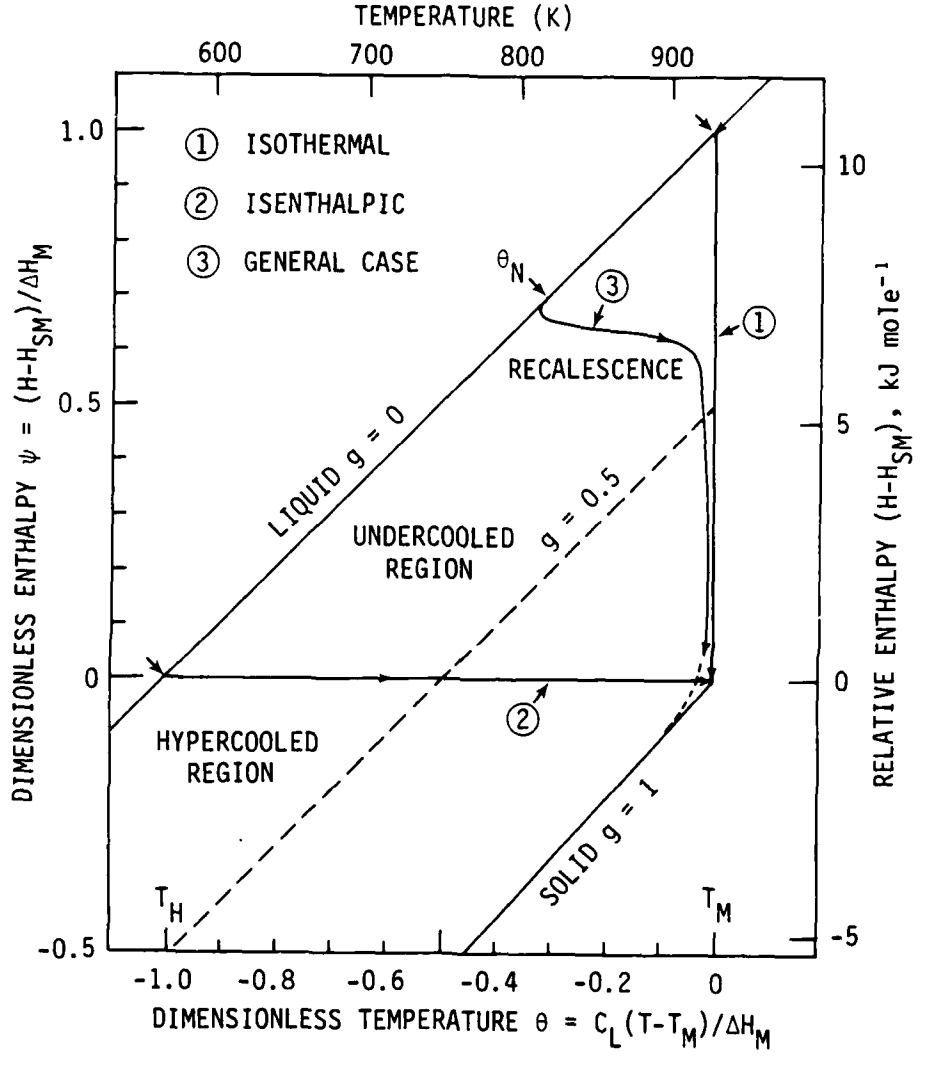

Figure 8. Enthalpy-temperature diagram showing possible solidification "paths". θ_N is the dimensionless temperature at the moment of nucleation.

"path" represents isenthalpic (or adiabatic) solidification. If nucleation can be suppressed until an amount of enthalpy at least equivalent to the heat of fusion has been removed (i.e., $\psi < 0$) the system can undergo complete solidification without further heat extraction ("path" 2 in Fig. 8). The region of the diagram for which $\psi < 0$ is known as "hypercooled". In the "path" such as that described by curve 3, two distinct solidification regimes can be identified. The first one is the recalescence or "rapid solidification" stage, where the supercooled droplet is absorbing most of the liberated heat of fusion and the heat loss to the surroundings is more or less irrelevant. The second regime is one of a "slower growth", and developed after the droplet undercooling has been largely relieved, thereby limiting the progress of solidification to the conditions imposed by the external heat flow. This regime usually involves temperatures close to the melting point of the metal and is roughly isothermal.

The thermal history reflects the competition between the external rate of heat extraction and the recalescence rate (release of latent heat) which is proportional to the solidification rate (change in fraction solid with time, (dg/dt). The latter is in turn a product of the solid/liquid interface velocity and its area. Predominance of the recalescence rate translates into a shallow negative slope for the ψ-θ curve in the "rapid solidification" stage. As the heat extraction process is able to relieve some of the heat of fusion being transformed

into sensible heat, the slope of the curve becomes steeper (more negative) and eventually positive if the external heat flow is dominant.

In addition to the two regimes noted above, there is usually an initial transient in the ψ-θ curve, during which time the overall cooling rate of the droplet decreases rapidly from its value at the moment of nucleation until it changes sign and recalescence begins. At the start of solidification, the solid/liquid interface velocity is finite but its interfacial area is very small-slow solidification rate. Therefore, the rate of heat extraction dominates the rate of recalescence and the droplet temperature drops further below θ_N. This period of decreasing enthalpy after nucleation may be sufficiently long to permit a large number of additional nucleii to form within the droplet.

Figure 9 shows the effect of the initial undercooling on the enthalpy-temperature curve for a constant K/Bi = 100, considering both linear and exponential kinetics. It is evident that increasing the undercooling prior to nucleation results in a corresponding increase in the solidification rate, thus reducing the initial transient and the relative contribution of the external heat extraction.

The dependence of the thermal history on the ratio K/Bi for a constant initial temperature $\theta_N = -0.5$ ($\Delta T_N = 182$ K) is shown in Fig. 10. Curves for K/Bi > 10^3 closely approach the limiting case of adiabatic (isenthalpic) rapid solidification

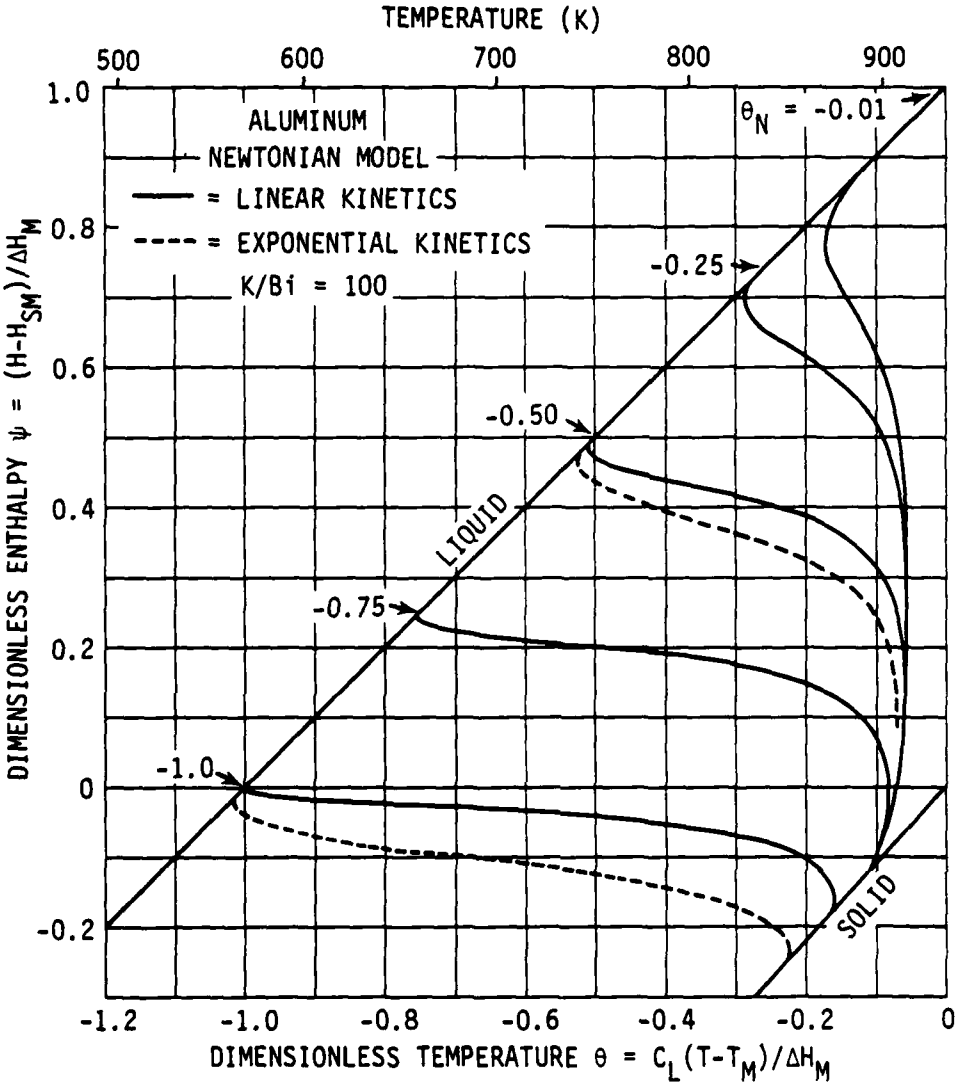

Figure 9. Effect of the nucleation temperature on the thermal history of undercooled droplets calculated from the Newtonian model.

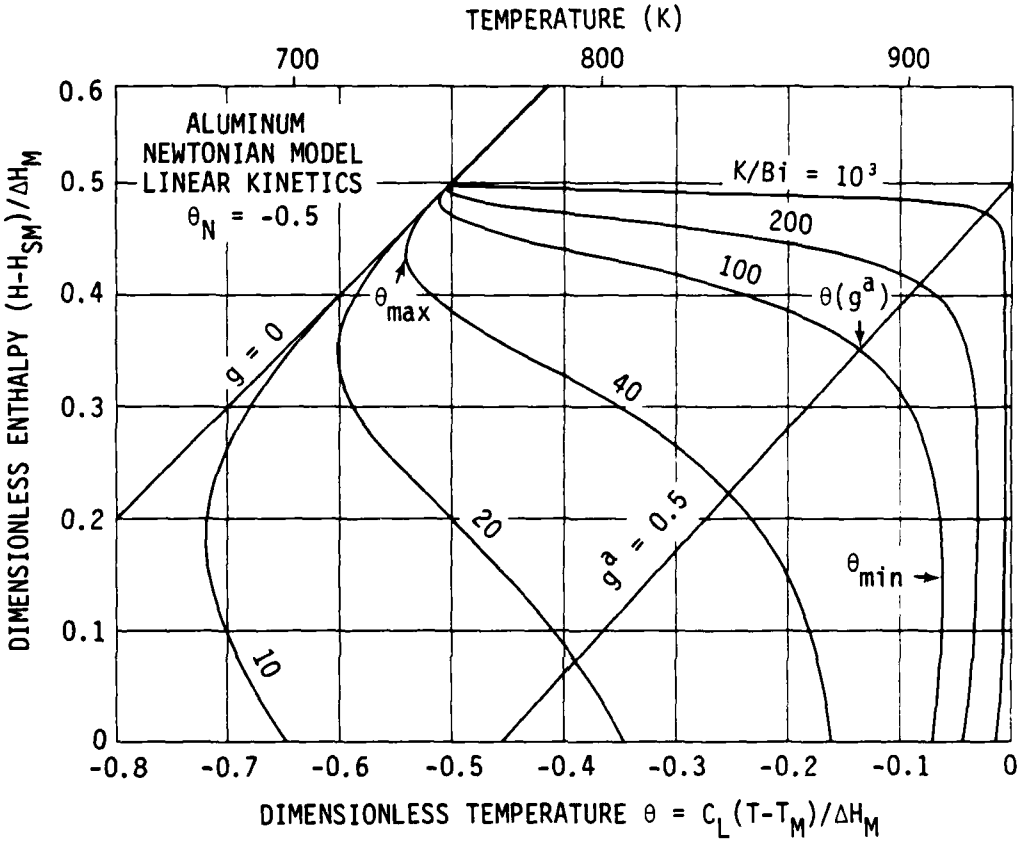

Figure 10. Effect of the ratio K/Bi on the thermal history of undercooled droplets for a fixed nucleation temperature. Note that for typical atomization conditions (K/Bi>100) the external cooling is not able to slow down recalescence to a significant extent.

followed by an isothermal slow growth regime at the melting temperature. As K/Bi decreases (slower kinetics or more efficient cooling), the curves show an increasing contribution of the heat extraction rate during recalescence. At the extreme, e.g., K/Bi = 10, the regime of "rapid solidification" is extended to a point where the droplet temperature never goes beyond its initial value Θ_N. However, even for a low kinetic coefficient K_M = 2 cm/s^{-1} (β=1), the heat transfer coefficient would have to be about 2 × 10^6 W/m^{-2} K^{-1} in order to produce this effect. For a higher β such as the value of 100 suggested by Cahn et al.[24], we would require an h = 2 × 10^8 W/m^{-2} K^{-1}, which is clearly above the values encountered in atomization.

Figure 11 shows the temperature profiles calculated from the non-Newtonian model along the growth axis, as a function of fraction solid for a fixed diameter droplet of 10 μm. The corresponding droplet temperatures and interface positions calculated from the Newtonian model are given for comparison. As expected from the Biot number, (Bi = 2.8 × 10^{-3}) the profiles are Newtonian prior to nucleation and after recalescence. However, substantial temperature differences Δ(T) are developed inside the droplet during the period of rapid growth. For example, maximum Δ(T) values of 7, 52 and 148 K occuring at fractions solid of 0.08, 0.108 and 0.126 were calculated for aluminum droplets of 1, 10, and 100 μm in diameter, respectively, under the conditions of this figure.

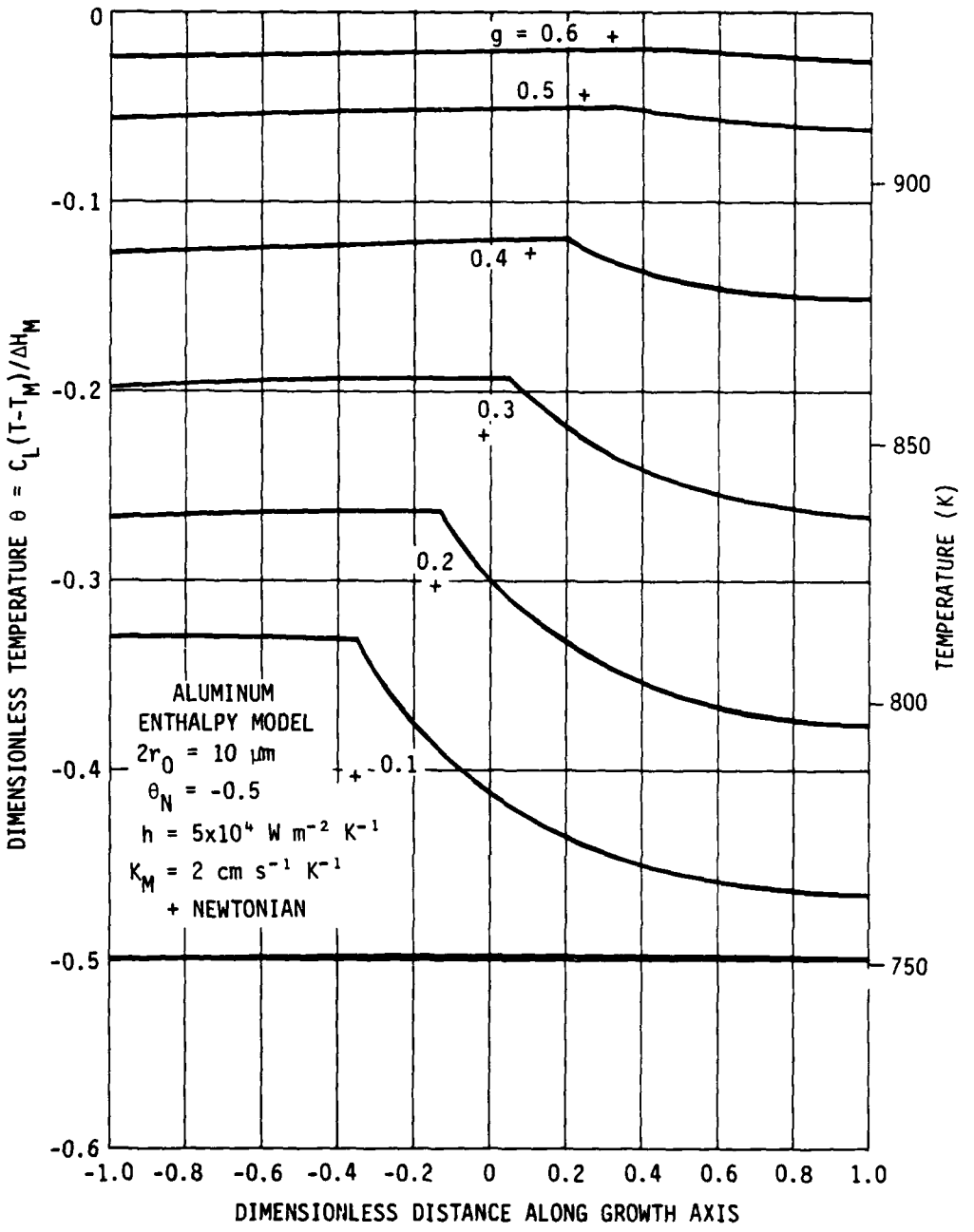

Figure 11. Thermal profiles developed inside the droplet as solidification progresses, for a constant particle diameter of 10 μm.

Figure 12 compares the position, shape and velocity of the solid/liquid interface as solidification progresses, for 1, 10 and 100 μm Al droplets and the corresponding Newtonian limit. As expected, the growth velocities increase as the radius decreases, and the values for a 1 μm particle are almost identical to those calculated from the Newtonian model (the interface and droplet undercoolings have similar values).

Figure 13 shows the transition from a convex to a concave solid front as Θ_N is reduced and r_0 is increased above 100 μm. In addition, increasing K_M will further magnify the concavity. In the limit, then, the droplet should get covered very rapidly with a solid "shell" after nucleation, and further solidification will proceed in a concentric pattern. This represents a fairly accurate picture of the solidification of large particles where dendrites shoot out from several nucleation sites along the surface of the particle.

An important conclusion of the study[23] was that for typical values of K/Bi encountered in atomization (K/Bi > 100), the external cooling has little or no effect in extending the "rapid solidification" regime to a fraction solid substantially larger than that dictated by the limiting case of adiabatic solidification. Furthermore, increasing the number of nucleation events further reduced the role of the external cooling during recalescence.

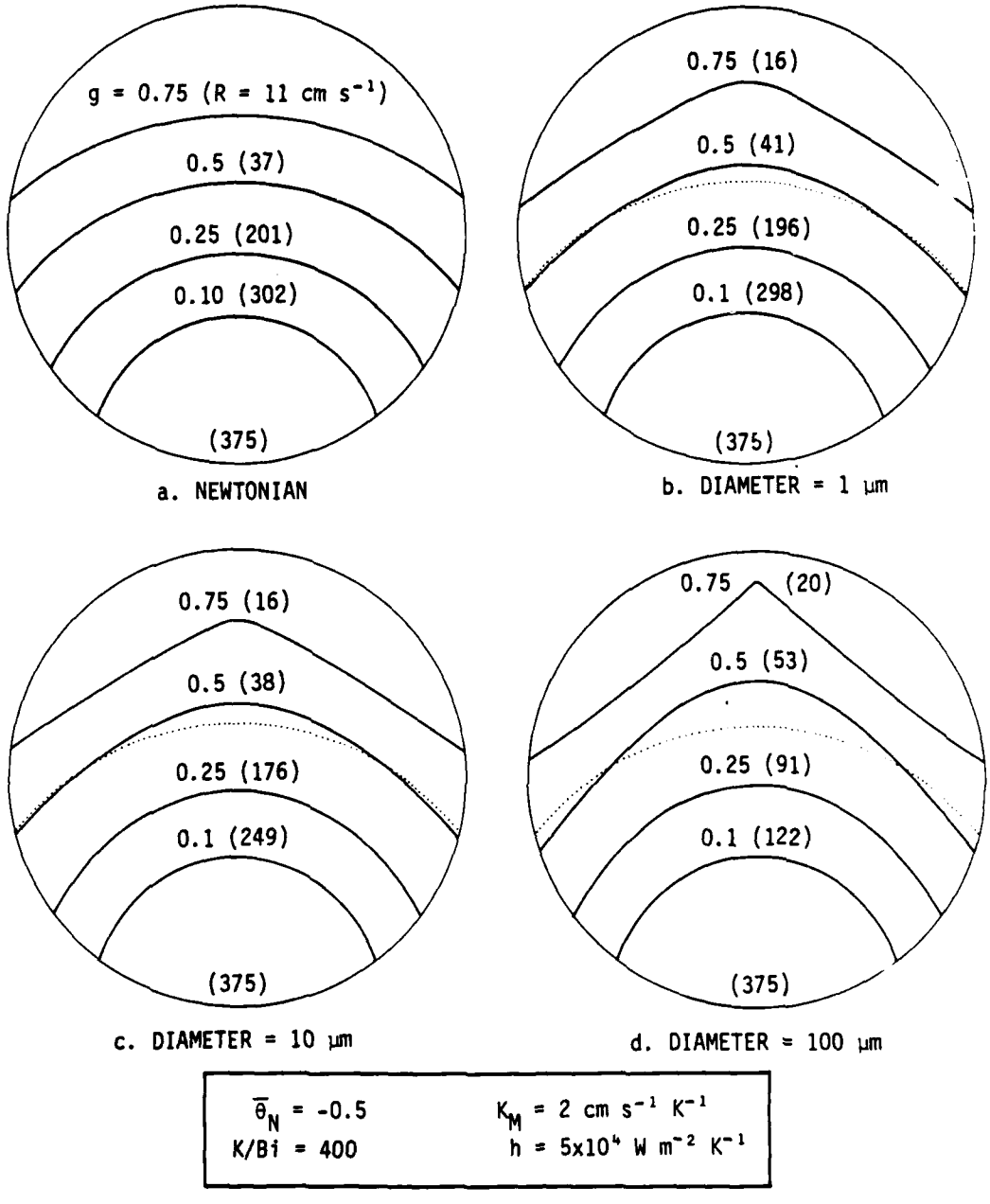

Figure 12. Interface profiles and velocities predicted from the Enthalpy model for undercooled solidification. The deviations from the Newtonian velocity limit increase with particle size, but the profiles for the recalescence stage are quite close in both models for r_0 < 100 μm.

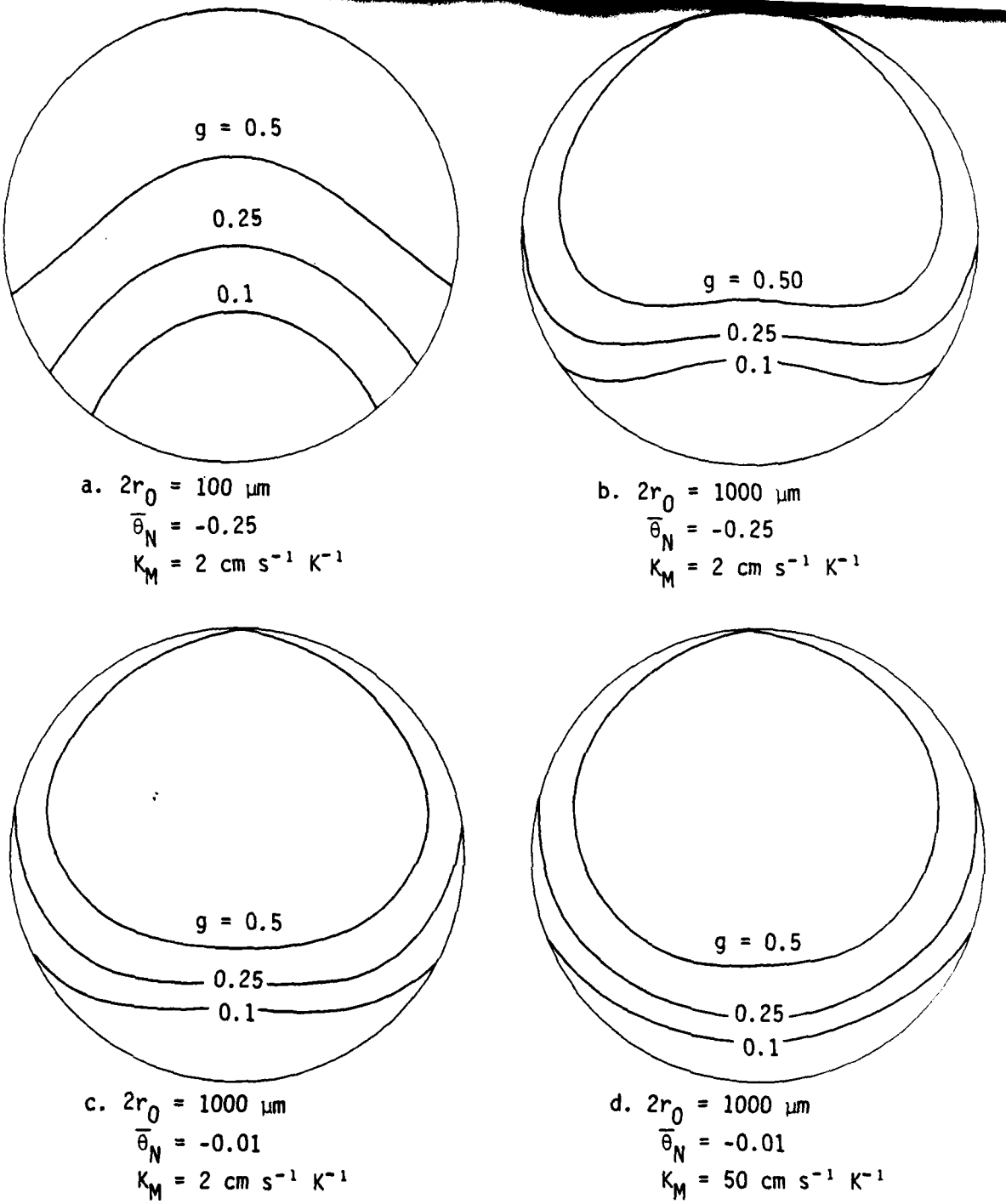

a. $2r_0$ = 100 μm
$\bar{\theta}_N$ = -0.25
K_M = 2 cm s^{-1} K^{-1}

b. $2r_0$ = 1000 μm
$\bar{\theta}_N$ = -0.25
K_M = 2 cm s^{-1} K^{-1}

c. $2r_0$ = 1000 μm
$\bar{\theta}_N$ = -0.01
K_M = 2 cm s^{-1} K^{-1}

d. $2r_0$ = 1000 μm
$\bar{\theta}_N$ = -0.01
K_M = 50 cm s^{-1} K^{-1}

Figure 13. Transition from convex to concave interface profiles is produced by increasing the particle size (a-b), reducing the initial uncercooling (b-c) and increasing the kinetic coefficient (c-d). In the limit, the interface tends to the concentric shape assumed in the no-undercooled solidification model.

STABILITY AT THE SOLIDIFICATION INTERFACE AND MICROSEGREGATION

Interface stability during solidification has received increased emphasis recently due to the emergence of rapid solidification as a field of technological interest. A most important contribution has been the extension of morphological stability theory to high interface velocities. It has been shown that plane-front solidification, which would avoid microsegregation effects, becomes increasingly stable with increasing interface velocity during rapid solidification of crystalline alloys. For most solidification processes at low interface velocities, the classical theory of constitutional supercooling[25] has been used as an adequate guideline to determine the growth conditions that result in unstable interfaces. The theory is basically an application of thermodynamics to determine if the liquid ahead of a moving interface is undercooled with respect to its composition. The undercooled liquid layer, due to rejection of solute by the growing solid, makes the shape of the interface unstable with respect to the formation of cells or dendrites that could protrude into it. The stability parameter emerging from this theory is the ratio of the temperature gradient in the liquid ahead of the moving interface (G_L) to its velocity (R). Greater stability is promoted by increasing G_L/R.

Figure 14 maps out the G_L and R combinations that lead to the three solidification-front morphologies shown. The line between the planar and cellular regions is the constitutional supercooling criterion for a binary alloy:

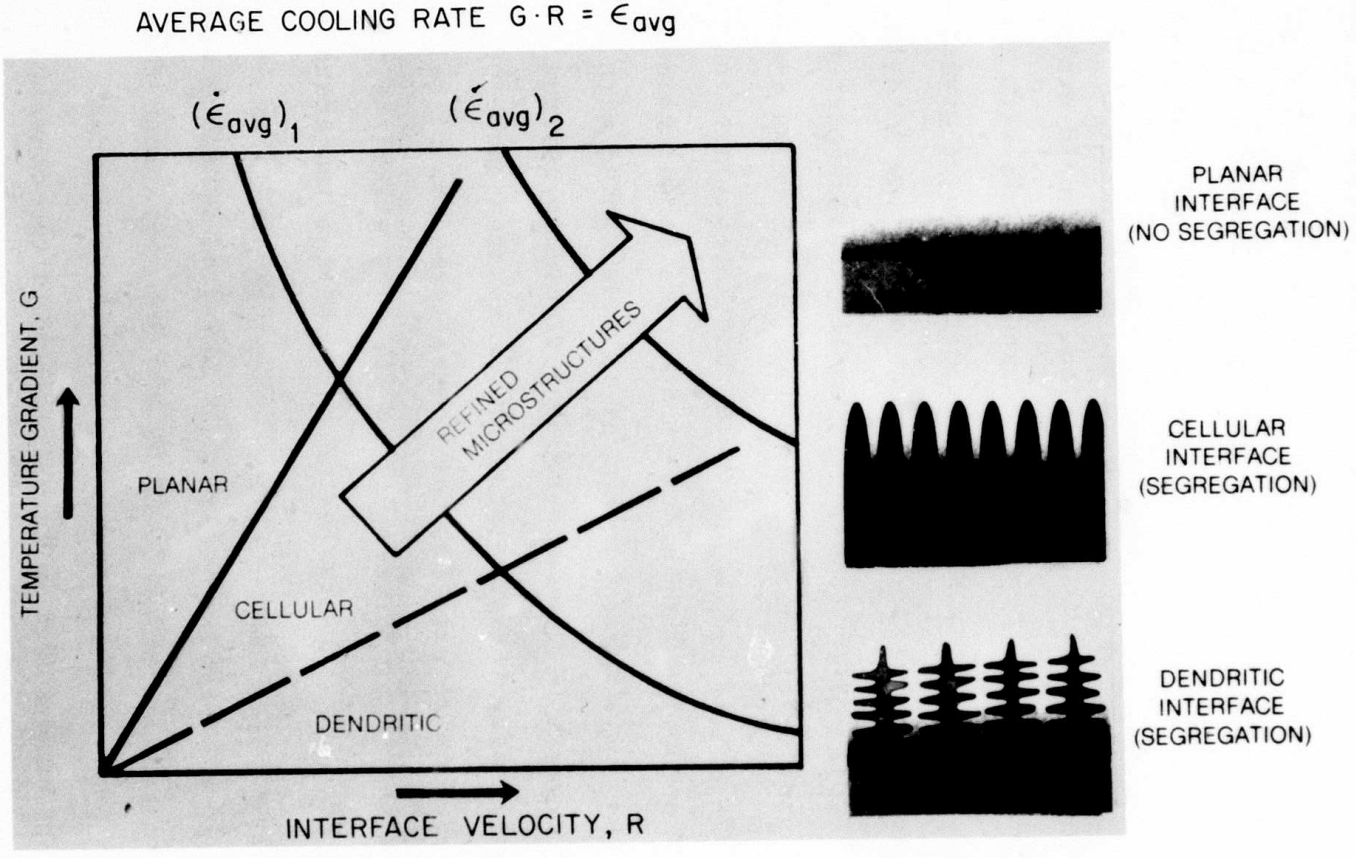

Figure 14. Dependence of solidification morphology on temperature gradient (G) and solidification rate (R). The qualitative effect of increasing cooling rate $\dot{\epsilon}_{avg}$ = Ga·R is indicated by the sloping effect.

$$G_L > m_L G_C = \frac{m_{LR} C_\infty (k-1)}{D_L k} \qquad (8)$$

where C_∞ is the bulk solute concentration, D_L is the liquid diffusion constant, G_C is the unperturbed solute-gradient at the interface, m_L if the slope of the liquidus line and k is the equilibrium distribution coefficient. To the left and above this line, the actual temperature gradient in the liquid is larger than that calculated from Eq. (8) and plane-front growth, with compositional homogeneity, is morphologically stable. To the right and below this line, the solute-gradient effect dominates (actual temperature gradient is smaller than that given in Eq. (8)) and chance proturberances can become pronounced leading to cellular structures and microsegregation. For small amounts of constitutional supercooling, the cellular interface is stable. This morphology reduces the constitutional supercooling ahead to the main interface by rejecting solute between the cells. With still larger solute concentrations, or faster interface velocities (R) relative to the operative temperature gradient, the familiar dendritic-growth morphology is encountered.

For the case of cellular or dendritic solidification, the temperature gradient and interface velocity in Fig. 14 could represent averages for the liquid plus solid "mushy" region. The product G·R is then a measure of the average cooling rate (ε_{avg}) during solidification. This variable is then directly

related to local solidification time (t_f) which is the time available for coarsening:

$$\varepsilon_{avg} = G \cdot R = \frac{\Delta T}{t_f} \qquad (9)$$

where ΔT is solidification temperature range.

Therefore, as indicated by the sloping arrow, moving out to larger G•R products in Fig. 14, shorter local solidification times, corresponds to the finer microstructures obtained in rapid solidification processing[26]. Note that the simple treatment here does not include growth into a supercooled liquid. Glicksman and Huang[27] have developed a series of relationships between the microstructural size scale (segregate spacing) and interface cooling. They concluded that for small undercoolings, the segregate spacing should be a fixed multiple of the critical nucleation radius. Furthermore, as dimensionless supercooling approaches unity, the scale of the morphology should rapidly decrease. They also studied the coarsening process during solidification of a transparent material and noted that the initial microstructure is produced far from equilibrium in order to comply with the transport processes during growth. The final microstructure tends to be substantially different from that produced in the vicinity of the dendrite tip, and can be correlated to the coarsening time, local solidification time, by a scaling law.

The constitutional supercooling theory predicts cellular or dendritic structures for most rapid solidification experi-

ments. However, for rapid solidification some of the assumptions and simplifications of this theory may not be valid. These include:

1. Surface tension (capillarity) and latent heat evolution which could stabilize the interface are neglected.

2. The constitutional supercooling theory takes into account a layer of liquid cooler than its local melting point, but it does not solve the kinetic equations for the thermal and diffusional fields to show how interface fluctuations lead to instability.

3. Local equilibrium at the interface -the equilibrium distribution coefficient is assumed to describe quantitatively the amount of solute rejected by the growing crystal.

The theory of morphological stability originally developed by Mullins and Sekerka[28-29] and Sekerka[30] considers the time dependence of a general sinusoidal perturbation of the interface with respect to solute and heat diffusion fields and surface tension. Extensive reviews of the theory are available in the literature[29-33]. It has been demonstrated that for a large number of conventional solidification processes, the constitutional supercooling and morphological stability approaches lead to similar results. This explains the popularity of the former approach due to its simplicity. On the other hand, since both surface tension and evolution of latent heat have a stabilizing influence, the morphological stability theory (even if local equilibrium at the interface is assumed) predicts far

greater stability during rapid solidification than predicted by the constitutional supercooling criterion. The two dominant effects are ascribed to the excess surface energy for short wavelength perturbations, common at high interface velocities and departure from local equilibrium at the solid-liquid interface[34].

The first treatments of morphological stability assumed local equilibrium at the solid-liquid interface and considered the transition from planar to non-planar growth during steady-state, constant velocity, unidirectional solidification of a binary alloy. A linear time dependent stability analysis was carried out[35] in which the perturbation at the solid-liquid interface growing in the z-direction is given by:

$$z = \delta \exp(\sigma t + i\omega_x x + i\omega_y y) \qquad (10)$$

where δ is the perturbation amplitude at time $t = 0$, and ω_x and ω_y are spatial frequencies. The interface is stable if the real part of σ is negative for all perturbations. The value of σ was determined[29,35] by solving the steady-state heat flow and diffusion equations with appropriate boundary conditions. For the stability-instability demarcation ($\sigma = 0$) the equation simplifies to a criterion which identified three factors contributing to the overall stability of the interface. These are; the solute field, the capillary forces and the thermal field given below:

$$+m_L G_c \frac{(\omega^* - R/D_L)}{(\omega^* - (1-k)R/D_L))} - \frac{T_M \gamma \omega^2}{\Delta H_M \rho_S} - \frac{k_S G_S + k_L G_L}{2\,\bar{k}} \gtrless 0 \qquad (11)$$

always > 0 solute field; always < 0 capillary force; $\lesseqgtr 0$ thermal field

where G_S is unperturbed temperature gradient in the solid, $\bar{k}$ = ($k_S + k_L/2$, k_L and k_S are thermal conductivities of liquid and solid, respectively, T_M is the melting point of the interface in the absence of solute and curvature, ΔH_M is the latent heat of fusion per unit mass, ρ_S is solid density, γ is the solid-liquid surface energy, and $\omega^* = f(R/D_L, \omega)$, where $\omega^2 = \omega^2_x + \omega^2_y$.

Thus, the interface is stable when the sum of the three terms in Eq. (11) is negative. The solute field is always destabilizing, but the capillary forces always oppose the growth of a perturbation. For large ω (short wavelengths), this term is large. The thermal field will be stabilizing if the numerator of the third term is positive, and destabilizing in the opposite case. Note that while the constitutional supercooling criterion predicts instability for all cases where $G_L < 0$, the morphological theory may predict a stabilizing thermal field if G_S is sufficiently positive to make the average gradient term also positive.

Two limiting cases are recognized for Eq. (11). First, we consider growth at slow interface velocities and where $\omega^* \sim \omega >> R/D_L$, lateral solute diffusion is complete, and capillary forces are small. If, in addition $R\Delta H_M \rho_S << 2k_L G_L$, then

Eq. (11) for the stability criterion becomes:

$$(k_L/\bar{k})G_L > m_L G_C \qquad (12)$$

which reduces to the constitutional supercooling criterion for $k_S \sim k_L$. Equation (12) is the solid line in Fig. 15 which shows the calculated critical copper concentrations in dilute Al-Cu alloys (below which the planar interface is stable) as a function of interface velocity R. A constant positive liquid temperature gradient in front of the interface $G_L = 2 \times 10^4 K/m$ was assumed. The wavelength $\lambda = 2\pi/\omega$ which corresponds to the onset of instability, i.e., to the value of ω for which $C_\infty(\omega)$ is a minimum, is shown in Fig. 16 to be a monotonically decreasing function of interface velocity. For the limiting case noted above (left top corner of this curve), λ is proportional to $R^{-1/3}$ [34].

For the second limiting case, high interface velocities, $\omega << R/D_L$, and a stabilizing thermal field, Eq. (11) becomes:

$$+m_L G_C (D_L^2/R^2 k)\omega^2 - \frac{T_M \gamma \omega^2}{\Delta H_M \rho_S} < 0, \text{ for stability}$$

or (13)

$$A = \frac{k\ T_M\ \gamma}{m_L G_C\ \Delta H_M \rho_S} (R/D_L)^2 > 1.0$$

Equation (13) is the absolute stability criterion[35]. It is good approximation at high interface velocities, right side of Fig. 15, and shows that in this region stability is practically independent of G_L. Furthermore, it has been shown[34] that the

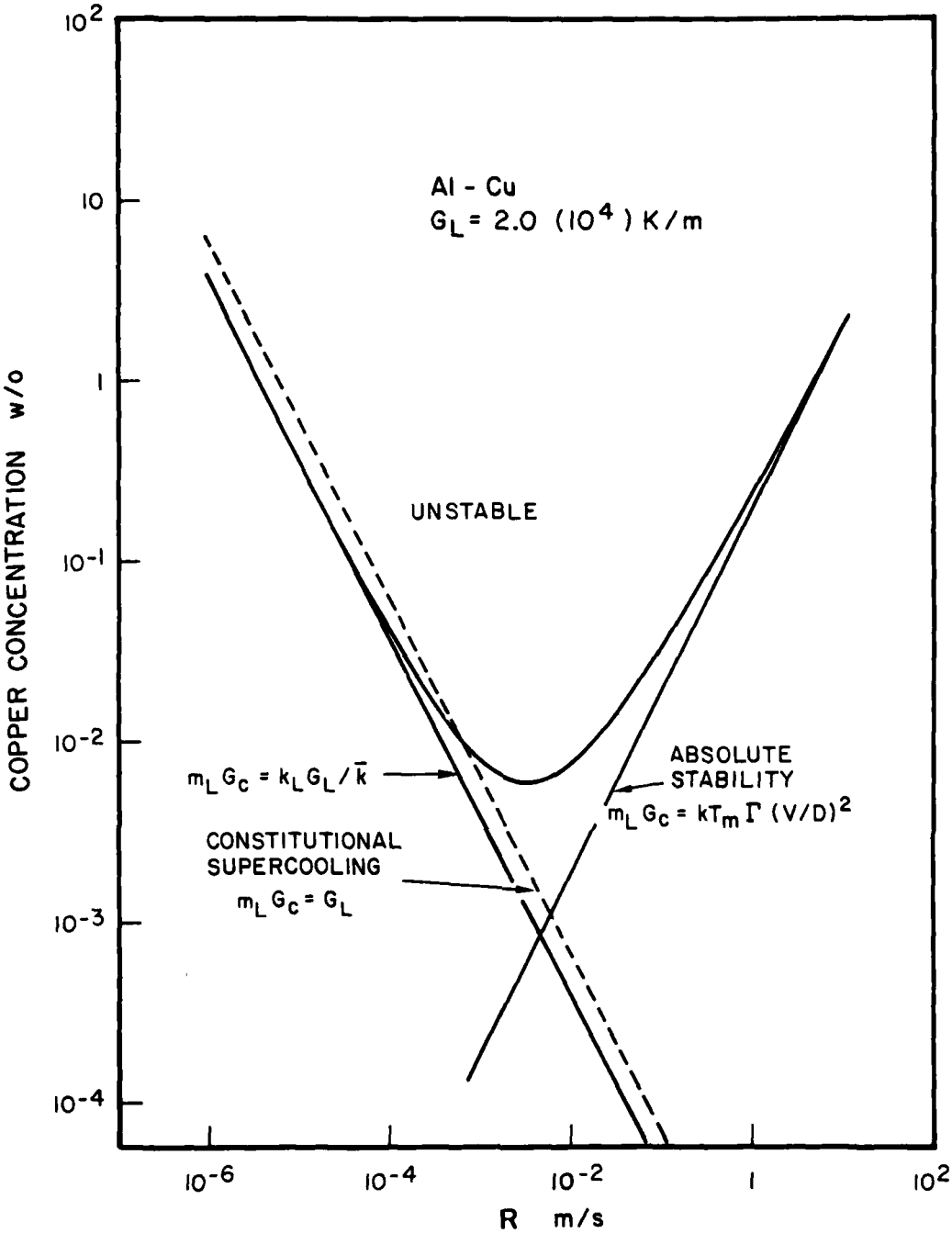

Figure 15. The critical concentration of copper above which interface instability occurs as a function of the interface velocity R in directional solidification of Al-Cu alloys for a temperature gradient in the liquid of 2.0(10^4)K/m. The curve is based on morphological stability theory while the lines correspond to constitutional supercooling, modified constitutional supercooling, and absolute stability[34].

wavelength for the onset of instability at such high velocities is proportional to $R^{-3/4}$. This is the lower right side of the curve in Fig. 16 where calculated wavelengths are shown for R = 10 m/s. It should be noted that the theory is no longer valid at such high velocities. Since, D_L for Cu in Al is $\sim 5\times10^{-9}$ m^2/s and the characteristic diffusion boundary layer, DL/R, is only a few atomic distances, and the use of macroscopic transport equations is not justified.

Figure 17 maps out the calculated G_L and R combinations that lead to homogeneous plane-front solidification as a function of copper concentration in Al-Cu alloys. This plot is similar to Fig. 14 except that now a new region of morphological stability is shown at high interface velocities which is independent of temperature gradient. As anticipated, the conditions under which plane-front solidification prevails become more restricted with increasing solute content.

Solidification into supercooled melts ($G_L < 0$) has also been recently discussed[34]. Of special interest is the solidification of very fine, less than 1 μm in diameter, supercooled droplets which are microstructurally analyzed in a subsequent section. In a small droplet the largest perturbation has to be less than the droplet size or $\omega > \pi/r$. Thus, for a 1 μm diameter droplet of pure aluminum $\omega > 6(10^6)m^{-1}$ the surface tension term in Eq. (11) is larger than $3.6\ (10^6)K/m$. Even if we assume that $G_S = 0$ a stable interface would be expected as long as $G_L > -1.2(10^7)$ k/m or R < 1.0 m/s. Addition of solute requires

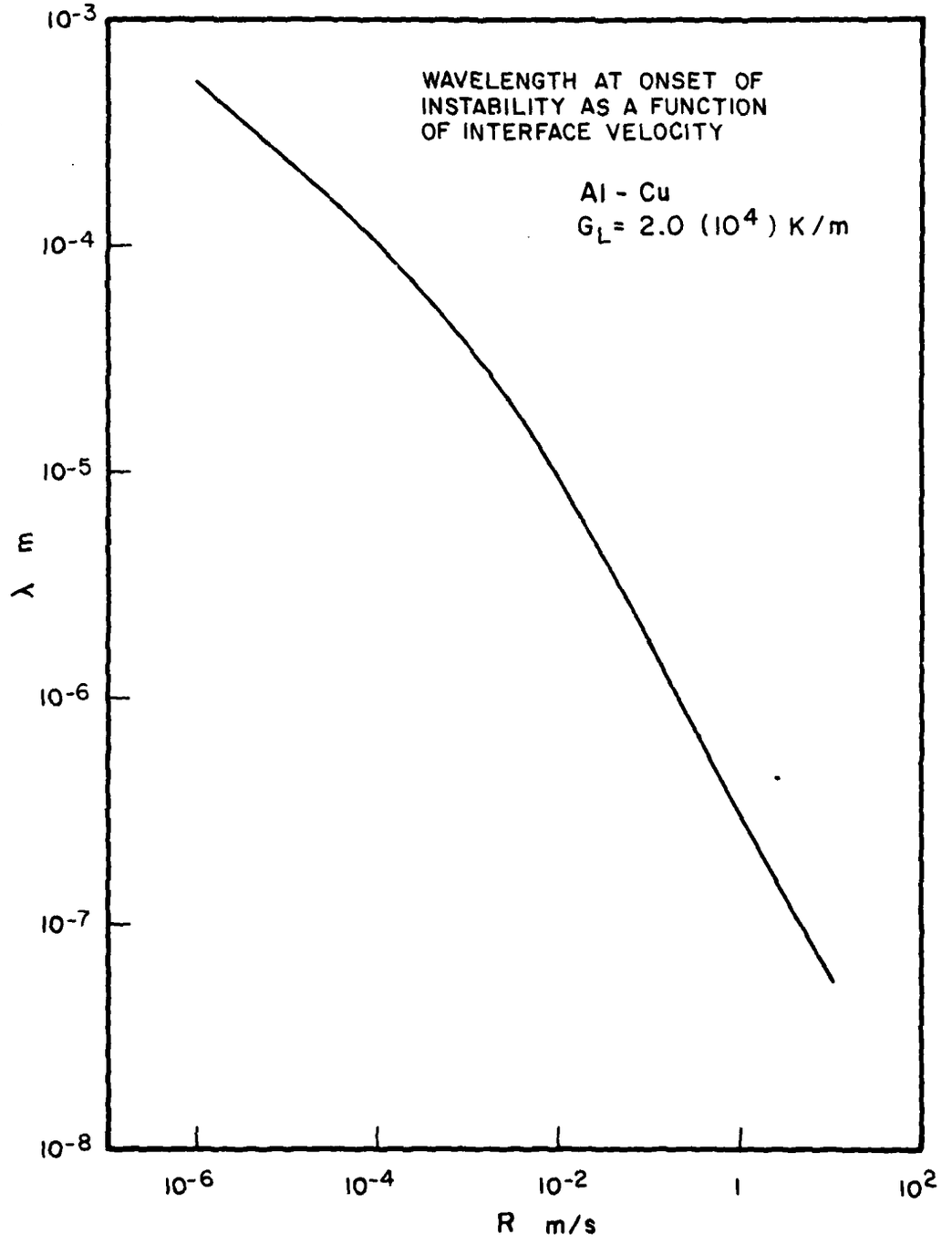

Figure 16. The wavelength λ at the onset of instability during directional solidification of aluminum containing copper as a function of interface velocity R.[34]

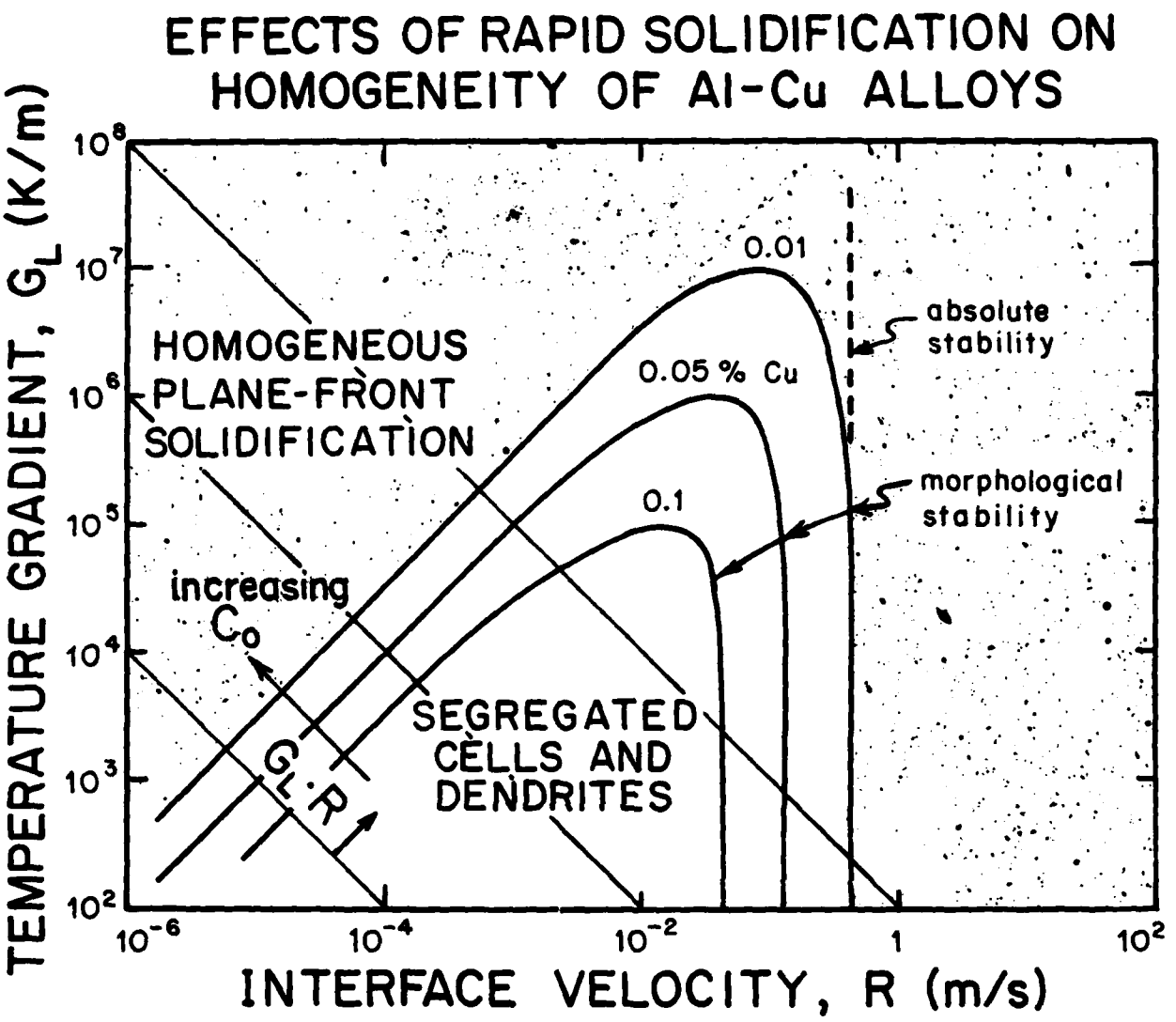

Figure 17. Regimes of homogeneous plane-front growth vs. segregated cellular and dendritic growth as determined by the liquid temperature gradient (G_L) and the interface velocity (R) in Al-Cu alloys. Cone-shaped lines separating the two regimes are the locus of morphological stability.

larger contribution from the surface tension term, since destabilization is now due to both the negative temperature gradient and the solute gradient terms in Eq. (11). Calculations for the Al-Cu system[34] have shown that some minimum composition, significantly less than 1 wt% Cu is needed for morphological instability to be observed in these fine particles. This is verified in a later section where the development of morphological instability in fine particles of aluminum containing 4.5 wt% Cu is noted.

While the assumption of local equilibrium has served to elucidate non-equilibrium solidification-segregation "paths" at low interface velocities - it falls short when interface velocities are high due to rapid rate of heat extraction as in atomization or splat cooling. Metastable structures, for example, extended solid solubility, cannot be always adequately explained when interface equilibrium in invoked. This extension in solubility can result from suppression of nucleation of the second phase below the eutectic temperature. The system thus follows the metastable solidus line as it moves into the two phase region of the phase diagram. Therefore, the maximum solid solubility is limited to the composition dictated by this metastable solidus at the solidification temperature. Experiments with Zn-Cd alloys, a system with a retrograde solidus, have proven the occurrence of solute trapping and deviation from local equilibrium at the solid-liquid interface[36]. Similar observations have been made on ion implanted dilute silicon alloys subjected

to laser melting and resolidification[37]. In a recent paper, Coriell and Sekerka[34] concluded that most departures from local equilibrium enhance interface stability, especially in the case where the partition coefficient tends to unity. Baker[38] has addressed the behavior of partition coefficient as a function of interface velocity for various models. In one such model where he permitted a variable solute energy at the interface he showed that given a sufficiently high velocity the partition coefficient will always tend toward unity.

In conclusion then, the present contributions of the morphological stability theory to rapid solidification, as well as its limitations, can be summarized as follows:

1. Short wave length perturbations at high interface velocities are stabilized due to capillary forces. If the thermal field is stabilizing, the interface velocity for absolute stability is a function of the solute content and is independent of the temperature gradient in the liquid.

2. Departures from local equilibrium at the solid-liquid interface tend to have a stabilizing influence on the interface. However, the exact form or magnitude of these departures are not known.

3. In undercooled melts, the temperature gradient in the solid plays an important role in interface stability.

4. In most rapid solidification experiments, interface velocity varies with undercooling and the changing thermal fields. Thus, the assumption of constant interface velocity has

seriously limited the design of conclusive experiments to test the theory. Some attempts have been made to overcome this assumption[39]. These have been for limiting special cases and this field remains ripe for investigation.

5. At very high interface velocities, the solute enriched layer approaches atomic dimensions and the macroscopic transport equations used to derive the stability criterion are no longer valid.

GLASS FORMATION

Theory has been developed providing boundaries for the region in the phase diagram where partitionless solidification is thermodynamically forbidden[36,40]. In this region, a two phase structure must be created if crystallization is to occur. It has also been shown[40,41] that, because diffusion processes are required to sort out the constituents into two phase eutectic microstructures in this region, crystallization velocities typically will not exceed 5 cm/s, making glass formation very probable during solidification. A short review of these findings is given below.

Solidification of crystalline structures is known to require nucleation and growth processes. On the other hand, attempts to predict the conditions for formation of metallic glasses usually focus on only nucleation, i.e., the degree of difficulty that atoms experience in joining an embryo - the viscosity is high or the diffusivity is low. Suppression of nucleation by rapid quenching of the liquid until the alloy reaches

its glass transition temperature is used to predict glass forming tendency of alloys. Recent investigations[40,41] have shown that amorphous solidification can be obtained in some eutectic and off-eutectic alloy compositions even in the presence of the crystalline phase. That is, crystalline solidification is growth limited. This is the case when the alloy is thermodynamically forbidden to form a single phase, and the solidification velocity is increased enough to overcome the diffusion controlled, partitioning process at the interface for the formation of a two-phase structure.

Baker and Cahn[36] have discussed the thermodynamics of nonequilibrium solidification in a binary alloy. With the aid of free energy (F) vs. composition (X) curves, they defined the domain of possible interface compositions for isothermal and steady state solidification. They concluded that the maximum solid composition X_S that can be formed from a liquid of composition X_L at the temperature of interest is determined by the point at which the liquid and solid free energy curves intersect. This is known as the $X(T_o)$ composition and the locus of all these points form a curve between the liquidus and the solidus for the equilibrium phase diagram. Partitionless transformations can only occur below the T_o curve ($T < T_o$ for a given X_L). Thus, for temperatures or compositions above the T_o curve the crystalline solid forming must be multiphase. The growth of a two (or more) phase solid from the liquid requires the diffusional sorting of the components in the liquid phase as well as

the creation of new surface area between the phases. These requirements for coupled growth lead to well known relationships between interface undercooling below the eutectic temperature, and interface velocity. For a given interface velocity, the interface undercooling required for eutectic solidification is much greater than for single phase crystallization. Due to this fact and the temperature dependence of the diffusion coefficient (related to the viscosity), a maximum velocity exists beyond which eutectic solidification cannot occur. Alloys required to crystallize at velocities greater than this maximum due to the rate of heat extraction and which cannot crystallize as a single phase material will form a glass.

It has long been known that alloys near eutectic compositions are often good glass formers. An interesting thing to note about compositions near eutectics is that for many alloys they must crystallize as multiphase solids regardless of the cooling rate. This is known by examining the T_o curves for all possible phases (stable or metastable). Figure 18 shows a hypothetical phase diagram with a stable and a metastable eutectic. If the composition range of an individual phase is very narrow or if the solidus is retrograde[36], the T_o curves will not extend far from that phase at temperatures of interest. This produces a rather wide range of alloy compositions between the T_o curves of the different phases which must crystallize as two-phase solids. Even partitionless (massive) crystallization of liquids in this composition range into a single phase is impossible.

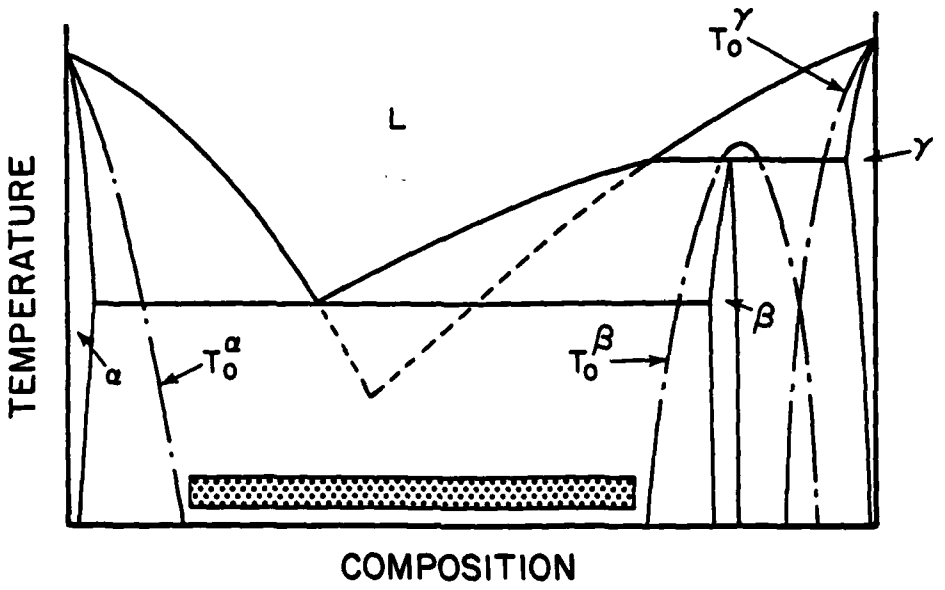

Figure 18. Hypothetic phase diagram with a stable and a metastable eutectic. The T_o curves for the three solid phases relative to the liquid are shown. In the shaded region of composition between T_o curves, crystallization to a single phase crystalline solid is impossible. From Ref. 40.

Wider composition ranges requiring two phase crystalliztion are possible if a particular phase fails to nucleate (for example, β in Figure 18).

In a recent paper[41], the microstructure of a range of compositions of an easy glass former Pd-Cu-Si as a function of growth rate up to the critical velocity for glass formation was investigated. The results showed that, in some cases, the transition from dendritic growth to eutectic growth with increasing growth rate for compositions away from the eutectic determines the critical conditions for the avoidance of crystallization. Figure 19 is a schematic illustration of these observations.

Examples of abrupt changes in microstructure of PdCuSi alloys are shown in Figure 20. Alloys with copper content of less than 6 wt% Cu form faceted and nonfaceted dendrites and eutectic a low interface velocity. With increasing interface velocity growth of a eutectic-like structure is obtained at these off-eutectic compositions. At still higher interface velocities, the eutectic structure becomes more refined until a sharp interface is formed during the acceleration mode which separates the eutectic from glassy alloy, Figs. 20(a) and (b).

In an alloy containing 9 wt% Cu, the transition from a refined eutectic with increasing interface velocity occurs at ~2.5 mm/s. However, the structure is now a mixture of glass alloy and small diameter crystallites, Fig. 20(c).

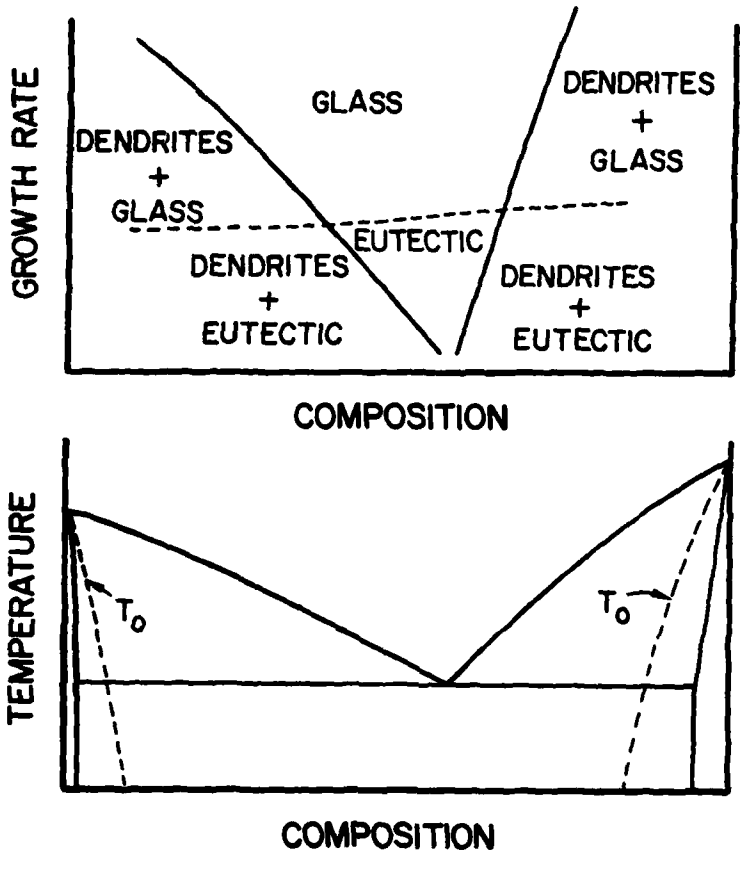

Figure 19. Maximum crystallization rates for alloys between T_o curves for a simple eutectic system (from Ref. 41).

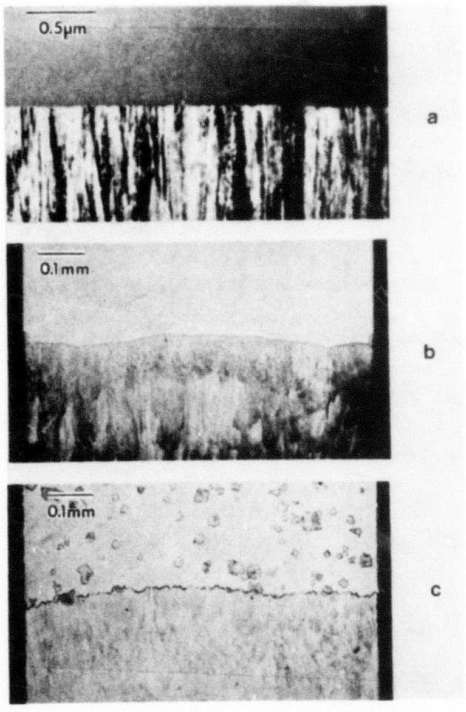

Figure 20. Interface between eutectic and glass in Pd-Cu-Si alloys (a) 6 wt.% Cu, TEM, (b) 4 wt.% Cu and (c) 9 wt.% Cu. Growth direction was vertical (from Ref. 41).

MICROSTRUCTURAL OBSERVATIONS

Some of the new theoretical developments have already been qualitatively verified on extremely fine powders of aluminum alloys, less than one micron meter in size, produced in a small laboratory-type atomization apparatus[18]. The submicron powders are electron transparent and it is possible to analyze the evolution of a complete microstructure from nucleation until the end of solidification without recourse to thinning procedures. For example, interface breakdown from planar to cellular in the middle of the powders is clearly delineated. Microstructural observations have been coupled with thermodynamic kinetic and heat flow concepts to elucidate the thermal history and solidification mode of the powders and their effects on the microstructure. A summary of these findings[18] is presented below.

The aluminum alloy powders used in this investigation were prepared by the electrohydrodynamic (EHD) atomization process[40]. Figure 21 shows a typical sample of powders as collected on a plastic substrate. They are nearly spherical and have smooth surfaces, although some appear to have solidified on the tape. Results of the heat flow studies on powder solidification, presented in a previous section, revealed that for typical atomization conditions the external cooling plays only a minor role during the recalescence stage of the thermal history. Therefore, the "rapid solidification" effects are usually limited by the undercooling achieved before nucleation occurs.

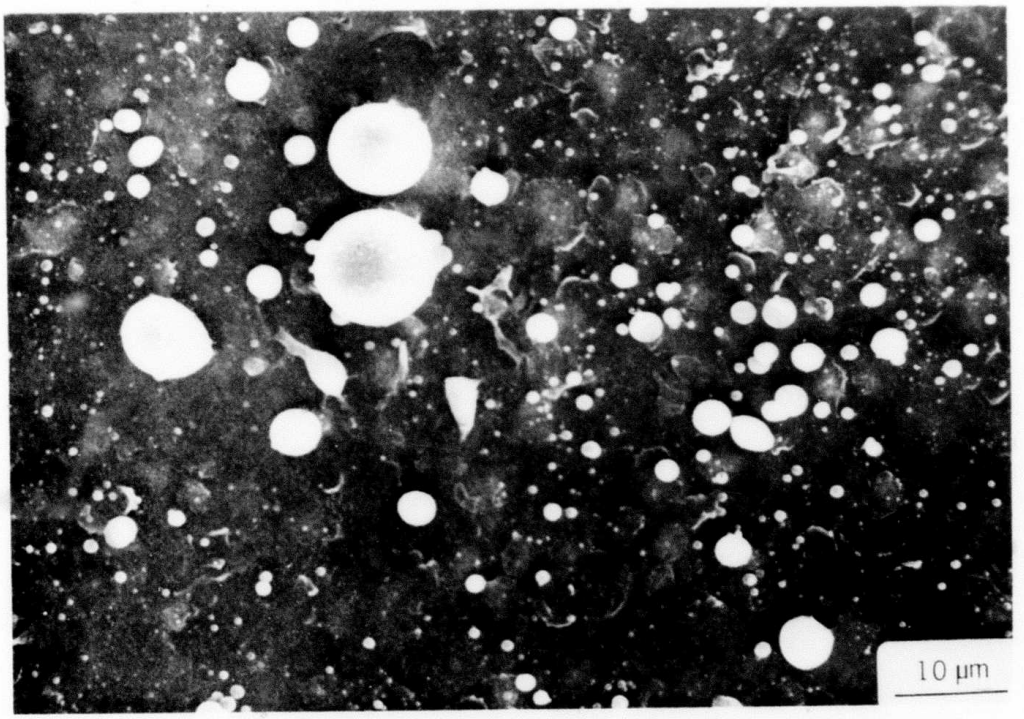

Figure 21. SEM view of Al-4.5 wt.% Cu powders produced by electrohydrodynamic (EHD) atomization process.

Most of the Al-Si EHD produced powders conform to a variant of the basic segregation pattern shown in Fig. 22. The microstructure exhibits a region (A) containing a uniform distribution of very fine precipitates or clusters of Si which, according to the electron diffraction evidence, have an orientation relationship to the primary α-aluminum phase. Dark field imaging of precipitates slightly coarser than those in the present figure suggest that they are either needles or platelets on the {111} α-aluminum planes. This finding is consistent with the decomposition kinetics of Al-Si solid solutions; the plates evolve from spherical clusters and needles that form in the early stages of precipitation[43-45]. It was concluded that this zone was originally a supersaturated solid solution.

Region (A) is followed by a precipitate-free zone (B), and the change in microstructure clearly delineates the solidification front. The latter is symmetric about the growth axis, which was consistently found to be close to a <111> direction.

Finally, the particle in Fig. 22 also has a well developed cellular region (C), with segregate spacings on the order of 0.1 μm. A similar structure in an Al-4.5 wt% Cu powder, shown at a different angle in Fig. 23, reveals the cellular pattern more clearly.

Figure 24, illustrates the general effect of particle size on the extent of the different zones in the powders. As the powder diameter decreases, the cellular structure becomes less defined 24(b), and eventually disappears, leaving only a

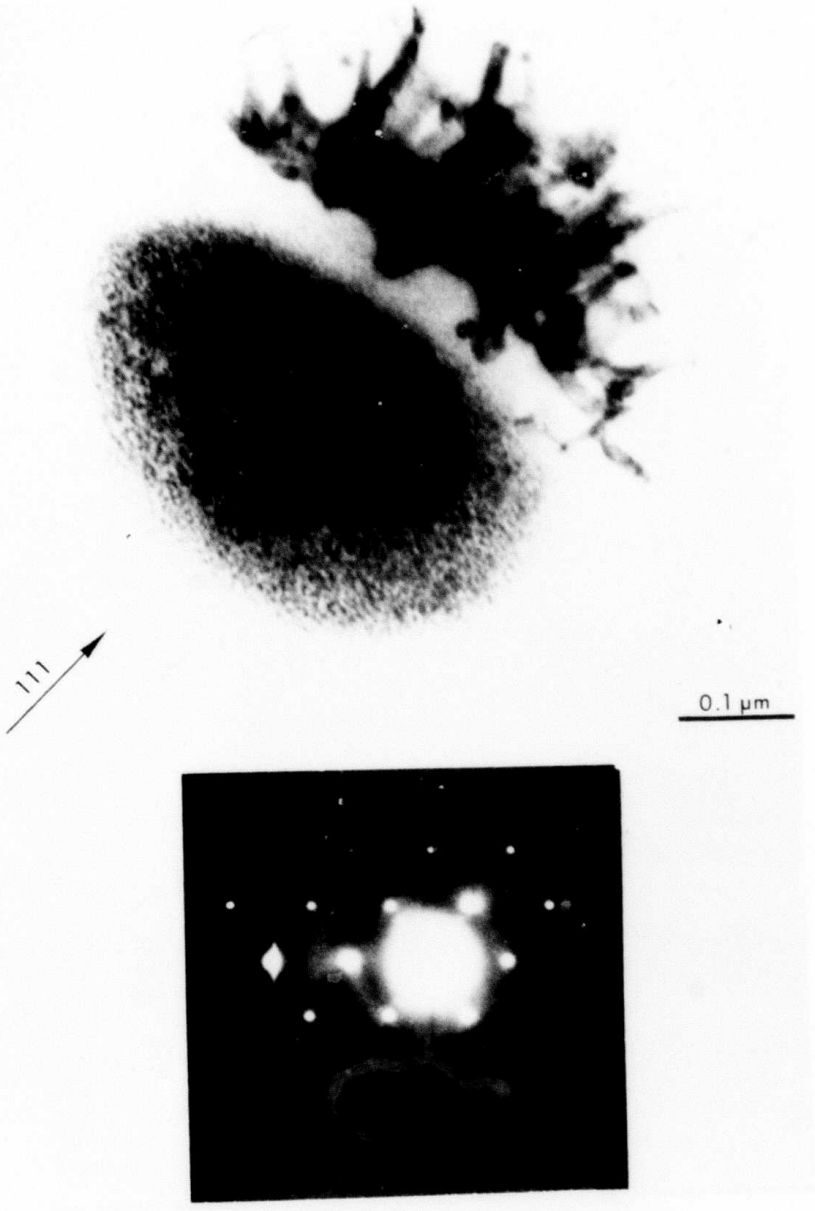

Figure 22. Typical segregation pattern for an Al-6 wt.% Si EHD submicron powder (1 μm>2r_o>0.5 μm) showing 3 distinct regions. The initial "rapid solidification" produces a supersaturated zone (A), which later breaks into cells (C) after the droplet recalesces. (B) is a transition zone where solute builds up in the liquid in front of the interface. The growth axis is close to a <111> direction.

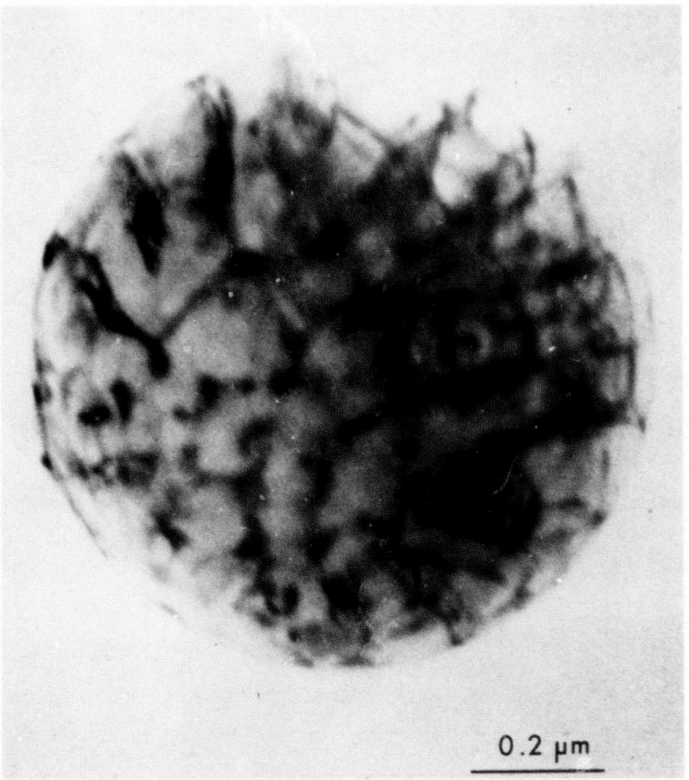

Figure 23. Cellular structures observed in Al-4.5 wt.% Cu EHD powders.

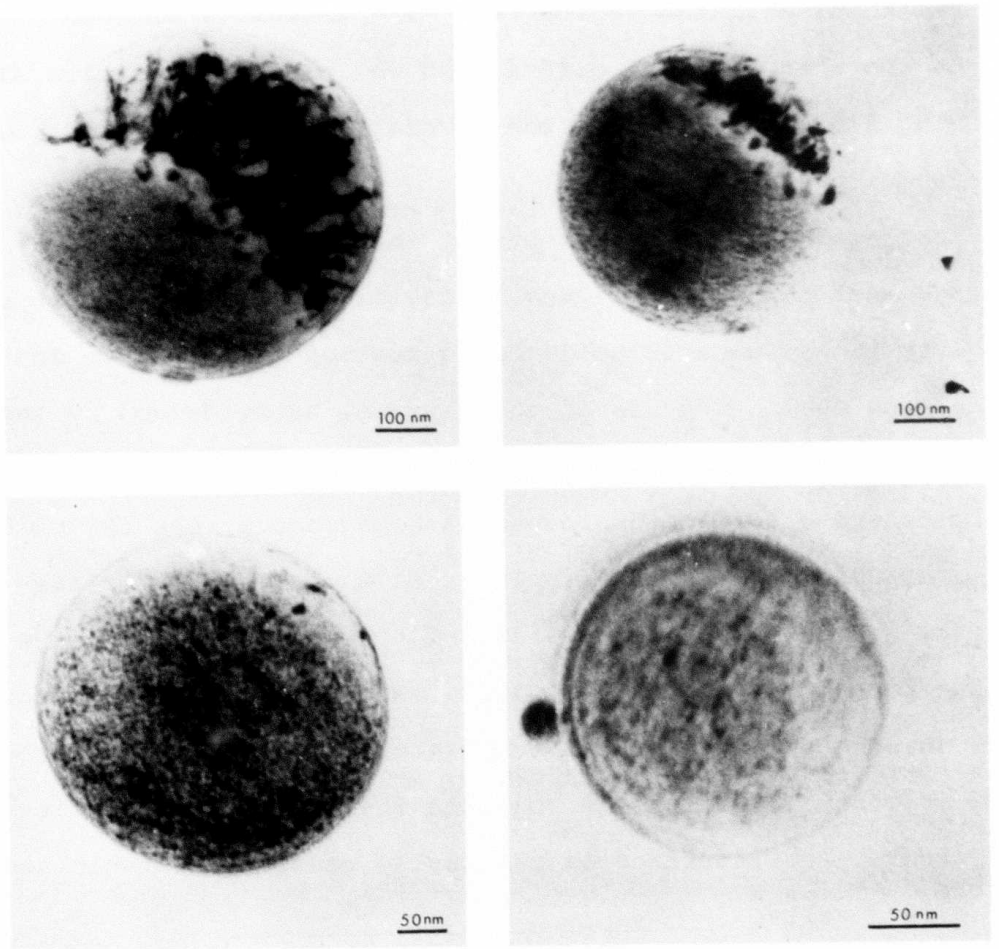

Figure 24. Transition from a partially segregated structure to a homogeneous one as powder particle size decreases in the Al-3 wt.% Si alloy. The diameters of the powders shown are (a) 570 nm, (b) 470 nm, (c) 220 nm and (d) 170 nm, respectively.

few segregates 24(c). At the lower end of the size distribution, the particles appear almost featureless 24(d), showing only the supersaturated region (A). The intensity of the silicon spots in electron diffraction was also reduced with diminishing diameter, although the crystallographic relationship noted above prevailed.

These microstructures reveal that substantial undercoolings must have been reached in the liquid droplets prior to solidification, which is believed to proceed as follows. In general, nulceation occurs at the surface, as evidenced by the growth direction. The subsequent "rapid solidification" into a highly undercooled liquid produces a homogeneous zone (A) of extended solubility. As the droplet recalesces, the interface velocity and undercooling are reduced, thereby decreasing the driving force for solute "trapping". When the interface temperature surpasses some critical temperature for the supersaturation process, T_C, solute is rejected ahead of the solidification front. The interface is eventually rendered unstable and breaks into cells.

The extent of homogeneous solidification can be rationalized in terms of the heat flow concepts previously discussed. Assuming that the thermophysical properties are reasonably constant, the behavior of an alloy growing in a plane front mode without solute partitioning is expected to resemble that of the pure metal.

The onset of segregation probably occurs at a temperature between the solidus T_S and the T_O curve. For purposes of illustration, we have arbitrarily assigned to T_O the average value of T_L and T_S from the Al-Si phase diagram, and estimated on this basis an upper bound to the hypercooling temperature T_H; see Table III. The lower bound to T_H corresponds to $T_C = T_S$. The values of Θ were calculated by substituting T_L for T_M in its definition and hence are proportional to the undercoolings. The values in this table indicate that dimensionless temperatures on the order of -1.18 ($\Delta T_N/T_L = 0.47$) and -1.36 ($\Delta T_N/T_L = 0.55$) may be necessary to eliminate segregation in aluminum alloys with 3 and 6 wt% Si, respectively. A large proportion of powders in the lower sizes experienced some segregation but no cellular breakdown. This phenomenon may simply reflect that the onset of segregation ($\Delta T^* < \Delta T_C$) occurred very late in the solidification process. ΔT^* refers to local undercooling at the liquid/solid interface in a general non-Newtonian heat flow model. On the other hand, interface breakdown may also be prevented by the stabilization of short wavelength perturbations due to surface tension effects as noted in an earlier section; the smallest perturbation that can grow is comparable to the particle size. High purity aluminum submicron powders, such as those in Fig. 25, do not exhibit any evidence of cellular structures that could have originated from thermal instability due to the negative temperature gradients in front of the interface. This observation lends support to the fact that the breakdown observed

TABLE III

EFFECT OF THE ALLOY COMPOSITION ON THE CRITICAL AND HYPERCOOLING TEMPERATURES†

		3% Si		6% Si	
		T	Θ	T	Θ
Liquidus	T_L	913	0	893	0
Critical	$T_C(T_O)$	848	-0.18	762	-0.36
	$T_C(T_S)$	782	-0.36	631	-0.72
Hypercooling	$T_H(T_O)$	484	-1.18	398	-1.36
	$T_H(T_S)$	418	-1.36	267	-1.72

†Estimated from the equilibrium phase diagram, T_S values are from the metastable solidus. $T_O = (T_L + T_S)/2$.

Dimensionless temperature $\Theta = C_L(T-T_L)/\Delta H_M$.

Figure 25. Typical structures in high purity aluminum (99.999%) submicron EHD powders. (a) shows a monocrystalline particle, and (b) a set of twin crystals.

in the alloys was mainly of constitutional nature. It could also be argued that thermal cells in a pure metal could be indistinguishable after solidification, unless they are decorated by impurities or strained areas caused by crystalline misorientations. Nevertheless, pure aluminum particles show some platelike features that can be interpreted either as clusters of impurities or vacancy condensation loops. The existence of denuded zones near the surface and crystal boundaries suggests that vacancies are involved in the formation of these features.

The microstructural analysis also revealed that most EHD powders are monocrystalline, indicating that nucleation was usually limited to a single event per droplet. A substantial proportion of them, however, consist of two or more crystals which could be either randomly oriented with incoherent boundaries, as in Fig. 26, or twins, as in Fig. 27. It was concluded that each random grain originates from an independent nucleation event, and its boundaries result from impingement with other growing crystals. On the other hand, twin crystals normally exhibit {111} coherent boundaries and it is unlikely that they were independently nucleated.

In summary then, the availability of submicron powders generated by the electrohydrodynamic atomization process has provided a suitable tool for fundamental solidification studies. In addition to having the potential to achieve substantial undercoolings prior to nucleation, these powders are electron-transparent and permit the microstructural examination of the

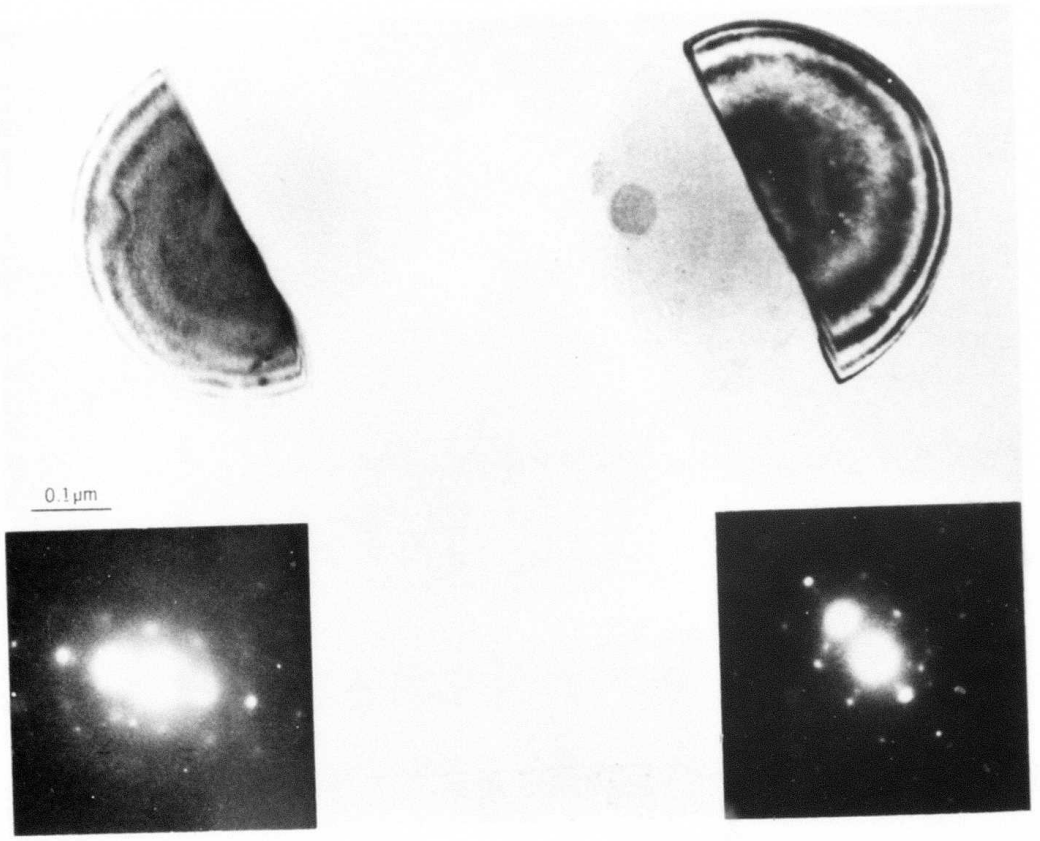

Figure 26. Typical polycrystalline powder of Al-3 wt.% Si alloy where two nucleation events occurred simultaneously in the droplet and formed an impingement boundary.

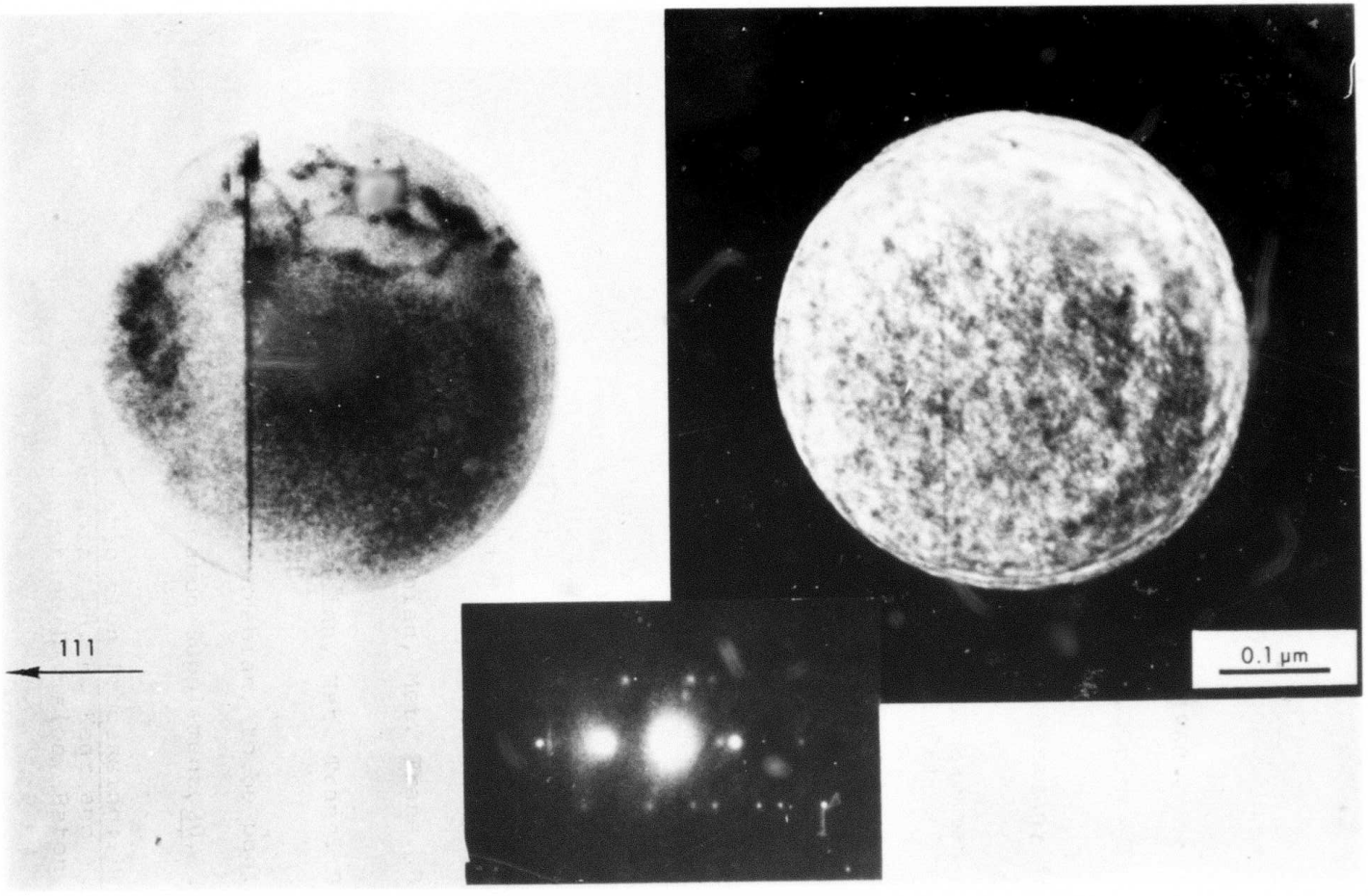

Figure 27. TEM of twin crystals in an Al-6 wt.% Si alloy powder. The segregation pattern suggests that nucleation occurred at a point on the line intersection of the powder surface and the twin boundary.

complete solidification structure of a small casting without thinning.

The investigation[18] revealed that decreasing the particle size - hence increasing the achievable undercoolings and liquid/solid interface velocities during growth - reduced the extent of segregation. The consequent supersaturation of the primary phase eventually results in homogeneously solidified powders with silicon contents as high as 6 wt%.

The observation of interface breakdown from planar to cellular in the middle of powder particles coupled with a solute depleted zone lends credence to the hypothesis that plane front homogeneous solidification was achieved due to the substantial undercoolings prior to nucleation and the high interface velocities during recalescence.

Some powders showed segregation but no cellular breakdown. This may be evidence of interface morphological stability due to surface tension effects, since the temperature gradient ahead of the interface is expected to be negative throughout solidification and therefore favor the growth of perturbations.

NONDESTRUCTIVE TESTING

A recent program at NBS co-sponsored by DARPA addresses the need for coupling of rapid solidification technology to nondestructive testing for on-line control of parameters during processing. Examples of fundamental studies in this area include:

The development of quantitative multichannel acoustic emission for monitoring the signals of cracks produced during surface modification by directed high energy sources, and

The development of ultrasonic scattering techniques for the characterization of metastable crystalline and glassy microstructures and their subsequent transformations into more stable structures during thermomechanical processing.

An example from the latter study on metallic glass ribbons of $Pd_{0.775}\ Cu_{0.06}Si_{0.165}$ alloy is given below. The objective of the investigation[46] was to study the crystallization kinetics of the ribbons (about 50 μm in thickness) by means of laser-generated and piezoelectrically detected, ultrasonic waves whereby the extensional wave velocity, and consequently the Young's moduli can be determined as a function of crystallization time. The amorphous-to-crystalline kinetics could thus be determined to a high degree of accuracy.

The inherent difficulty of measuring sound-wave velocities in thin ribbons was overcome by developing a technique whereby a load was applied on the specimen by means of rapid deposition of energy from a single-pulse of a Q-switched Nd:YAG laser. A state of unbalanced compressive thermal stress is produced. The stress gradient propagates along the ribbon in the form of an elastic wave. The piezoelectric crystal, at a distance from the spot where the laser radiation was deposited, detects the local displacement. Thus, the transit time of the

propagating wave could accurately be determined by means of a transient-pulse recorder. Results of the investigation[46] indicate that the transition from the amorphous-to-crystalline state in Pd-Cu-Si is time and temperature dependent, Fig. 28. The kinetics was determined at three isothermal-holding temperatures, and the activation energy for recrystallization was found to be 55 Kcal/mole. From the time dependence of the transformation kinetics an insight was gained into the nucleation and growth mechanisms. Corroborative metallographic evidence was found to be in qualitative agreement with the ultrasonic data, Fig. 29, suggesting a linear growth law whereby the crystallization front moves from the free surfaces toward the interior. The investigation[46] also revealed an initial increase of about 7.4% in the elastic modulus, out of 40% for the complete transition from the amorphous to the crystalline state. It appears that his initial increase can be related to a structural relaxation of the amorphous phase that may precede the crystallization process.

ACKNOWLEDGEMENT

This paper was written under the auspices of the DARPA Materials Research Council, Contract #MDA903-80-C-0505 with the University of Michigan.

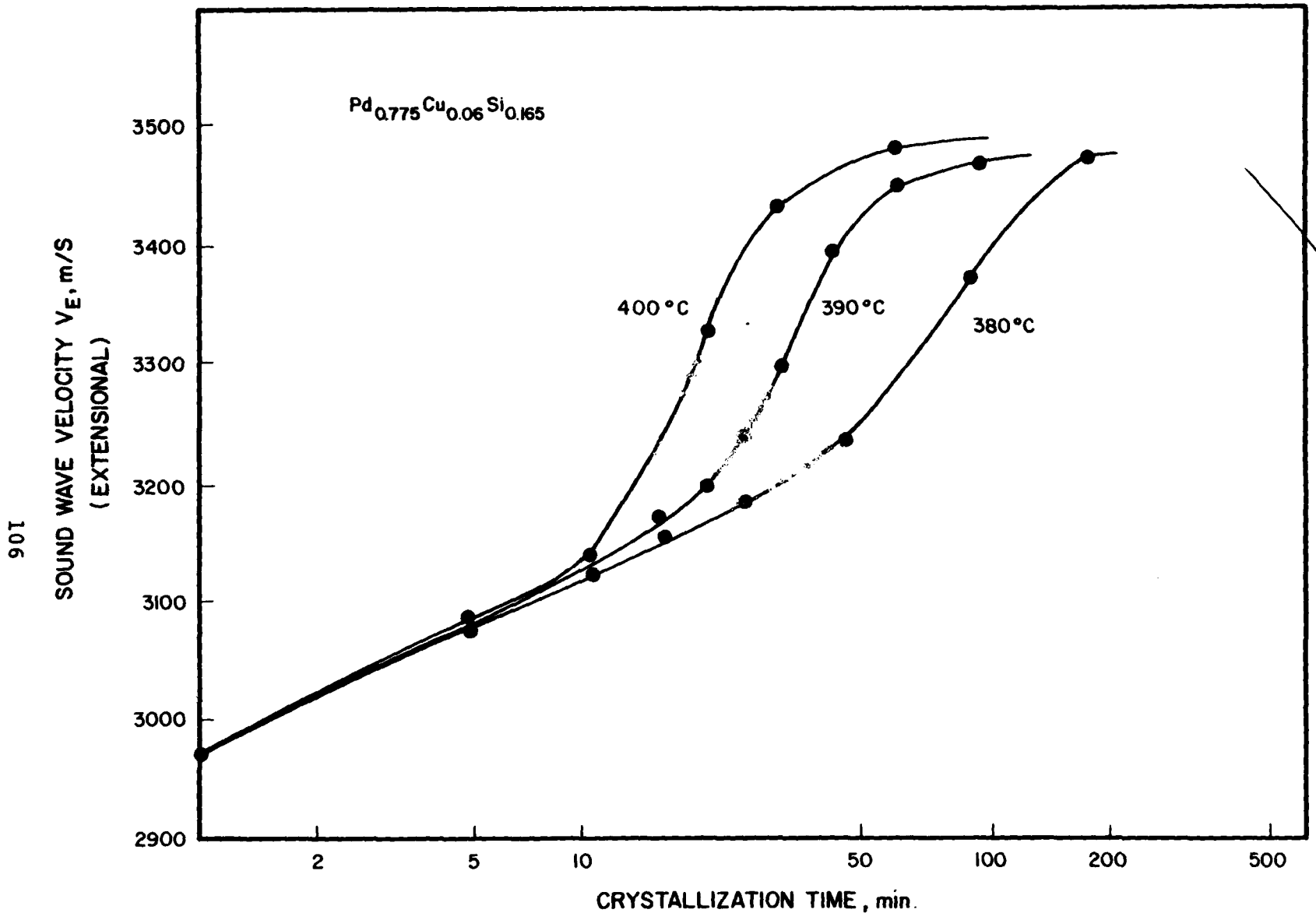

Figure 28. Variation of the sound wave velocity as a function of crystallization time during the amorphous to crystalline transition in Pd-Cu-Si at 380, 390, and 400°C.

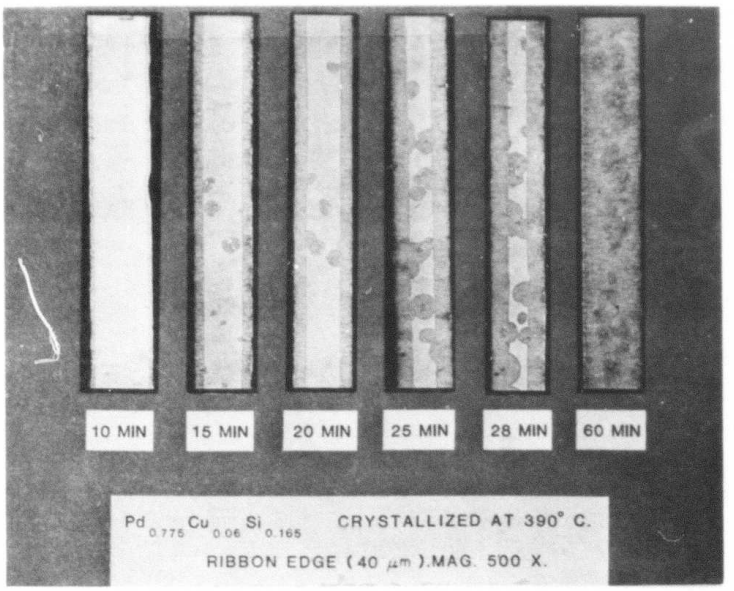

Figure 29. Changes in microstructure as a function of time during the amorphous-to-crystalline transition in Pd-Cu-Si at 390°C. View from the ribbon edge.

REFERENCES

1. J. L. Murray, Metallurgy Divison, National Bureau of Standards, private communication.

2. R. K. Linde, J. Appl. Phys. 31, 1136 (1960).

3. P. Predecki, A. W. Mellendore and M. J. Grant, Trans. Met. Soc. AIME 233, 1581 (1969).

4. D. R. Harbur, J. W. Anderson and W. J. Maraman, Trans. Met. Soc. AIME 245, 1055 (1969).

5. S. E. E. Ramati, G. J. Abbaschian, D. G. Backman and R. Mehrabian, Met. Trans. B, 9B, 279 (1978).

6. S. Hong, D. G. Backman and R. Mehrabian, Met. Trans. B, 10B, 229 (1979).

7. R. C. Ruhl, Mat. Sci. Eng. 1, 313 (1967).

8. P. H. Shingu and R. Ozaki, Met. Trans. A, 6A, 33 (1975).

9. D. R. Uhlmann, J. Non-Cryst. Solids &, 337 (1976).

10. F. Spaepen and D. Turnbull: Proceedings of Second International Conference on Rapidly Quenched Metals. Edited by N. J. Grant and B. L. Giessen, M.I.T. Press, Cambridge, MA, p. 205 (1975).

11. S. C. Hsu, S. Chakravorty and R. Mehrabian, Met. Trans. B, 9B, 221 (1978).

12. S. C. Hsu, S. Kou and R. Mehrabian, Met. Trans. B, 11B, 29 (1980).

13. S. Kou, S. C. Hsu and R. Mehrabian, Met. Trans. B, 12B, 33 (1981).

14. J. A. Sekhar, S. Kou and R. Mehrabian, to be published.

15. D. Rosenthal, Weld. J., Research Supplement 20, 2205 (1941).

16. R. Mehrabian, Rapid Solidification Processing: Principles and Technologies, R. Mehrabian, B. H. Kear and M. Cohen (eds.), p. 9, Claitor Publishing Division, Baton Rouge, LA (1978).

17. J. P. Hirth, Met. Trans. 9A, 401 (1978).

18. C. G. Levi and R. Mehrabian, submitted for publication to Met. Trans.

19. T. Z. Kattamis and R. Mehrabian, J. Vac. Sci. Tech. 11, 6, 1118 (1974).

20. J. H. Perepezko, D. H. Rasmussen, I. E. Anderson and C. R. Loper, Jr., Solidification and Casting of Metals, Proc. of Conference held at the University of Sheffield, July 18-21, 1977, p. 169, The Metals Society, London (1979).

21. J. H. Perepezko, Rapid Solidification Processing: Principles and Technologies II, R. Mehrabian, B. H. Kear and M. Cohen (eds.), p. 56, Claitor Publishing Division, Baton Rouge, LA (1979).

22. C. G. Levi and R. Mehrabian, submitted for publication to Met. Trans.

23. C. G. Levi an R. Mehrabian, Met. Trans. 11B, 21 (1980).

24. J. W. Cahn, W. B. Hillig and G. W. Sears, Acta Met. 12, 1421 (1964).

25. W. A. Tiller, K. A. Jackson, J. W. Rutter and B. Chalmers, Acta Met. 1, 428 (1953).

26. R. Mehrabian, Rapid Solidification Processing: Principles and Technologies I, R. Mehrabian, B. H. Kear, and M. Cohen, Eds., Claitor Publishing Division, Baton Rouge, LA, p. 7 (1978).

27. M. E. Glicksman and S. C. Huang, Rapid Solidification Processing: Principles and Technologies II, R. Mehrabian, B. H. Kear and M. Cohen, eds., Claitor Publishing Division, Baton Rouge, LA, p. 68 (1980).

28. W. W. Mullins and R. F. Sekerka, J. Appl. Phys. 34, 323 (1963).

29. W. W. Mullins and R. F. Sekerka, J. Appl. Phys. 35, 444 (1964).

30. R. F. Sekerka, Crystal Growth: An Introduction, P. Hartman, ed., North Holland, Amsterdam, p. 403 (1973).

31. R. T. Delves, Crystal Growth, B. R. Pamplin, ed., Pergamon Press, Oxford, 1, 40 (1974).

32. D. J. Wollkind, Preparation and Properties of Solid State Materials, Marcel Dekker, New York, 4, 111 (1979).

33. J. S. Langer, Rev. Mod. Phys. 53, 1 (1980).

34. S. R. Coriell and R. F. Sekerka, Rapid Solidification Processing: Principles and Technologies II, R. Mehrabian, B. H. Kear and M. Cohen, eds., Claitor Publishing Division, Baton Rouge, LA, p. 35 (1980).

35. R. F. Sekerka, Crystal Growth, H. S. Peiser, ed., Pergamon Press, Oxford, p. 691 (1967).

36. J. C. Baker and J. W. Cahn, Acta Met. 17, 575 (1969).

37. C. W. White, S. R. Wilson, B. R. Appleton, F. W. Young, Jr., J. Appl. Phys. 51, 738 (1980).

38. J. C. Baker, Ph.D. Thesis, M.I.T., Chapter V (1970).

39. J. S. Wey, K. A. Gautesen and J. Estrin, J. Crystal Growth 19, 169 (1973).

40. W. J. Boettinger, F. S. Biancaniello, G. M. Kalonji and J. W. Cahn, Rapid Solidification Processing: Principles and Technologies II, R. Mehrabian, B. H. Kear and M. Cohen, eds., Claitor Publishing Division, Baton Rouge, LA (1980).

41. W. J. Boettinger, submitted for publication.

42. J. Perel, J. F. Mahoney, P. Duwez and B. E. Kalensher, Rapid Solidification Processing: Principle and Technologies II, R. Mehrabian, B. H. Kear and M. Cohen, eds., Claitor Publishing Division, Baton Rouge, LA (1980).

43. K. M. Entwistle, P. Fuller and I. Brough, Acta Met. 26, 1055 (1978).

44. L. F. Mondolfo, Aluminum Alloys: Structure and Properties, p. 373, Butterworths, London, England (1976).

45. H. Matyja, K. C. Russel, B. C. Giessen and N. J. Grant, Met. Trans. 6A, 2249 (1975).

46. M. Rosen, H. N. G. Wadley and R. Mehrabian, submitted to Scripta Met.

AMORPHOUS POWDERS VIA THE P&WA RSR PROCESS

R. J. Patterson, II

For almost two years, amorphous materials have been produced in the form of gas quenched powders using the P&WA RSR process. Major objectives of the internally funded work have been to extend our knowledge of the capabilities and limitations of the process and to apply that understanding toward possible process improvements. The amorphous alloys are an extremely useful tool in this evaluation because; 1) the existence of the amorphous state is now easily and readily verified by techniques such as DSC, TEM, and X-ray diffraction, and 2) the alloys provide a simple "yes-no" condition. That is, one must quench from the liquidus to the glass transition without nucleation and growth if the powder is to be amorphous, and thus a powder particle will either be amorphous or it will be crystalline. The fact that we do not have to be concerned with varying degrees of supercoolings which vary with quench rate, and hence, particle size, vastly simplifies the investigation.

Two systems have been used in the effort: FeBSi (c.f. Luborsky et al., IEEE Trans. Mag., Sept. 1979) and NiBSi (c.f. Donald & Davies, J. Mat. Sci. 15, (1980), pp. 2754-2760). Major findings to date include the following:

1. The original device, utilizing a high velocity annular gas jet designed to clear the outer edge of the turbine housing, apparently had an abnormal "hot zone" around the atomizer

approximately 11 inches in diameter, resulting in reduced quench rates for particles solidifying within this zone. This has been solved with the new gas manifold incorporated in the helium recirculator added to the machine last year. This manifold utilizes sets of swirl nozzles which provide greater quench gas into the immediate vicinity of the atomizer.

2. Unlike melt-spun foils, residual strain in the powder particles does not seem to be anisotropic (or perhaps it is radially anisotropic).

3. Unlike the results reported by Berkowitz & Walter (Reston, 1980), no substantial variation in the magnetic Curie transition has been found. They reported a variation for powder produced by the spark discharge (EDM) technique on the order of 2°C per micrometer of particle diameter. The RSR powders show Curie transitions, essentially identical to those reported for melt-spun ribbon, which may show a variation on the order of 0.02°C per micrometer of particle diameter.

4. The thermal stability of the RSR produced powders does seem to show substantial variation with particle size. In the Ni-base system, for example, the alloy studied shows that at about 413°C, the -15+10 mm size fraction requires about 70 minutes for onset of crystallization while the -65+55 mm fraction requires about 42 minutes.

The latter two findings are of interest because of speculation that amorphous materials quenched at different rates might show differences in their thermophysical properties. We

should also point out that these studies indicate something about the time at which the powder is at temperature while in the collection canisters on the machine. Finding 4, for example, indicates that the powder has seen temperatures at or below about 400°C for times less than an hour. Future studies with less stable alloys are expected to refine this figure.

Major problems in this effort have been twofold. First, "proper" atomization (characteristic of, for example, superalloys and aluminum alloys) has yet to be achieved (believed due to excessive superheat prior to atomization). Second - and a problem widespread in rapid solidification work - is that the total lack of thermophysical properties makes it most difficult to correlate the experimental data with theoretical work in the areas of droplet production and quenching. Such properties include the variation of viscosity, density, surface tension, specific heat, and thermal conductivity with temperature and chemistry, and the variation of the latent heat of fusion with chemistry.

AN APPROACH TO ALLOY DESIGN BASED ON RAPID SOLIDIFICATION

Morris Cohen

Special attention is given here to the control and resulting role of second phase dispersions as obtained by rapid solidification processing. Although the present emphasis is on ferrous alloys, both austenitic and martensitic, it is evident that the principles involved can be applied to alloy systems more generally.

In most of the studies on rapidly solidified steels thus-far, a conspicuous resistance to austenitic grain growth has been noted, even on heating up to 1200°C for steels having normal austenitizing temperatures of about 900°C. This circumstance offers new opportunities for achieving superior combinations of strength and toughness in a wide variety of alloy compositions.

It is well recognized in physical metallurgy that precipitated particles can pin the grain boundaries of a matrix phase and thereby cause resistance to grain growth at elevated temperatures, whether during fabrication or heat treatment. Gladman[1] has derived the following relationship between grain size (2R) and second phase particles (volume fraction F_v and mean diameter $2\bar{r}$):

$$2R = \frac{\pi}{6} \frac{2\bar{r}}{F_v} \left(\frac{3}{2} - \frac{2}{Z}\right), \qquad (1)$$

in which Z is a measure of the grain size contrast between a

growing grain and the surrounding grains. Z can also be regarded as an adjustable parameter to fit experimental data; it is found that Z typically lies between 4/3 and 2. In this expression, 2R is a limiting grain size which reaches an interfacial tension balance with the interfacial tension represented by the second phase dispersion, and so results in minimum interfacial energy of the alloy system for any given F_v and $\bar{r}$ of the dispersion. The above equation assumes that the specific grain boundary energy of the matrix is the same as the matrix precipitate interfacial energy.

Clearly, then, the limiting grain size is smaller, the smaller the precipitate size and the larger its volume fraction. As it happens, rapid solidification favors both of these factors by making it possible to dissolve alloying components in the liquid state, which are relatively insoluble in the solid state, and then maintaining such phases in finely dispersed form when they are precipitated during, or subsequent to, the rapid solidification process. We have found, for example, that MnS (which often appears as undesirable inclusions in ordinary steels) can be tolerated in larger quantities--and in a beneficial way for pinning austenitic grain boundaries--as a result of rapid solidification.

However, in order to maintain a small grain size at very high temperatures, the ratio $\bar{r}/F_v$ must remain small, i.e., the second phase particles must resist coalescence (Ostwald ripening)

as well as resolution in the matrix phase. These interrelationships are reflected in the kinetic equation[2]:

$$\bar{r}^3 - \bar{r}_o^3 = \frac{8DC}{9R_gT}\,\sigma\, V_m^2 t, \qquad (2)$$

where r_o is the mean precipitate radius at zero time,

D is the diffusivity (in the matrix) of the rate-controlling specie,

C is the solubility concentration (in the matrix) of the rate controlling specie,

R_g is the gas constant,

T is the absolute temperature,

σ is the specific interfacial energy,

V_m is the molar volume,

t is the time at temperature T.

It is seen that, in order for $\bar{r}$ to be small, the initial precipitate size $\bar{r}_o$ must also be small. In addition, for $\bar{r}$ to remain small on heating at high temperatures, the temperature sensitive product DC should also be small. If the second-phase precipitate is designated as MX (e.g., MnS), then the precipitate coalescence will be controlled by D_XC_X if $D_XC_X < D_MC_M$, or by D_MC_M if $D_MC_M < D_XC_X$. This makes it possible, for a given precipitate stoichiometry, to alloy the melt in such a way as to minimize DC in Eq. (2) and, at the same time, to maximize F_v in Eq. (1). Helpful guidelines for achieving small C and large F_v are provided below by thermodynamic equations for the appropriate solid-solubility products.

Table I indicates the solubility products as a function of temperature of several second phase precipitates relative to the austenitic solid solution in steels. Experimental data are available in several instances, and the necessary interaction parameters are also available for computing the solubility products in similar cases. The agreement is only fair, but it is believed that the arrangement in Table I correctly establishes the order of decreasing solubility products. The previously mentioned MnS falls in the mid-range of the compounds listed, whereas TiN looks much more effective in terms of the alloy-design principles being discussed. That potential is now being investigated at MIT.

Although the control of second phase precipitates by rapid solidification processing has been directed here to grain size phenomena, it is also evident that the capability of achieving and maintaining fine second phase dispersions with large volume fractions are just what is needed for dispersion strengthening. Again, rapid solidification and the alloying guidelines being proposed here offer many new pathways for such alloy development.

ACKNOWLEDGEMENT

This technical note is based on ONR-supported research at MIT under Contract N00014-81-K-0013. The foregoing part of the work was carried out by Dr. H. C. Ling, now at Western Electric Engineering Laboratories, Princeton, NJ.

TABLE I

SOLUBILITY RELATIONSHIPS FOR VARIOUS
SECOND-PHASE PRECIPITATES IN AUSTENITE

	log [M w/o] [X w/o]	
Precipitate	Data from Literature	Calculations by H. C. Ling*
VN	-8330/T + 3.46	-7242/T + 3.32
Nb(C, N)	-6770/T + 2.26	-9516/T + 439
TiC	-7000/T + 2.75	-10470/T + 4.91
MnS	-9020/T + 2.93	--
AlN	-7500/T + 1.48	-12882/T + 5.09
TiB_2	--	-14964/T + 5.67
TiN	-8000/T + 0.32	-14990/T + 4.39

* See Acknowledgments.

REFERENCES

1. T. Gladman, Proc. Roy. Soc. A294(1966) 298.

2. S. K. Bhattacharyya and K. C. Russell, Met. Tran. 3 (1972) 2195.

ANALYTICAL ELECTRON MICROSCOPY IN RSP

H. Fraser

Rapid solidification is expected to lead to refined microstructures and increased homogeneity, and it is important to apply techniques that can probe structure and determine chemical changes on a very fine scale. These requirements are met in large part by analytical electron microscopy (AEM). The term AEM includes transmission electron microscopy (TEM), scanning transmission electron microscopy (STEM), energy dispersive X-ray spectroscopy (EDS), Auger electron spectroscopy (AES), scanning electron microscopy (SEM) and electron microscope analysis (EMPA).

While these various techniques have been well-developed, in the case of microchemical determinations of thin foils (typically achieved by the use of STEM coupled with EDS and/or EELS) there exists a major problem which prevents accurate analyses from being effected. Thus, there appear to be surface layers associated with electropolished metal foils. For example, in the case of Ni-based superalloys, small precipitates form on the surfaces of polished foils after a relatively short exposure to an intense electron beam. These precipitates have been identified as Al_3Ni_2 (from selected area diffraction analysis); clearly, the composition of these precipitates is markedly different from that of the "bulk" foil and an accurate determination of phase (e.g., γ/γ') chemistries is not possible.

Work is in progress aimed at determining the origin of these surface layers and establishing ways in which they may be avoided.

Three examples of the use of AEM in RSP studies are given:

ORIGIN OF MICROCRYSTALLINE POWDERS

The microstructure of RSR powder (produced at GPD-PWA, West Palm Beach) has been fairly widely studied. In general, two types of microstructure have been identified, namely dendritic and microcrystalline. AEM was usefully used in the following way; individual powders were thinned for STEM analysis and it was found that whereas the dendritic structures were heavily segregated (as expected), the microcrystalline material exhibited very small amounts of elemental segregation. The experimental observations on this type of powder may be summarized as follows:

1. The population of microcrystalline material increases with decreased powder size (and therefore increased cooling rate).
2. There are a large number of equiaxed grains.
3. Solidification is effected in an essentially segregation free manner. Calculations for pure Ni have been carried out assuming homogeneous nucleation (B-D), Newtonian cooling, and a growth equation which includes a curvature term to account for the very small size of nuclei

at large undercoolings. The results show a dramatic increase in the number of grains expected for powder less than ~20 μm in diameter. Furthermore, the undercooling necessary to permit homogeneous nucleation to occur is close to that for hypercooling; in this way it may be possible to account for the observed segregation-free solidification.

IN-SITU RAPID SOLIDIFICATION STUDIES

Alloy powders produced by electrohydrodynamics (EHD) are often sufficiently small to permit direct imaging using transmission electron microscopy. When supported on a thin carbon film, it is possible, then, to make studies of the as-solidified microstructure without resorting to complicated specimen preparation techniques. In the present set of experiments, these studies have been carried one step further, where the electron beam has been used to melt powders in situ, and, by shifting the electron beam, the powders have again been rapidly solidified. Since the carbon film provides conductive cooling not afforded by the EHD process, the cooling rates are somewhat faster, and in this way, it has been possible to produce a supersaturated solid solution of 30 at% Ge in Al. AEM is used in effecting the identification of phases, present in these powders.

PRODUCTION OF A FINE DISPERSION OF Y_2O_3 IN Ti ALLOYS

There have been several attempts using conventional processing to produce a fine thermally stable distribution of Y_2O_3

in Ti alloys to impart elevated temperature strength. It is felt that this may be achieved using RSP, and as a preliminary set of experiments, laser surface melting of a Ti-8Al-4Y alloy has been performed. Initially the arc-melted microstructure has been fully characterized, and is found to contain interdendritic regions of Y_2O_3. Within the dendrites, there are small (~1000Å) particles the nature of which have not yet been identified, but AEM analysis reveals that they are rich in Y. The as-rapidly solidified microstructure shows a marked refinement of the interdendritic phase, and a matrix consisting of lath martensite. An interesting observation concerns the dispersion of a very fine phase (~100Å diameter), often lying on the lath interfaces. These phases are found (by AEM) to be rich in Y. Further work involving the possible refinement of dispersion of Y-based phases using RSP is in progress.

DISCUSSION

John B. VanderSande

In the quest for novel alloys and microstructures, little emphasis has been placed (at this conference) on the possibilities for precipitation hardening of austenitic steels. Nick Grant at M.I.T. has some preliminary observations on Ti and C additions to 316 stainless steel. Precipitates of TiC with approximately 140Å diameter are uniformly distributed after extrusion of RS flakes. The room temperature and elevated temperature properties are greatly improved compared to compositionally conventional 316 stainless steel. The possibility of adding elements to the melt which produce fine, stable precipitates in the powders or flakes after consolidation, should be pursued in order to improve low and high temperature mechanical properties of austenitic steels.

Observations on fcc and bcc stainless steel powders routinely show a high dislocation density which is inherited from the solidification process. The origin of this high dislocation density has not received very much attention. Surely this dislocation substructure may play an important role in the development of the final microstructure of the alloy after consolidation. These inherited dislocations may, after rearrangement, contribute to the development of the observed fine grain size and/or act as important heterogeneous nucleation sites for precipitation and otherwise influence phase transformation kinetics.

The thought of adding relatively small amounts of elements which can be kept in the liquid state and which can form stable compounds (oxides, carbides, sulfides, nitrides) to act as durable grain boundary pinning phases in steels, deserves careful consideration. Since bcc metals show such a strong grain size dependence in their mechanical properties, efforts to obtain and retain fine grains in steels constitute an important research area. The possibilities of improving room temperature mechanical properties "across the board" by grain refinement and inhibiting grain growth during heat treatment is an exciting prospect.

Much effort, time, and money is being expended to rapidly solidify materials. However, only a fraction of that effort is being directed toward research on the consolidation variable. The benefits in refined microstructures which RS produces may be lost by the coarse way in which materials are consolidated. Most of us are happy to get powder, flakes, etc. into three-dimensional form so that we may test our materials. Seldom do we have the control over this consolidation variable, to know if it has been optimized.

DARPA would do well to set aside some funding so that worthy projects might investigate dynamic (low T) compaction routines for promising alloys. A blanket funding for CERAC, for instance, similar to the early blanket funding of P&WA, W.P.B., for RS powders, might be in order.

Some of the results presented at this conference, where particle size did not seem to influence properties, might be the consequence of the consolidation variable overwhelming the RS microstructure. Additionally, some materials may show metastable microstructures only at certain particle sizes (as we have observed in 303 S.S.). It is for that particle size fraction that novel compaction routines might be more profitable in producing novel end-product properties.

SUMMARY OF STRUCTURE/PROPERTIES TALK

J. C. Williams

INTRODUCTION

Powder metallurgy, especially using rapid solidification technology (RST), can provide opportunities for new or improved alloys. These opportunities can somewhat arbitrarily be stratified into three groups as follows:

1) RST provides the opportunity to make components from alloys which are not very workable.
2) RST provides the opportunity to make alloys which cannot be made by ingot metallurgy.
3) RST provides the opportunity to create entirely new/novel microstructures when coupled with novel consolidation processes.

These opportunities, especially the latter two, provide enormous potential for the metallurgical and the solid mechanics communities to work together to synthesize microstructures which have improved properties.

However, with these opportunities are a number of legitimate questions including the following:

1) What structures and compositions are really attractive?
2) If the new class of materials are stronger, how can we design with them to minimize loss of damage tolerance?
3) Can the microstructure be manipulated to improve damage tolerant properties without impairing the other property improvements?

4) Can we extend the potential of RST still further by combining the intrinsic microstructural refinement with novel processing to achieve an entirely new class of materials?

In this summary, selected examples which illustrate both the advantages and difficulties of RST powder products will be described. These are not exhaustive or complete, but do provide some concrete examples regarding structure and properties in this class of materials.

RESULTS

The examples which will be described below represent three classes of alloys; those based on Ni, Al and Ti. Each has its own characteristics, areas of competitive advantage and shortcomings. As a result, each class will be discussed separately.

Ni-Base Alloys

The Ni-base alloys discussed here are those belonging to the high Mo group of Ni-Mo-Al-X alloys, where X can be W, Ta, Nb or other elements. These alloys are always used in the directionally recrystallized condition and are characterized by extremely high creep strengths compared to the best conventional alloys, e.g. D.S.Mar-M-200+Hf. The source of the high creep strength in these alloys is not clear at this juncture, but several interesting microstructural-related observations are worth mentioning. First, because of the high Mo content of these alloys and because the Mo is a large atom which partitions away

from the γ' phase, the γ/γ' misfit in these alloys is negative (i.e. $a_0^{\gamma'} < a_0^{\gamma}$), whereas it is positive or zero in conventional superalloys. Second, the high Mo content in these alloys, coupled with the partitioning of Mo to the γ phase leads to the formation of one or more additional Ni-Mo ordered phases. These are based on Ni_2Mo (Pt_2Mo prototype structure) Ni_3Mo (DO_{22} structure) and Ni_4Mo (Dl_a structure). Third, these alloys exhibit a significant tendency for microstructural instability at elevated temperatures. For example, significant cellular or discontinuous coarsening of the γ' phase is observed to initiate at grain boundaries during prolonged elevated temperature exposure. Another elevated temperature instability which occurs is formation of high aspect ratio phases. Currently they have been shown to be the non-coherent equilibrium versions of Ni_2Mo and NiMo, both of which have an orthorhombic structure. Further work is continuing in this area.

Since the current plan is to use these alloys in the directionally recrystallized (DR'd) condition no grain boundaries will be present. Thus the extent to which the cellular coarsening reaction poses a problem is not clear because it is not well-known if this reaction will initiate within the grains if there are no grain boundaries present to accelerate the onset of the reaction. The formation of high aspect ratio phases is a source of ongoing concern and the current trends in alloy development are to reduce the Mo content so as to reduce the driving force for formation of these phases.

The analysis and characterization of these new alloys has been aided significantly by the use of Scanning Transmission Electron Microscopy (STEM). This technique permits the solute partitioning to be rapidly measured in a semi-quantitative way. This is important because the high Mo concentration tends to affect the way other elements such as Ta, Cr and others partition. Quantitative analysis with STEM is fraught with problems as was described by Fraser in another talk at this session. Despite this the semi-quantitative STEM analysis which can be done fairly routinely provides useful guidance in selecting alloying elements and their concentrations.

Conventionally atomized Ni base alloys were not discussed in the talk due to time limitations but it is worth noting that RSP turbine disks are currently being manufactured by both large U.S. engine companies. One serious failure has been encountered in an as-HIP'd powder turbine disk from a military engine. It has not been possible to determine the exact nature of this failure but it is most likely to have been caused by low cycle fatigue. Renewed consideration is now being given to whether as HIP'd or HIP + forged disks are the most suitable. This area of concern may not bear any direct relationship to RSP technology but is certainly a potential problem in the performance of all powder metallurgy products. The central question is whether consolidation such as HIPing leads to adequate product integrity or if more vigorous mechanical working is required to ensure particle-particle bonding or to more finely distribute any other

defects which may be present. This is an area of study where more systematic investigation is clearly warranted.

Al Alloys

The Al alloys discussed here are those which are strengthened by dispersoids of intermetallic compounds such as Al_6Mn or $Al_{10}Mn_3Si$. These alloys are attractive because they exhibit improved elevated temperature strength up to ~250°C. Another class of alloys which is also very interesting is the high modulus alloys based on Al-Li. These alloys will be described in a separate presentation by I. Palmer. The alloys are fabricated from air atomized powder by hot pressing and then extruding. The hot pressing temperature is always higher than the extrusion temperature and thus tends to fix the microstructural scale by controlling both the subgrain size and the coarseness of the dispersoid. The strengths of alloys hot pressed at ~400 and ~500°C differ by ~20%. It is also interesting to note that the observed yield stress is the combined result of dispersoid strengthening and substructure strengthening, but the larger contribution to strength is due to the dispersoid. The tensile ductility is very good, especially in comparison with other dispersion strengthened alloys such as Thoria dispersed Ni. The reasons for this appear to be related to the strong interfaces between the dispersoid and the matrix in the Al alloys. In support of this, TEM observations within the neck of a tensile specimen show no voids at the dispersoids even when the strain is ~.35. By contrast, the larger particles which are occasionally

found in this material crack at relatively low strains and these cracks then propagate into the ductile matrix to form voids. Other sources of fracture initiation in these materials are oxide particles. These are especially prevalent in air atomized powders. These lead to early formation of voids which then link together by shear cracks to produce failure. It is interesting to note that fractographic examination of failed specimens shows that small microvoids have formed during final fracture. The mechanism of formation of these is worthy of more detailed consideration. For example, is there a size effect with respect to the case of void formation at particle/matrix interfaces? If so, what are the governing factors (if any) in addition to size?

Finally, the fatigue properties of the dispersion strengthened RSP Al alloys are interesting. Based on the limited data available so far, it appears that the smooth bar fatigue strength of these alloys at 10^7 cycles is consistently > 0.7 of the yield strength, whereas it is typically < 0.5 for precipitation hardening alloys such as 2024 or 7075. In contrast the cyclic stress intensity for fatigue crack growth is very low ($\sim 1.5\text{-}2 MNm^{-3/2}$) compared to typical values reported for heat treatable alloys. However, there have recently been extensive discussions regarding the role of residual stresses generated during quenching after solution treatment on fatigue crack growth rate threshold. In this regard, the dispersion hardened alloys do not have the same thermal history and may therefore be nominally free from residual stress. Very recent threshold measure-

ments in 7000 series alloys which have been stress relieved have produced values in the 2-3 $MNm^{-3/2}$ range which supports this suggestion.

Titanium Alloys

Considerably less effort has been expended on RSP Ti alloy powder metallurgy and what work has been done has been confined to products made from rotating electrode process (REP) powder or powder made by variants of REP. The work has also been confined to alloys which have been successfully made by ingot metallurgy methods. Thus the benefits of the current Ti powder metallurgy effort must be economic rather than performance based. To date no convincing demonstration of the economics of RSP Ti powder based on REP (or variants thereof) has been completed. This is in part due to the nature of REP which requires a mechanically sound concentric bar for an electrode. A significant amount of value added labor is required in manufacturing this bar which is lost once the bar is atomized by REP. In the opinion of the author, a more productive approach to Ti RSP powder lies in direct atomization of the liquid metal. In the case of Ti, a skull furnace or some type of directed energy beam furnace will be necessary because of the extreme reactivity of the molten metal. If this can be accomplished then a broader scope of alloy compositions can be atomized and examined. In particular, there are a number of Ti eutectoid systems which might have the potential for elevated temperature strength. These have never been systematically investigated because they are potentially diffi-

cult or even impossible to cast into ingot by the conventional consumable electrode processes used in the Ti industry.

It is worth briefly reviewing the Ti RSP work which has been done because it demonstrates a potential benefit and a potential problem, the latter of which is not unique to Ti alloys made from RSP powder. Studies completed so far using Ti-6Al-4V have shown that P/M product did have a somewhat higher oxygen content as expected. Microstructural analysis showed that the P/M product had a somewhat finer grain size and a quick calculation suggests that this factor in conjunction with the oxygen content can account for the increase in strength. In addition to tensile data, tension-tension fatigue tests have been performed on both ingot and powder metallurgy products. These tests show that the fatigue strength of the P/M product is consistently much poorer than that of the ingot product and that the variability of the fatigue strength in the P/M product is extreme. Further, the difference in fatigue strength between powder and ingot products became greater in higher strength conditions. Metallographic examination showed a wide range of metallurgical defects in the P/M product. These were in part traceable to contaminants in the powder (Fe, Si, Ni, Co) and in part due to W contamination of the powder which is intrinsic to the REP. The latter type of defects have been removed by altering the REP machines to eliminate the W electrode, but the contamination problems are potentially still in existence. Fractographic examination of the failed fatigue specimens showed that those specimens with abnormally short fa-

tigue lifetimes all exhibited sub-surface crack origins. SEM/EDX analysis showed that each of these origin areas was contaminated with an impurity such as Fe, W, Si, Ni+Co, etc. This points out the need for more careful handling of the powder. It also raises an interesting but somewhat more fundamental question as will be described below.

Sub-surface fatigue crack initiation sites have been observed in Ti and Ni base RSP powder products. These cracks appear to initiate at small microstructural defects which are initially $\tilde{<}$ 20μm in diameter. Analysis of the growth of such a small flaw using linear elastic fracture mechanics is a questionable proposition. Thus a renewed effort to analyze the growth of small cracks would seem to be an appropriate undertaking for the mechanics community. Such an analysis is essential to any sensible scheme of lifetime prediction of fatigue limited components.

CONCLUSIONS & RECOMMENDATIONS

In view of the foregoing the following conclusions and recommendations are offered. Several general conclusions seem warranted first.

1. RST offers the opportunity for producing new alloys and microstructures from alloy compositions which are not considered producible by ingot metallurgy. The need for novel low temperature consolidation techniques is clear if the fineness of RSP powder products is to be fully retained.

2. The higher strengths of RSP powder products and the inherent possibility of defects leads to a defined need for better analytical techniques for predicting the behavior of small flaws.

3. New alloy compositions must be selected with metallurgical stability questions in mind, especially for high temperature applications.

4. The potential for microstructural design is significantly enhanced by the availability of RST.

With regard to the alloys and alloy systems described above several specific conclusions and recommendations can be offered.

1. The lack of detailed understanding of the high temperature (~1025°C) creep strength of Ni-Mo-Al-X alloys suggests that additional fundamental studies are needed.

2. The factors which promote stability of the various Ni-Mo ordered phases are not clear; accordingly work on simpler systems seems to be warranted.

3. The cause and nature of high aspect ratio phases and their effect on mechanical properties should be studied.

4. The propensity for formation of cellular coarsening within grains is not well characterized. This should be studied in view of the impact of this reaction on the performance of DR'd material.

5. The small dispersoids in Al-Mn and Al-Mn-Si alloys do not contribute to premature fracture by nucleating voids but the large ones do.

6. Air atomized Al alloys can contain sufficient quantities of Al_2O_3 to degrade properties.

7. Further studies of the relationship between dispersoid size and tendency for matrix decohesion should be conducted.

8. Lower temperature consolidation leads to better strength and ductility in dispersion strengthened RSP Al alloys.

9. RSP powder products of conventional Ti alloys do not exhibit remarkably better properties than wrought material.

10. The real potential for RSP Ti alloys is through new alloy compositions which will capitalize on the potential of RSP methods.

11. The low cycle fatigue debit in RSP Ti alloys is more obvious because wrought Ti alloys are essentially inclusion free.

MICROSTRUCTURE-PROPERTIES IN RAPIDLY SOLIDIFIED P/M Al-Li-X ALLOYS

R. E. Lewis and I. G. Palmer

New P/M techniques using rapidly solidified particulate are being used in an effort to overcome the problems which have been experienced with conventional ingot cast Al-Li alloys, in particular low ductility and low fracture toughness. The program (Contract F33615-78-C-5203) is sponsored by DARPA, Materials Sciences Division, and managed by the Materials Laboratory, AFWAL. The objective is to develop alloys meeting certain room temperature property goals. The most significant microstructural features of the alloys, and their correlation with mechanical properties were described. Some of the work was performed at LPARL and some at Georgia Institute of Technology, on subcontract to LPARL.

Oxide Particles

The distribution of oxide particles was revealed by etching in hot bromine/alcohol solution. In alloys made from splat particulate the distribution of oxide particles on prior flake boundaries was clearly revealed. Increasing the extrusion ratio from 8:1 to 20:1 improved the distribution of particles. No significant improvement was observed in longitudinal tensile properties, however it is expected that transverse properties will be improved by the higher extrusion ratio. Improved distribution of oxide was also seen in alloys made from fine atom-

ized powders, together with slightly improved longitudinal tensile properties.

Constituent Particles

In the Al-Cu-Li alloys investigated, the use of rapidly solidified particulate produced significantly fewer constituent particles than in ingot cast alloys of similar composition. However in the Al-4Cu-3Li P/M alloys the high volume fraction and brittleness of the particles resulted in low tensile ductility. The best tensile properties were exhibited by the Al-3Li-2Cu alloy which contained the smallest amount of undissolved second phase.

Dispersoid Particles

Significantly finer dispersoid particles were obtained than in ingot cast alloys of similar composition. The extended solid solubility achieved by the rapid solidification also allowed higher volume fractions of dispersoids to be obtained. The dispersoid particles have two beneficial effects (1) to inhibit the localization of slip which occurs in ingot cast Al-Li alloys and which leads to low toughness, (2) to stabilize a very fine grain size which should increase both strength and toughness.

Precipitate Particles

In the Al-Li-Cu and Al-Li-Cu-Mg alloys, prestraining followed by aging resulted in finer and more uniform distributions of θ' and S' precipitates. This produced a significant increase in yield strength with only a small decrease in elongation.

Precipitate Free Zone

The increase in precipitate free zone width with increase in aging time results in slip localization occurring within the precipitate free zone and low ductility intergranular failure, especially in the overaged condition. Prestraining followed by aging results in a decrease in the precipitate free zone width for the θ' and S' precipitates, and a consequent improvement in ductility.

Grain and Subgrain Structure

Grain size and shape, degree of recrystallization, and texture were found to have significant affects on strength and ductility. The best properties were obtained in fully unrecrystallized microstructures. The most effective element for preventing recrystallization was found to be Zr. The dispersoid formed, Al_3Zr, is coherent and this is believed to be the reason for the more effective pinning of grain bounderies shown by this dispersoid.

The aspect (width/thickness) ratio of P/M extrusions was found to have a significant effect on strength and ductility, with the highest strength exhibited by axisymmetric extrusions, and the highest ductility by the most asymmetric extrusions. This effect is related to the degree and type of crystallographic texture developed in the different extrusion geometries.

Comparison With Other Data

Comparisons have been made of the tensile data obtained for the best alloys developed on this program, with the limited published data for Al-Li based alloys of similar lithium constant. At both the 3 wt.% Li level and the 1.5 wt.% Li level the P/M alloys showed equivalent or slightly better combinations of strength and ductility. The DARPA program alloy 1.12 (Al-3Cu-2Li-1M_g-0.2Zr) showed a better combination of strength and ductility than any other alloy.

I/M Versus P/M Al-Li Alloy Development

Improvements are being made in I/M Al-Li alloy development technology which are expected to lead to the development of I/M alloys having acceptable combinations of mechanical properties, at Li levels up to about 3 wt.%. However, improvements are also being made in P/M Al-Li alloy technology and it is considered equally certain that rapidly solidified Al-Li-X alloys will be developed having better combinations of properties than the I/M alloys, at both room temperature and elevated temperature. The situation is analogous to the development of the 7000 series alloys in which rapidly solidified P/M alloys (X-7090 and X-7091) are currently being developed by Alcoa, having better combinations of properties than the best available ingot alloys (e.g., 7475 and 7050). Thus although rapid solidification is not required to make 7000 series Al alloys, better properties can be obtained by use of this new technology.

DISCUSSION

Alan Lawley

Williams and Palmer have presented data/observations on powder processed Al-Mn, Al-Mn-Si and Al-Li alloys. We have recently completed a detailed study of the fatigue response of fully-dense high-strength P/M aluminum alloys (Al-Cu, Zn, Mg, Co) of compositions equivalent to ingot metallurgy 7075 and 7675. Particular emphasis was given to the interplay of the mode of powder processing and cobalt level on microstructure and load-controlled fatigue and resistance to fatigue crack progagation. The fatigue response has determined in air and salt-fog.

Briefly, in air the fatigue life of the P/M alloys was superior to that of the I/M material, Figure 1. This is attributed to the higher resistance to crack initiation in the P/M alloys and is the result of the fine grain size and relative absence of constituent particles in the matrix. Fatigue crack propagation rates in the P/M processed alloy are lower than in the I/M material at high levels of K but the behavior is reversed at low ΔK values, Figure 2. This can be explained in terms of the interplay of microstructural parameters (grain and subgrain size, dispersoids, precipitates, oxide content/ distribution, the cyclic plastic zone size and the density of secondary fatigue cracks.

The fatigue life of the P/M and I/M material suffered serious degradation in salt fog and is similar in both forms of

the alloy, Figure 3. Similarily, the fatigue crack growth rates increase significantly in salt fog compared to air for both P/M and I/M materials. Propagation rates in the P/M material are higher than in I/M material at high ΔK but the response is reversed at low ΔK. The presence of secondary cracks and a large grain size in the I/M alloy can explain the superior resistance to crack propagation in the ingot material at high ΔK levels.

Acknowledgement

This research was sponsored by AFOSR.

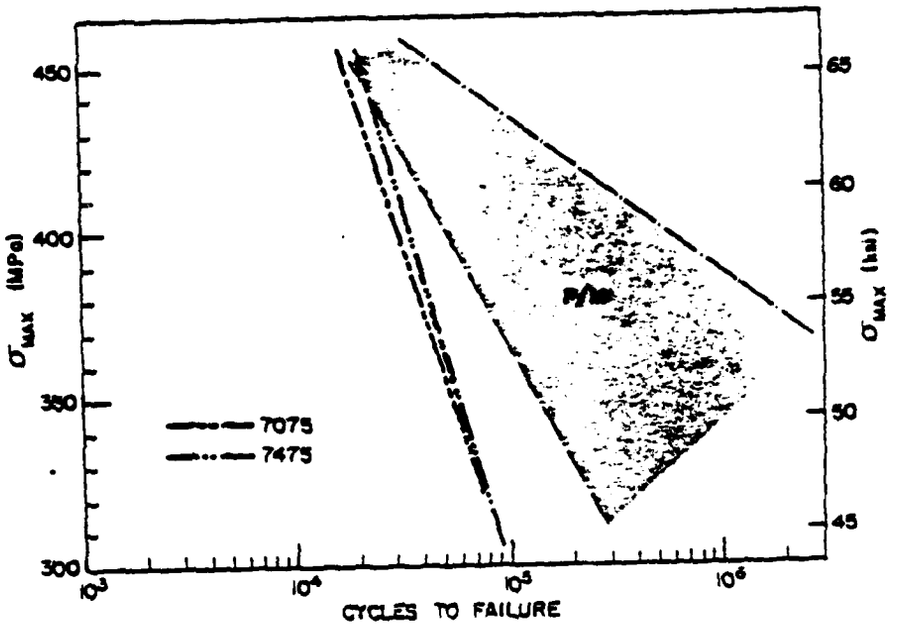

a

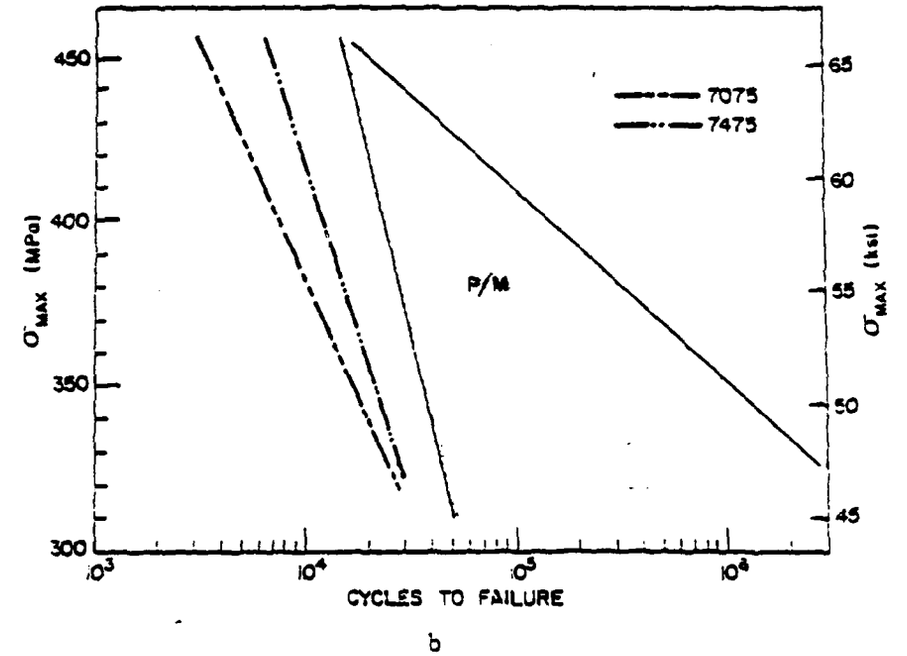

b

Figure 1. Comparison of S-N curves of I/M 7475 and I/M 7075 with P/M materials, tested in laboratory air. a) L orientation, b) ST orientation.

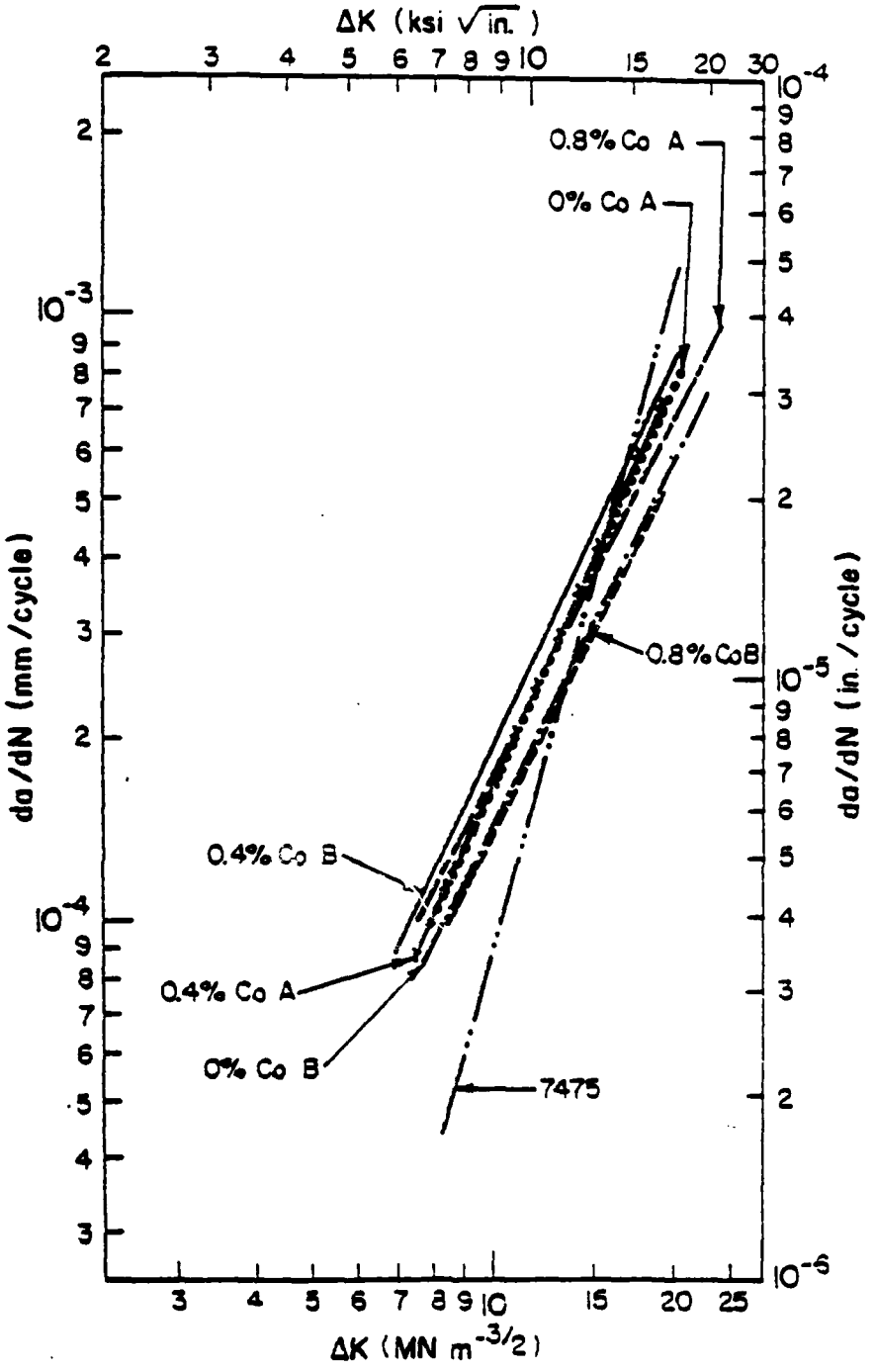

Figure 2. Crack Propagation rate as a function of ΔK in laboratory air for the L orientation; 7475 I/M, A = P/M A processing, B = P/M ABC processing.

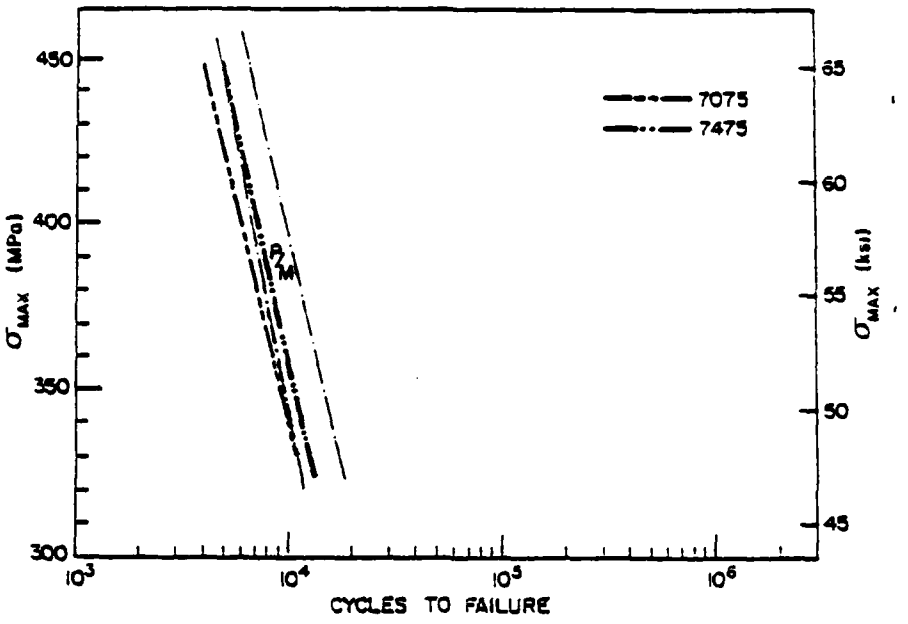

a

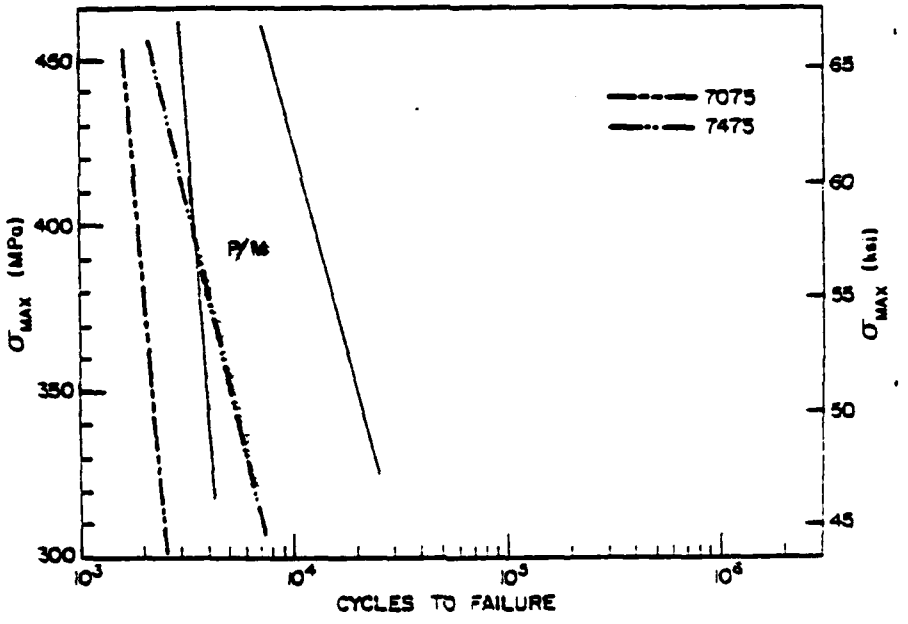

b

Figure 3. Comparison of S-N curves of I/M 7475 and I/M 7075 with P/M materials, tested in 3.5% NaCl solution salt-fog. a) L orientation, b) ST orientation.

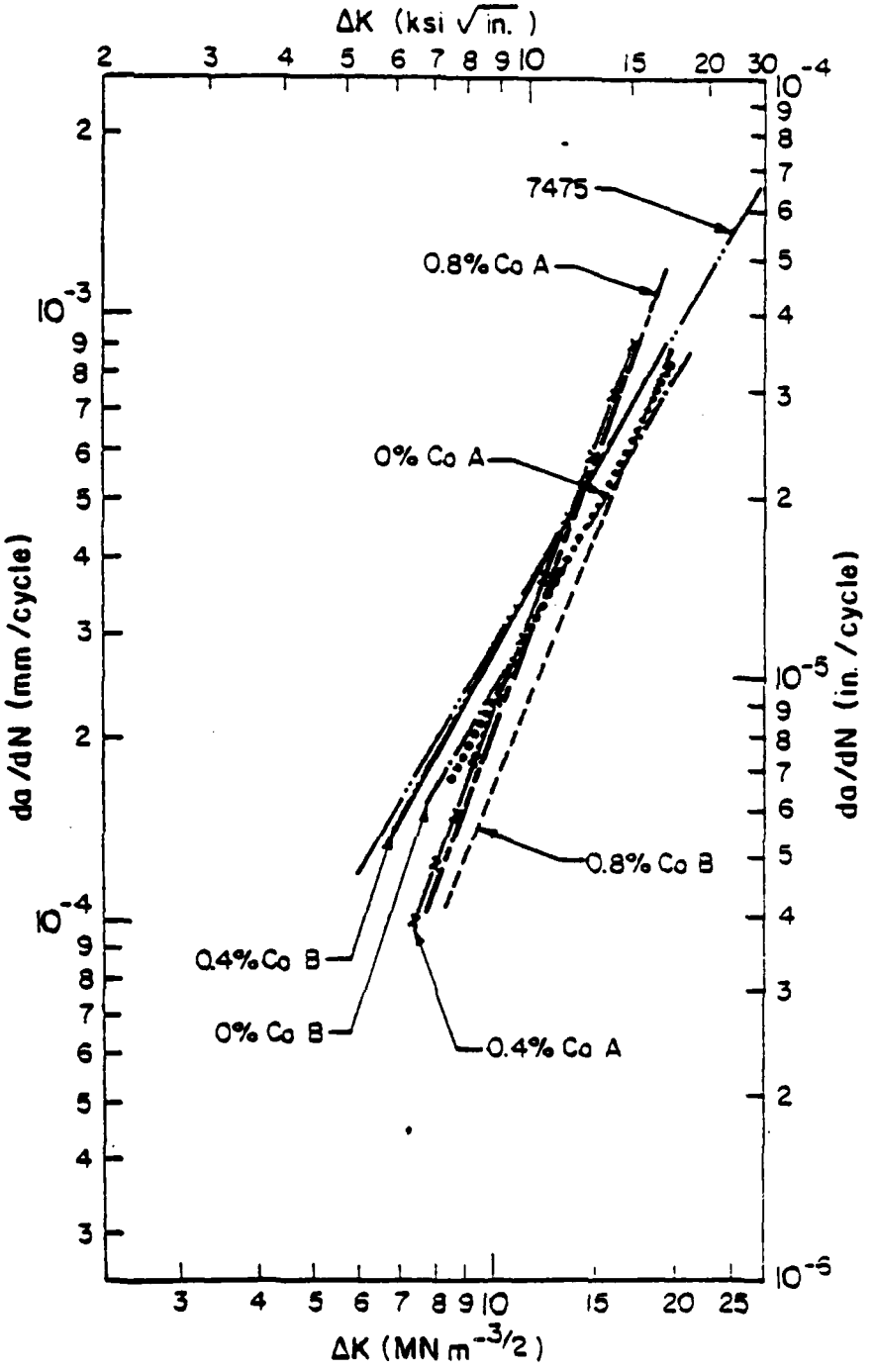

Figure 4. Crack propagation rate as a function of ΔK in 3.5% NaCl solution salt-fog for the L orientation; 7475 I/M, A = P/M A processing, B = P/M ABC processing.

COMMENTS

D. Apelian

In this discussion there are two points which I want to raise. (i) The need for fundamental research to better characterize and understand structure-sensitive properties, and (ii) the need to address the feasibility of alternative RST routes. These are further discussed below:

Structure-Sensitive Properties

The excellent review of the developments in RSR-185, Al-Mn, Al-10%Mn-2.5%Si and Al-Li alloys along with the Ti alloys presented by Williams and Palmer point out the need for fundamental research in several arenas:

a. Characterization and understanding of the crack propagation rate in rapidly solidified metals as a function of structural parameters is needed. Materials having different structures and/or processed at different cooling rates (i.e., P&W RSP and conventional P/M) need to be evaluated.

b. Low cycle fatigue properties of the above materials processed at different cooling rates need to be characterized, and the structural factors controlling or having a dominant effect on low cycle fatigue need to be understood.

c. The defect tolerance levels of RSR materials need to be addressed and understood. In addition to this, effort should be addressed towards cleaning the melt prior to atomization and "casting" using innovative processing technologies.

Alternative Processes

There are several other processing routes to achieve the over all goal of RST which need to be evaluated:

a. Low pressure plasma processing where the plasma source is used to "atomize" the injected powders which are then deposited on a substrate.

b. The Osprey process where the melt is atomized and the produced powders are directly deposited and compacted into a die. Subsequent inert forging can be done.

c. Fine grain ingot processing such as the drip casting process where macrosegregation is eliminated and undercooling and fairly rapid solidification rates in the ingot are achieved. The resultant ingot is subsequently processed (HIP + isothermal forge) and upon testing (United Technologies data) the properties are superior to those obtained from the same alloy processed via the conventional P/M route.

In these processes unique microstructures are obtained. Alloy development to take advantage of these processing routes should be carried out. Finally, the flexibilities offered by these various processes should be evaluated.

LONG TERM STABILITY OF HIGH TEMPERATURE ALLOYS

H. A. Lipsitt

The long term microstructural stability of RSR superalloys produced by Pratt & Whitney, Government Products Division, under contract to DARPA and AFWAL/ML has been continuously assessed since the inception of the program. Three types of instability are evaluated in these alloys. These are the precipitation of equilibrium phases upon long term exposure, perhaps these phases are TCP types; the general growth or Ostwald ripening of the γ' cuboidal precipitate; and cellular coarsening of the grain boundary γ'. The first of these can produce a sudden marked loss in ductility, and/or stress-rupture life although no such loss was determined in this case. The latter two processes will produce a slower, insidious and continuing loss of strength with time at temperature. Assessment is made initially for 250 hours at 1700°F since some early alloys in the program did precipitate a TCP phase, NiMo, in as little as 50 hours at 1700°F. Any alloy that is receiving closer scrutiny by P&W, GPD, is given a fuller assessment; 100, 500 and 1000 hour exposures at temperatures in the range 1600-2000°F.

The first major shift in the program was to reduced Mo content which eliminated the TCP phase and shifted the mechanism of coarsening to Ostwald ripening of the γ'. However, recent alloying additions of Cr, Ta, and Y have changed the coarsening

mechanism back to one of grain boundary cellular growth. Our studies indicate that this mechanism produces a considerable loss in yield strength and in ductility at temperature, since slip tends to become localized in the coarsened regions. The most recent RSR alloy to be investigated (RSR-606) fully was at least as unstable as the early alloy, RSR-185. Early stress-rupture data indicate that a low Mo version of RSR-606 containing only 5.2 a% Mo may have vastly improved stability as well as remarkable stress-rupture life.

Iron Aluminides

A brief presentation was made to show that, for reasons unknown, grain size control in RSR Fe_3Al is no problem whatsoever, whereas grain size control in cast and wrought Fe_3Al is extremely difficult. This is taken as an indication that something exists in the RSR prior particle boundaries which helps to control grain growth at temperatures below 1000°C. It was suggested that Al_2O_3 may form on the powder particle interfaces and serve to control grain size.

The point was made that such factors constitute extremely important technological differences between otherwise identical materials and that these factors should be isolated, studied, and used wherever possible. Tensile ductilities as high as 8% have been measured in stoichiometric Fe_3Al at room temperature.

POWDER ATOMIZATION SYNTHESIS OF ACTIVATED NICKEL-- A NEW ROUTE FOR PREPARATION OF SKELETAL CATALYSTS

F. D. Lemkey and C. Adam

Powder atomization procedures such as centrifugal (RSR), and hydrogen soluble (HMI) developed within UTC have recently demonstrated a promising route for the preparation of enhanced skeletal metal catalytic materials. Catalytic metals which can be synthesized include non-noble transition elements such as nickel, cobalt, iron, or molybdenum and noble elements such as platinum, palladium, rhodium, ruthenium, iridium, etc. in a highly dispersed state as either skeletal (Raney® type) or supported (metal/alumina or metal/silica) configurations.

Several DoD missions involving metal and metal oxide catalysts may benefit from these novel synthesis procedures, e.g. (1) upgrading hydrocarbon fuels, (2) contaminant removal in atmospheric control systems (space and submarine), (3) propellant (hydrazine and hydrogen peroxide) decomposition reactions, (4) fossil fuel combustion exhaust cleanup, and (5) selective hydrogenation catalysis in the synthesis of organic compounds of military significance.

There are some impressive economic advantages in preparing transition metal catalysts with improved specific catalytic activity providing sustained activity can be maintained. An example can be cited of the cost advantages for methanation of $3H_2/CO$ over an experimental UTRC activated nickel catalyst com-

pared with a currently available commercial Raney nickel based on small laboratory tests conducted at UTRC. Using a Detman type formula[1] we have calculated that synthetic natural gas would cost $3.29/10^6 Btu representing a cost reduction of 32 percent for a nickel methanation catalyst prepared from an activated proeutectic nickel-aluminum alloy synthesized by RSR atomization procedures compared with a cost of $4.85/10^6 Btu cited for currently available methanation catalysts[2]. Principle assumptions made in this calculation are that catalyst cost represented 20 percent of the total plant investment and that our experimental catalyst cost might be as much as three times that of currently available commercial nickel methanation catalysts. Observed methanation rate for our RSR activated nickel was twice that of a commercial Raney® nickel activated in the some manner and tested under the same conditions.

Nickel catalysts prepared by caustic activation of nickel-aluminum alloys synthesized by RSR and HMI atomization procedures have shown superior physical properties and outstanding catalytic performance for selected hydrogenation reactions compared with commercial cast and pulverized Raney® nickels (W. R. Grace).

In Table I a summary of results on the liquid phase hydrogenation activities of three activated nickels is presented. The superiority in reaction rate data for the RSR produced precurser for nickel compared to commercial Raney is impressive for this stage in their development.

TABLE I. Comparative Hydrogenation Reactivity of Catalytic Nickel Derived from DS Eutectic Alloys, RSR Proeutectic Powders and W. R. Grace Bulk Case Ni/Al Alloys.

	Hydrogenation Reaction Rate moles H Absorbed per g cat. per min.			Reaction Conditions		
Reactant	Fibrous Ni from DS Alloy 6.2 w/o Ni in initial alloy	RSR Powder 28.4 w/o Ni in initial alloy	W. R. Grace bulk cast alloy 50.2 w/o Ni in initial alloy	Temp. °C	Pressure Atmos.	Test Duration Min.
Acetone	280	226	180	22	0.86	10
Nitrobenzene	397	239	66	22	0.86	10
	722	1808	599	80	3.2	60
Itaconic Acid	186	225	90	22	0.86	10
Butyronitrile	142	242	11	22	0.86	10
Toluene	540	640	475	80	3.3-3.8	60
Dextrose	599	1246	271	80	3.2-3.5	60

The atomization procedures (HMI and RSR) provide unique control over size and amount of the peritectic Al_3Ni phase, which is known to be the most effective precursor of catalytically active nickel for hydrogenation reactions. In addition, the rapid solidification rates achieved in these atomization processes provide the small crystallite sizes of the Al_3Ni phase essential for production of large specific surface areas on the part of the nickel activated by caustic extraction of the aluminum matrix phase. This is shown graphically in Figure 1.

Another feature of catalytically active nickels prepared by these processes is the production of porosities and pore size distributions quite different from conventional Raney® nickels.

The nickel prepared from the RSR alloy shows a larger pore volume in sizes less than 100Å with a conspicuous maximum for pore sizes below 20Å.

Some examples of the physical properties, particularly total surface area, nickel metal surface area, porosity, pore size distribution, and the amount of residual aluminum after caustic activation are shown in Figures 2, 3, and 4. The activated nickel catalysts prepared from RSR nickel-aluminum alloys provide an unusually high porosity in large pores compared with W. R. Grace nickel catalysts. On the other hand, activated nickel prepared from HMI nickel-aluminum alloys provides unusually large surface areas in quite small pores.

These preliminary results indicate that atomized nickel alloys provide a unique new approach for preparation of a wide

Al_3Ni DENDRITE SPACING VS COOLING RATE

Al – 28.4 w/o Ni

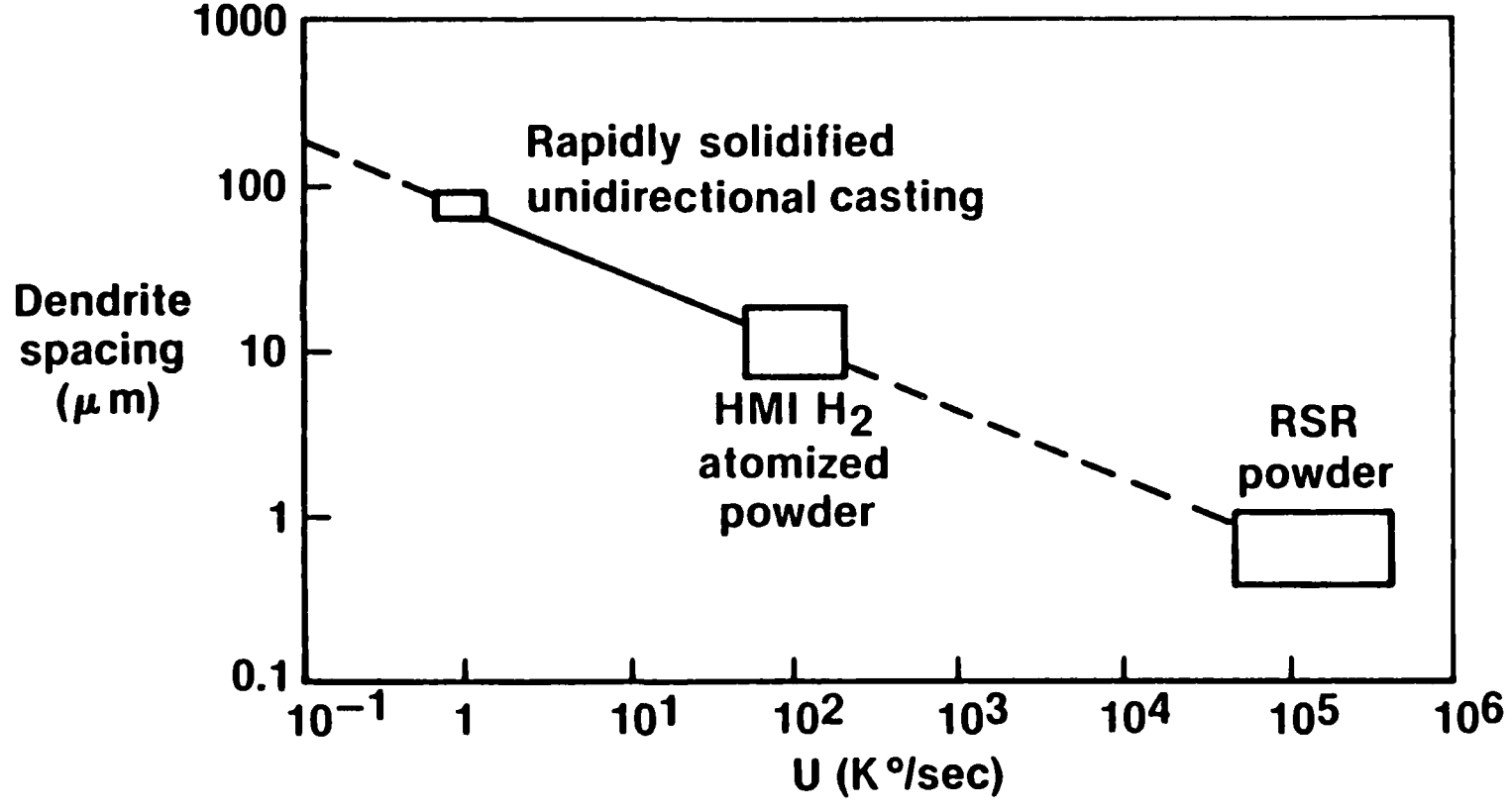

156

PORE VOLUME – PORE SIZE DISTRIBUTION

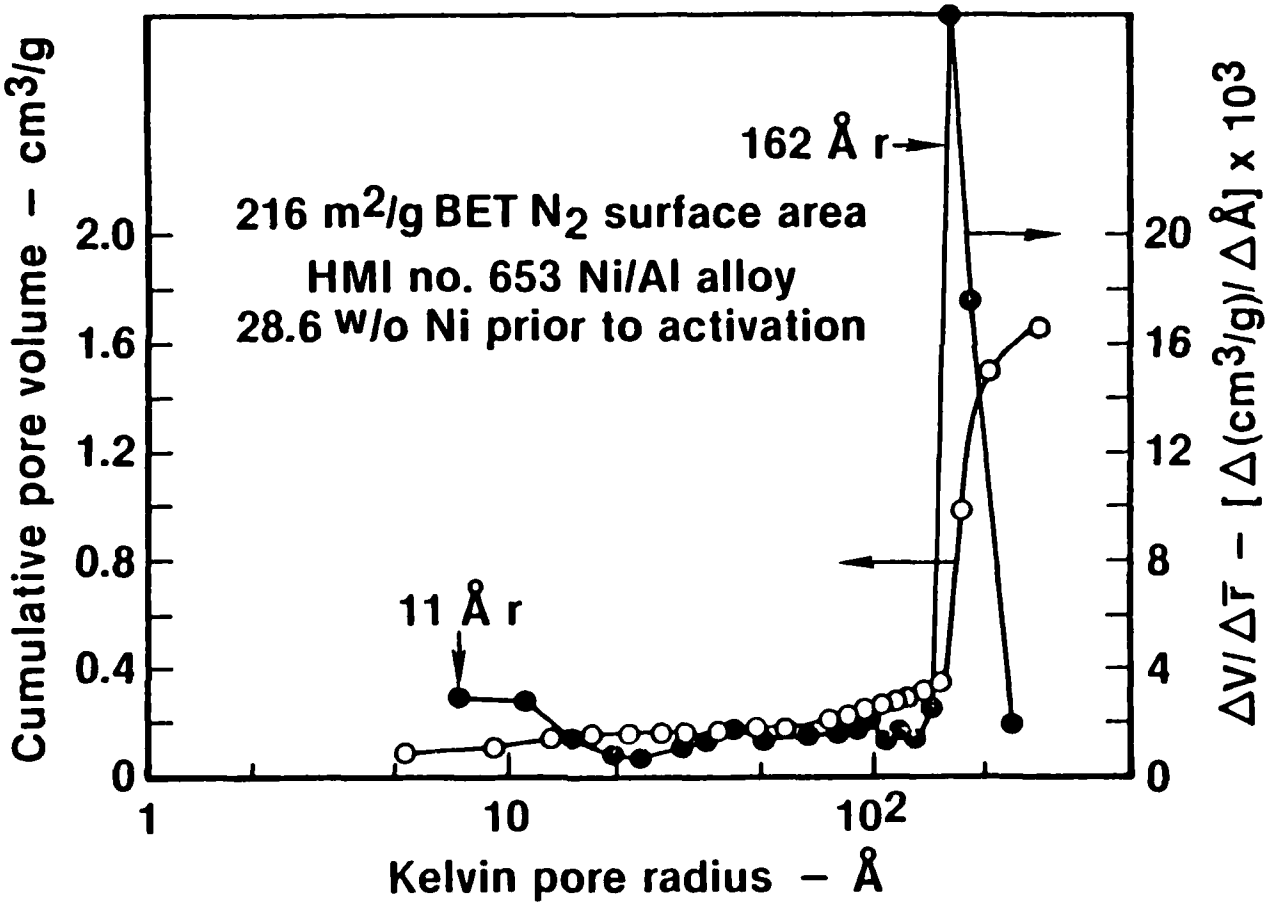

PORE VOLUME – PORE SIZE DISTRIBUTION

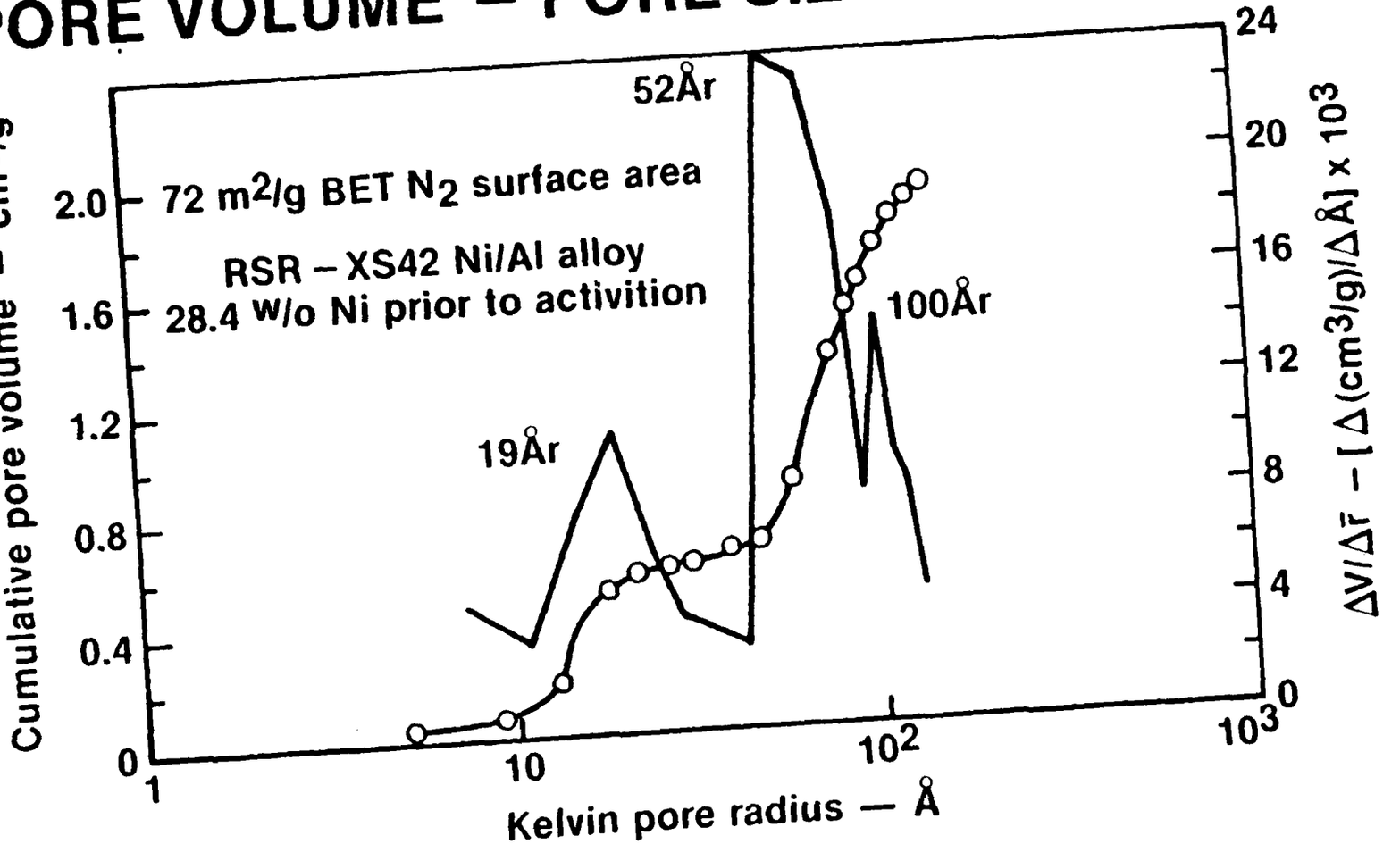

PORE VOLUME – PORE SIZE DISTRIBUTION

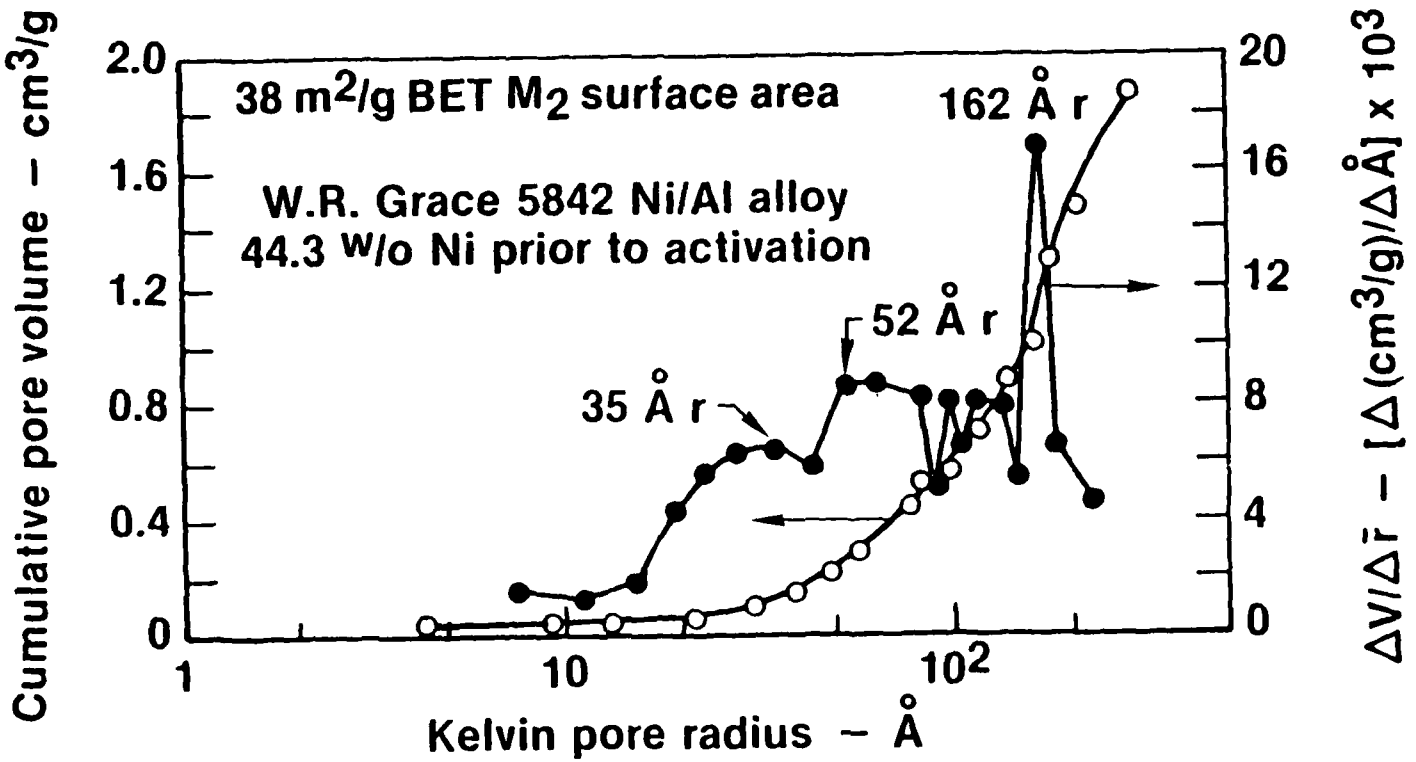

range of catalytically active nickel alloy surfaces with an opportunity to exercise control over selectivity in catalytic processes by varying pore structure and nickel alloy composition. Forseeable catalyst applications are in selective hydrogenation of a wide variety of organic compounds, hydrazine and hydrogen peroxide decomposition and in the preparation of a wide range of binary metal oxide (NiO/Al_2O_3, NiO/SiO_2, NiO/ZnO, NiO/MgO) oxidation catalysts. Physical forms of catalysts fabricated can be as powders, granular pellets or various porous inserts for use in slurry, fixed bed or monolithic catalyst configurations. Applications can be made to either liquid phase or vapor phase reactant systems.

Attached is a summary of a recent research program conducted to evaluate and characterize nickel catalysts derived from aluminum-nickel and aluminum-molybdenum-nickel RSR alloy powders and represents a beginning of an alloy development program directed toward providing homogeneous precursors for improved catalysts.

REFERENCES

1. "Coal Gasification Commercial Concepts-Gas Cost Guidelines", Project 4568-NW, U.S. Energy Research and Development Administration, Washington, D.C., Jamuary 30, 1976.

2. Anderson, L. L. and D. A. Tielman -"Synthetic Fuels from Coal," John Wiley and Sons, New York (1979).

BULK MICROCRYSTALLINE ALLOYS

Ranjan Ray

Rapid solidification processing techniques (RSP) offer outstanding prospects for snythesis of many new and improved engineering alloys which are likely to play important roles in building up future technologies.[1] Through extensive R & D efforts in recent years, a number of new RSP alloys have already reached the advanced stage of development.[2]

A new class of RSP alloys with technological potential are briefly reported in this note. These are bulk microcrystalline alloys made from metallic glasses.

Most metallic glasses, known to date, phase transform (i.e. devitrify) into very brittle, crystalline phases at low temperatures, i.e., 350-500°C (669-930°F)[3,4]. This rules out their uses at high temperatures. Besides, because of the need for fast heat extraction during solidification, fabrication of metallic glasses is restricted to thin bodies, e.g., ribbons; henceforth, inspite of their outstanding mechanical, corrosion resistance and/or magnetic properties, metallic glasses have not yet found widespread applications.

A new family of metallic glasses were synthesized in the recent past by the author based on Fe, Ni and/or Co which upon heat treatment at temperatures sufficiently above crystallization temperature (T_c) of the glassy phase and preferabley between 0.6 and 0.95 of the solidus temperature (T_s) are converted

into devitrified, multiphase crystalline alloys possessing high tensile strength, good ductility and high thermal stability.

The novel metallic glasses, above, were formulated with certain critical combinations of transition metals and metalloids. The total contents of metalloids, e.g., B, P, C, and Si, range between 5 to 13 atom percent; boron is the dominating metalloid element in these alloys. Typical examples include (subscripts are in atom percent) $Fe_{75}Cr_8Mo_5W_2B_{10}$, $Ni_{40}Cr_{13}Ni_2Mo_1B_9Si_1$, $Fe_{78}Cr_5W_7B_8C_1Si_1$, $Ni_{40}Cr_{25}Co_{10}Fe_{10}Mo_5B_{10}$, $Ni_{57}Cr_{10}Mo_{25}B_8$ and $Co_{40}Cr_{30}Ni_{10}Fe_{10}B_{10}$.

A number of low metalloid metallic glasses were prepared as ribbon by melt-spinning.[5] The glassy ribbons were devitrified-heat treated at 850-950°C up to 1 hour. Tensile tests of the devitrified, crystalline ribbons (parallel edged) were carried out on an Instron machine. Their UTS values, typically ranging between 205,000-330,000 psi (1414-2277MPa) are listed in Table 1.

The devitrified ribbons having alloy compositions of the present research possess remarkable thermal stability at elevated temperatures.

Metallic glasses having composition, $Ni_{40}Co_{10}Fe_{10}Cr_{25}Mo_5B_{10}$ and $Fe_{40}Cr_{30}Ni_{10}Co_{10}B_{10}$ were crystallized at 950°C and 900°C, followed by isothermal annealing at 700°C. No change in hardness was observed on aging up to 200 hours at 700°C.

Table I

Composition of Devitrified Alloys (at. pct.)	Ultimate Tensile Strength (PSI)	(MPa)
$Fe_{39}Cr_{25}Ni_{15}Co_{10}Mo_3W_2B_6$	205	1414
$Fe_{57}Co_{10}Ni_{15}Mo_{12}B_6$	260	1794
$Fe_{35}Cr_{25}Ni_{15}Co_{10}Mo_3W_2B_{10}$	325	2242
$Ni_{44}Co_{10}Fe_{12}Cr_{18}W_5Mo_5B_6$	294	2028
$Ni_{40}Co_{10}Fe_{10}Cr_{25}Mo_5B_{10}$	286	1973
$Ni_{45}Co_{20}Fe_{15}Mo_{12}B_8$	315	2173
$Ni_{57}Fe_{10}Co_{15}Mo_{12}B_6$	255	1759
$Co_{40}Ni_{10}Fe_{10}Cr_{30}B_{10}$	330	2277
$Co_{55}Ni_{10}Fe_{15}W_6MO_6B_8$	287	1980

The superior physical properties of the new devitrified alloys have their origin in their microstructures. TEM studies revealed that the devitrified alloys exhibiting high tensile strengtn values consist of unique aggregates of microcrystalline phases. The matrix is constituted typically of sub-micron grains (0.2-0.3 micron) of a Fe, Ni and/or Co base solid solution phase uniformly dispersed with 0.1-0.2 micron sized intermetallic phases, e.g., borides.

The present microcrystalline alloys can be classified as new generic alloys based on composition/microstructures/processing principles. They have evolved from a series of hypoeutectic metallic glass alloys. Low metalloid content is critical to achieve the desired microstructures of the devitrified alloys of the present scope. In contrast, most metallic glasses of the metal-metalloid type, previously known, have eutectic/ hypereutectic compositions, i.e., high contents (20 atom percent) of metalloids, B, P, C and/or Si and as such, these alloys in the devitrified state are rendered brittle by the formation of excessive amounts of the brittle intermetallic phases, i.e., borides, phosphides, carbides etc.

The important finding, i.e., strong, thermally stable microcrystalline alloys via metallic glasses of specific compositions led to the next step: powder metallurgical hot-consolidation of metallic glasses into bulk microcrystalline alloys on a best effort basis. The objective was to explore the potential of the bulk microcrystalline alloys with respect to various structural/engineering applications.

A number of metallic glasses of the present category were converted into fully dense, bulk microcrystalline alloys, i.e. bars, by hot extrusion and hot isostatic pressing of glassy powders (-100 mesh) at temperatures between 900 and 1050°C (1650 and 1920°F). Metallic glass powders were prepared by pulverization of melt-spun ribbons. Note, the present metalloid-lean glassy ribbons are brittle in as cast condition and hence, are readily amenable to pulverization to powders by standard equipment, e.g. a rotating hammer mill. In powders made by pulverization of melt-spun ribbons, particles of all sizes have experienced essentially the same quench history.

Initial test data appears to indicate excellent prospects for engineering applications of bulk microcrystalline alloys at both room and elevated temperatures. Microcrystalline alloys as hot extruded bars having compostions such as $Fe_{70}Cr_{13}Ni_6Mo_1B_9Si_1$, $Fe_{62.5}Cr_{16}Mo_{11.5}B_{10}$ etc., exhibited UTS values in the range 200,000-230,000 psi (1380-1587 MPA). The consolidated microcrystalline alloys based on Fe contaning Cr and/or Mo, W possess high hot strength/hardness and excellent oxidation resistance in the temperature range, 1000-1200°F.

A microcrystalline alloy in bulk form having composition $Fe_{63}Cr_{22}Ni_3Mo_2B_8C_2$ exhibited about ten times the resistance to sulfuric acid of 1N concentration at room temperature as commercial AISI 316 and 304 stainless steels.

The microcrystalline alloys containing small additions of carbon such as $Fe_{75}Cr_5W_7B_8C_1Si_1$ have capability to respond to

neat treatment to change their hardness and ductility, analogous to the manner in which hardness and ductility of steel may be changed by heat treatment (i.e. hardening, tempering, annealing etc.). Hardness values in excess of Rockwell C68 can be achieved in these bulk microcrystalline alloys by suitable heat treatment procedures. High hardness values of these boron-carbon containing alloys are believed to be due to the unique microstructures consisting of ultrafine boride dispersoids in ultrafine grained microcrystalline matrix.

It is evident, from the above discussion, that the bulk microcrystalline alloys of the present scope have prospects for practical applications as structural/engineering materials upon further advancement of the manufacturing technology. The new technology of bulk microcrystalline alloy prepared from metallic glass alloys can advance rapidly taking full advantages of the vital fabricating principles involved, i.e. melt-spinning, pulverization and powder metallurgical consolidation, which are well known techniques.

REFERENCES

1. Rapid Solidification Processing, Principles and Technologies, II (R. Mehrabian, B. H. Kear and M. Cohen, Eds.), Claitor's Publishing Division, Baton Rouge, Louisiana, 1980.

2. A. L. Bement and E. C. vanReuth, in Ref. 1, p. 404.

3. Rapidly Quenched Metals III, 3rd. Int. Conference Vol. 1 and 2 (B. Cantor, Ed.) The Metals Society, London, 1978.

4. Metallic Glasses (J. J. Gilman and H. J. Leamy, Eds.), American Society for Metals, Metals Park, Ohio, 1978.

5. S. Kavesh, in Ref. 4. p. 36.

This work was carried out by the author at the Corporate Development Center, Allied Chemical Corporation, Morristown, NJ 07960.

METALLIC GLASS APPLICATIONS

L. A. Davis

Metallic glass science began in 1960 with the work of Klement, Willens and Duwez. For all practical purposes, metallic glass technology began in 1973 when the first samples of metallic glass were offered commercially by Allied Corporation. Two key events presaged the technology development in the pre-1973 period; Chen and Polk broadly delineated the myriad of possible alloys which may be fabricated based on reasonable inexpensive metals (Fe, Ni, Co) and Bedell and Wellslager invented a practical, continuous, ribbon casting process. In 1976 Narasimhan invented a method by which wide sheets may be produced, a development key to the application of metallic glasses in magnetic devices.

Since the work of Chen and Polk, alloy development has continued unabated. The most important "base" system identified is Fe-B. Alloys, additionally containing C and Si, have been formulated which exhibit ~1/4 the core losses of 3%Si-Fe, the standard magnetic core material in distribution transformers.

Potential energy savings provide an enormous economic driving force for the use of amorphous alloys to replace Si-Fe; one estimate predicts a $30 billion savings over the next 15 years (this includes savings which would accrue due to reduced need for new generating capacity, amounting to seven 1000 megawatt stations). However the need for new transformer manu-

facturing techniques represents a deterent to the use of amorphous alloys, particularly in view of the present soft market for transformers, since the above savings will accrue to the user rather than the transformer manufacturer. Consideration should be given to government support for the development of such techniques; in all likelihood, cooperation between government and industry in Japan, where the economic incentive is even greater, will lead to the development of amorphous alloy distribution transformers. The world market would then come to be dominated by Japanese manufacturers, if U.S. manufacturers are caught lagging.

Metallic glasses also exhibit outstanding high frequency magnetic properties. They can be used in place of permalloy, superper malloy and ferrites in airborne transformers, switched mode power supplies, magamps, saturable reactors, magnetic switches, etc. They also have great potential for use in consumer electronic devices such as tape heads, stereo cartridges and the like. Efforts in the latter area are primarily conducted by device manufacturers in Japan.

Structural applications of metallic glasses, per se, will likely be limited. There is, however, great potential for the synthesis of bulk structural components with unique microstructures and properties, based on the controlled crystallization of consolidated glassy ribbons or powders.

AN ASSESSMENT OF RST AND ITS DoD APPLICATIONS

T. F. Kearns

A review of service plans for design and construction of new weapons systems indicated that there are about 75 such systems to be brought to the initial production stage between now and the year 2000. At first glance, this would appear to offer multiple opportunities for introduction of new materials during this period. However, when we recognize that there is a lead time of about 10 years required between original design and first production and that many new systems are really up-dates or modest modifications of current systems, in which opportunities for material changes are quite restricted, this number is drastically reduced. Fortunately there are introduction opportunities after original design, i.e. during prototype development and inservice, which render the picture less bleak. We would be well advised to scrutinize introduction opportunities in systems that have already passed the orginal design stage, to maximize this number of these opportunities. In these actions we will be seeking to remedy defects in the originally planned design or to produce modifications thereof needed by or advantageous to DoD. Assuming that all of the materials development work has been successfully completed on a new alloy, there are many system-related factors which influence decisions to use or not use an alloy in a new or modified weapons systems. A few of the more significant of these follow:

Requirements specified for the vehicle

Once the performance requirements for a new vehicle have been established, its materials of construction have been essentially determined. The designers job thereafter is to meet that performance, on time, with reliability in the vehicle and at lowest possible cost. There is usually no advantage to the designer to increasing performance beyond that specified, and it is disadvantageous for him to do so if cost is increased.

Material at production stage

We cannot expect a system designer to base his design on use of a material which has not reached the production stage. His supply of material must be assured, and this will often require the existence of more than one source of supply.

Knowledge and facilities available in user organization

Particularly when a new manufacturing process, such as powder metallurgy, is involved we must recognize that manufacturers may not plan to use new materials unless their organizations are competent in their design and manufacturing technology and are equipped to do so. This barrier favors materials supplied to system manufacturers in conventional, i.e. bar, sheet, forgings, etc., form.

Criticallity of the parts

We should expect greater difficulty in introducing new materials into critical parts than into those less critical. If possible, it would seem advantageous to introduce new, untried, materials into less critical parts to avoid the major system

problems incident to possible failures of critical parts. In RST materials there are many requirements that must be met before we can expect new alloys to be developed, scaled-up to production and characterized for design use. Some of the more significant of these are:

Alloy/process development

Universities need RST material with which to work or equipment to produce it. Industry must perceive an economic benefit to the company in alloy development efforts. Non-profit labs need economic support and government labs need both people and money for alloy/process development efforts. Developments made outside of the material producing industry must be transitioned to a producer(s) to achieve production status.

Scale-up and production

The principal roadblock here involve convincing industry that there is a demand for the RST products and that the demand will be lasting. The technical and economic information must be generated which will convince producer management that investment in RST production is sound business.

Material characterization

The main roadblock in generating the needed engineering data base of new RST alloys is creating on the part of design organizations a desire to use the materials. Neither industry or government support adquate to the task can be expected unless this desire exists.

Where We Stand

Thus far we see tool steels, powder metallurgy superalloys and Metglass products in production and two aluminum alloys at pilot plant stage. Attractive laboratory test results have been reported. There is, as yet, little user demand for additional RST products outside the materials development community. RST is, however, a government thrust area which implies significant economic support.

What We Need

A more extensive theoretical base

Attractive alloys with optimim balance of properties for a variety of applications

Low cost, high volume production processes and associated quality control practice

What We Don't Need

Multiple failures of production parts

Extravagent claims of advantages or applications which reduce the credibiliy of the RST materials development community

Impediments to information exchange that could arise in connection with control of the export of technology

DISCUSSION ON APPLICATIONS AND TECHNOLOGY

E. J. Dulis

We recently investigated the effects of using different atomizing gases, argon, nitrogen and helium, on the particle size and dendritic arm spacings of Rene 95 powder particles. The actual measured dendritic arm spacings are shown for particles -105 μm to 88 μm (-140 to +170 mesh) and -37 μm (-400 mesh) for each of the three different atomizing gases. In addition to powder particles made by our gas atomization process, included in the investigation were the Pratt & Whitney spinning disk RSR Rene 95 powder particles. A size analysis of all particles is shown in the attached tables. The dendritic arm spacings versus particle size were plotted for the three different atomizing gases using gas atomization as well as the Pratt & Whitney spinning disk RSR process powder particles. In general, little difference was found on the effect of gas used. Helium has a much larger thermal conductivity and heat capacity than argon and thus the dendritic arm spacings of the helium atomized particles are somewhat less than those of argon atomized particles. However, in general, the differences are minor, considering the dendritic arm spacings range in size from about 1 to almost 2 micrometers. The room temperature and 1200°F tensile properties of products made from the aforementioned powders show little difference among the three starting powders. All of the products met the GE specifications for room temperature and 1200°F,

150 ksi, for the different starting powder particles show that all of the products met the GE Class A specification requirements. The spinning disk Pratt & Whitney powder was slightly low in ductility.

In a GE/Crucible investigation on the effect of hot isostatic pressing temperature and the effect of different solution treating temperatures on low cycle fatigue properties, as-HIPed bars were prepared of Rene 95 made from -140 mesh powder (-105 μm to less than -37μm). To evaluate the effects of processing parameters, Van Stone and Gangloff of GE used the defects tolerance fatigue test in which a controlled EDM defect is imparted to the surface of the test specimens. The defects tolerance test establishes the crack growth rate per cycle, da/dm, as a function of the stress intensity factor, ΔK. This test showed good agreement with low cycle fatigue tests. As the hot isostatic pressing temperature was increased from 1800 to 2200°F, the fatigue properties improve substantially. Also, after hot isostatic pressing at 2050°F, solution treating at 2000, 2090, and 2175°F showed the defect tolerance fatigue properties increased as the solution treated temperature increased. Thus, both the temperature of hot isostatic pressing and the temperature of solution treating have an important bearing on the fatigue properties of the final product.

The effect of cooling rate, as manifested by the final powder particle size was investigated by comparing -105 micrometer (-140 mesh) material with -53 micrometer (-270 mesh)

material. A negligible difference in room temperature tensile properties were found in comparing these materials. The Van Stone and Gangloff data on the effect of particle size and thus cooling rate and HIP temperature (as well as the difference in atomizing gas) showed that the effect on defect tolerance fatigue of particle size was minor compared to the effect of HIP temperature. However, the best properties were obtained on argon atomized particles, -270 mesh or -53 micrometers in size, that was hot isostatically pressed at 2200°F.

RENE 95 POWDER ANALYSIS

Screen Analysis (% Undersize)

Mesh Size	Size(mm)	P&WA* RSR Powder	CRC** Argon Atomized	CRC** Nitrogen Atomized	CRC** Helium Atomized
-140 +170	-105 +88	100.00	100.00	100.00	100.00
-170 +200	-88 +74	90.58	90.59	84.94	88.50
-200 +230	-74 +63	76.11	72.30	74.04	79.50
-230 +270	-63 +53	67.59	58.14	64.71	73.10
-270 +325	-53 +44	55.03	53.96	54.64	66.30
-325 +400	-44 +37	33.07	36.39	35.59	49.40
-400	-37	26.57	30.36	28.72	43.30

---

* Spinning disk, He gas cooling
** Gas atomization

TEXTURE CONTROLLED DIRECTIONAL GROWTH IN Ni-BASE SUPERALLOYS

B. B. Rath

INTRODUCTION

A program has been initiated to systematically evaluate the role of composition, thermomechanical processing and post processing treatment on the growth of single crystals in a series of Ni-base superalloys. An extensive study performed by Pratt & Whitney has established the effects of processing conditions on the evolution of crystallographic texture in the alloys and the consequences of these textures on the ease of crystal growth along the desired [111] direction. Early studies had established that the presence of grain boundaries with grain misorientations, as low as 6 degrees, contribute to a reduction in performance due to creep rupture. It became apparent that relatively defect-free single crystals must be grown in these alloys.

Growth of crystals from the solid in these alloys under conditions of a temperature gradient revealed a large accumulation of twins and occluded grains imbedded in the crystal. The number density and the volume fraction of these twins and grains remained relatively unaffected by the growing crystal orientation, crystal growth rates, prior thermo-mechanical history, minor variation in composition, grain size or the texture of the polycrystalline matrix. Unlike the frequently observed occluded grains in the surface region of crystals grown by the strain-

annealing method, the twins and occluded grains in Ni-base alloys were found in equal density throughout the crystal, i.e., the number density was independent of thickness.

The first phase of the program was directed towards (a) determining the origin and morphology of the twins and identifying the factors influencing their formation and growth and (b) reducing or eliminating twins and freckles by suitable metallurgical processing.

EXPERIMENTAL PROCEDURE

The alloys chosen for the study were RSR-185, RSR-606, and their minor modifications. They were produced in polycrystalline form by a RSR process and then given the following mechanical treatment resulting in texture.

Material	Composition in%	Fabrication	Texture
RSR-185	Al 6.8 W 6.0 Mo 14.4 Ni balance	Cold Cross rolled 75:25	Sharp texture $(011)[\bar{2}11]$ $(011)[211]$
RSR-185	"	Straight cold rolled	Texture spread $(011)[\bar{2}11]$ $(011)[211]$
Modified RSR-606	Cr 3.0 Al 6.7 W 6.2 Ta 1.5 Mo 11.0 Y 0.1 Hf 0.2 Ni balance	Hot Cross rolled	Weak texture

Interrupted directionally recrystallized specimens of these materials were also studied. Optical microscopy, electromicroscopy and x-ray techniques were extensively used in this study.

RESULTS

Figure 1 is a typical light micrograph composite showing twins and freckles in a single crystal of RSR-185 which was diffusion bonded and then directionally recrystallized. The single crystal interface is seen on the lower left. Notice the alignment of the twins in this and the following figures. Similar twins and island grains in a directionally grown crystal of alloy x are shown in Fig. 2. The twins and freckles densities are not dependent on the depth in the material. Figure 3 shows micrographs of front and side views, respectively, of interrupted and directionally recrystallized alloy x showing no change in frequency of twins with depth. A grain size distribution was observed during directional recrystallization as shown in Fig. 4 and plotted in Fig. 5 as a function of distance from the polycrystalline matrix. The relative frequency of grain size in an interrupted and directionally recrystallized alloy x is given in Fig. 6. A sharp peak in grain size is obtained for all the grain distributions studied. Figure 7 shows the grain size distribution and regions for texture evaluation in alloy x during directional recrystallization. The texture gradient along the growth direction of an interrupted and di-

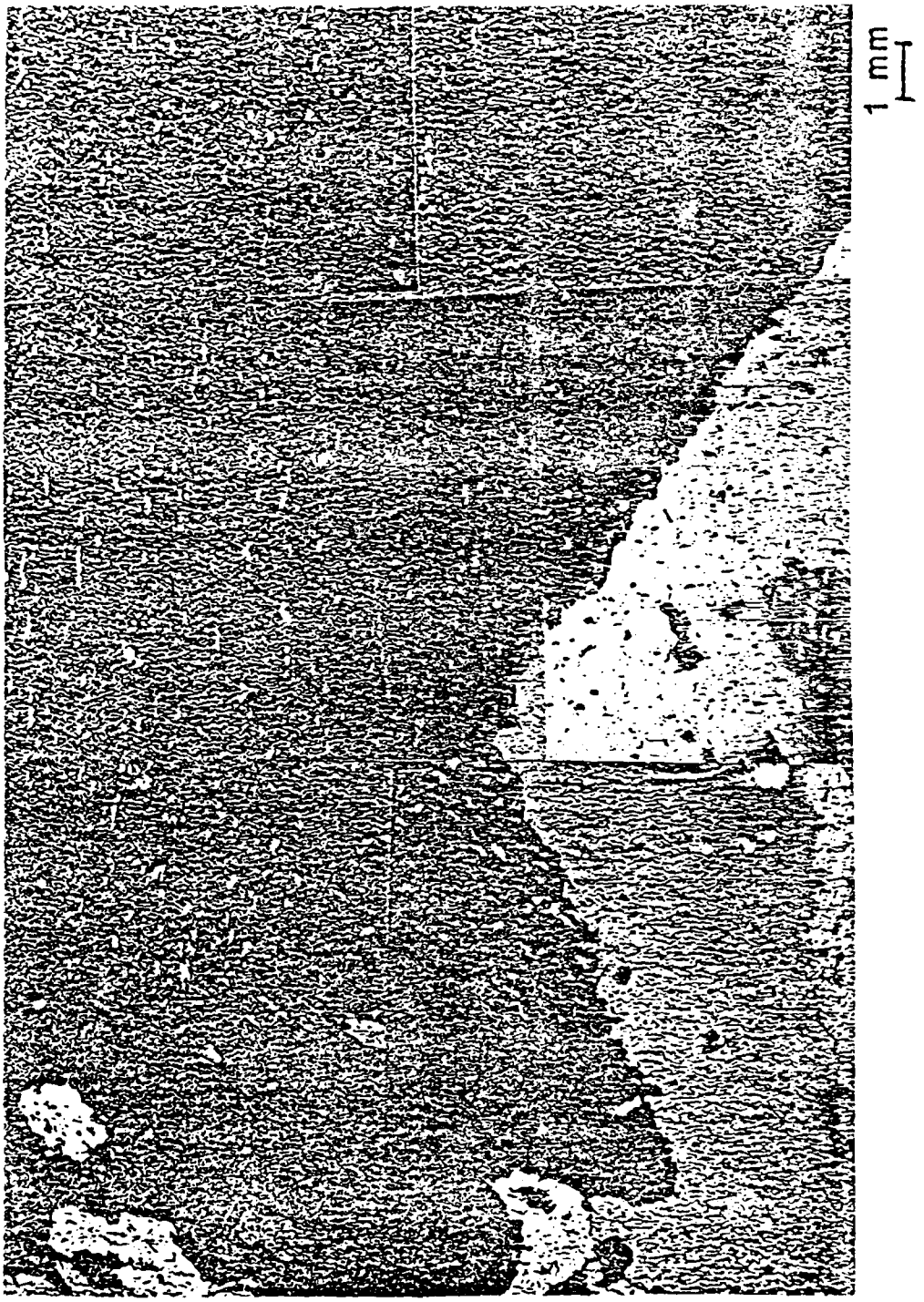

Figure 1. Single Crystal in a DB/DR Sample, Alloy 185 (Sample 0)

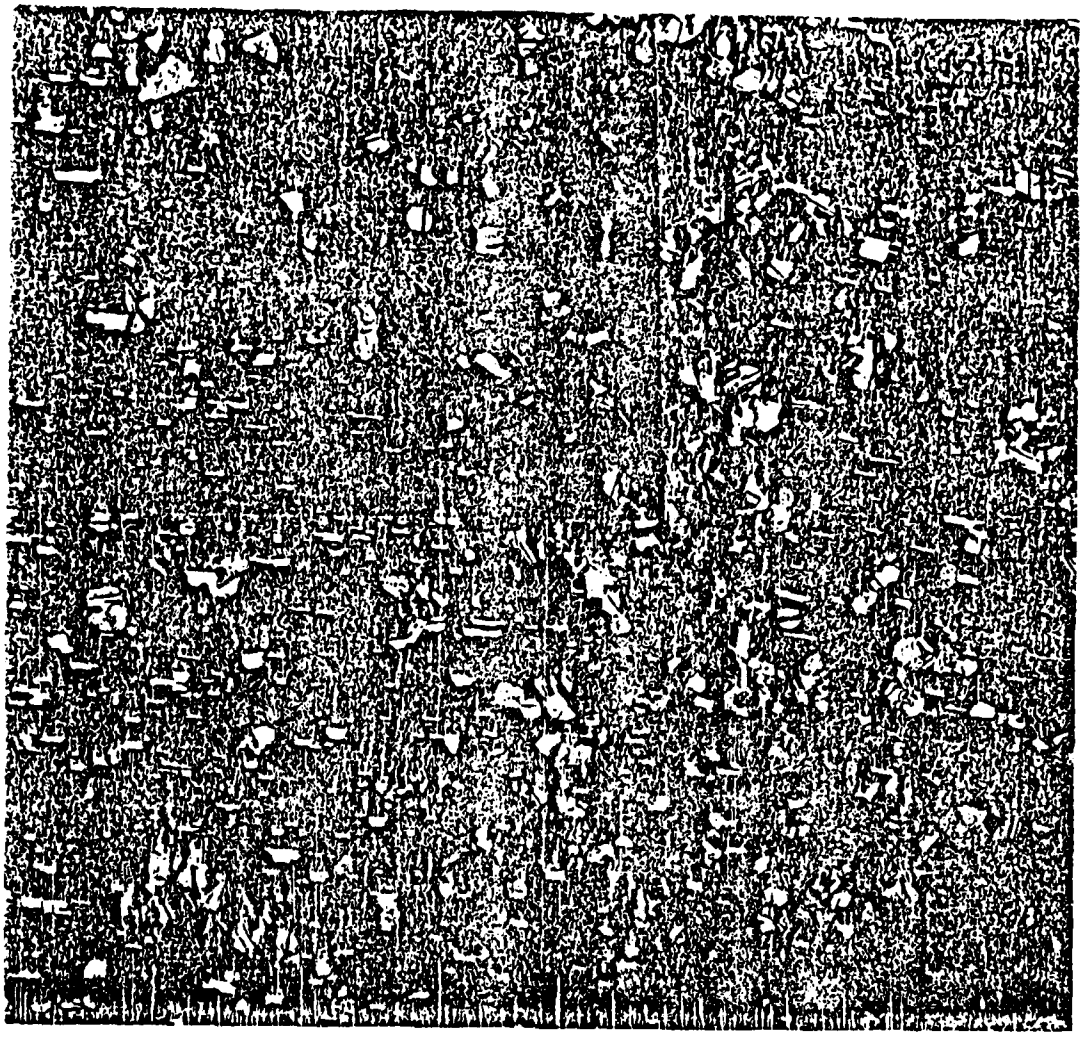

Figure 2. Twin and Island Grain Frequency in a Directionally Grown Crystal, Alloy X, Sample 5.

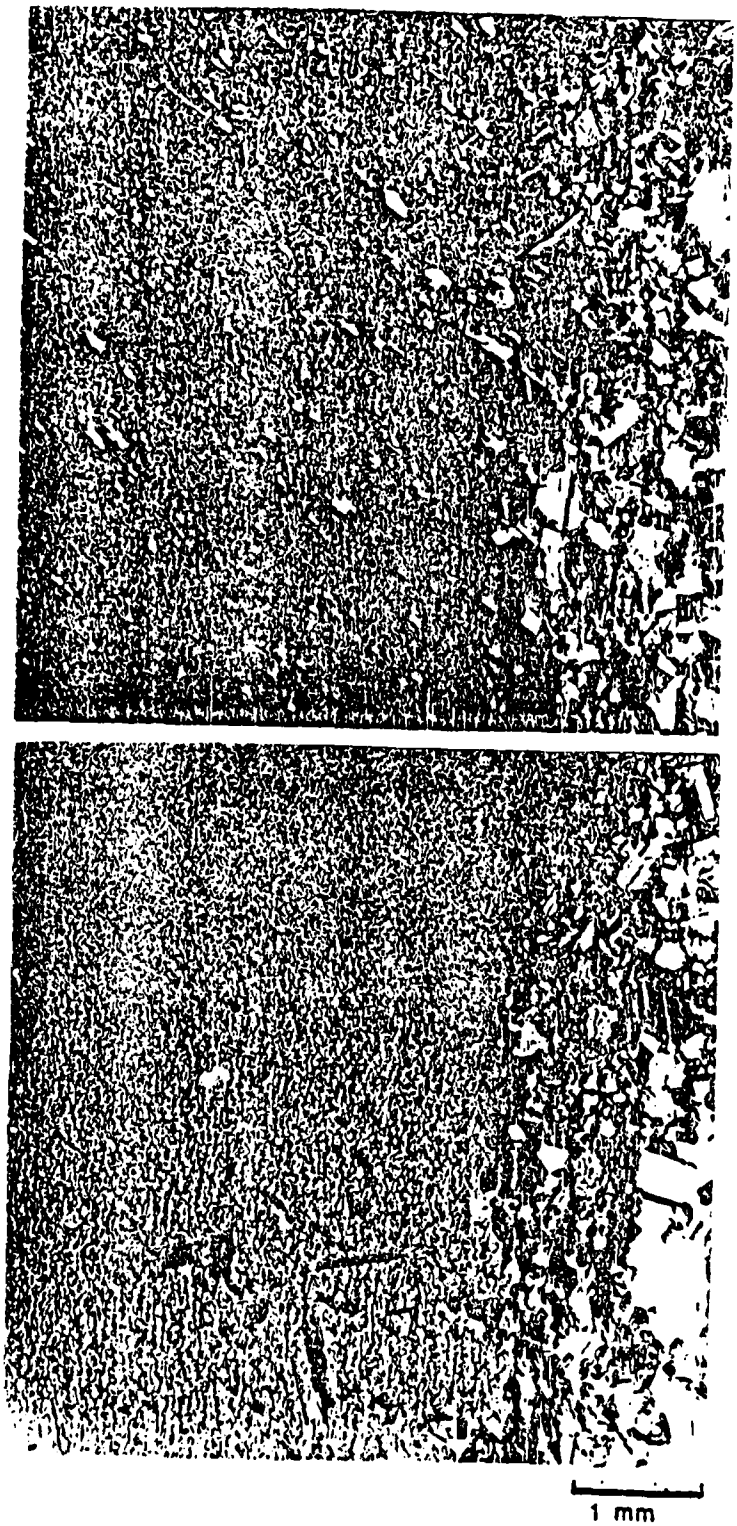

Figure 3. Interrupted DRed Crystal, Alloy X, Sample 5. (Side view).

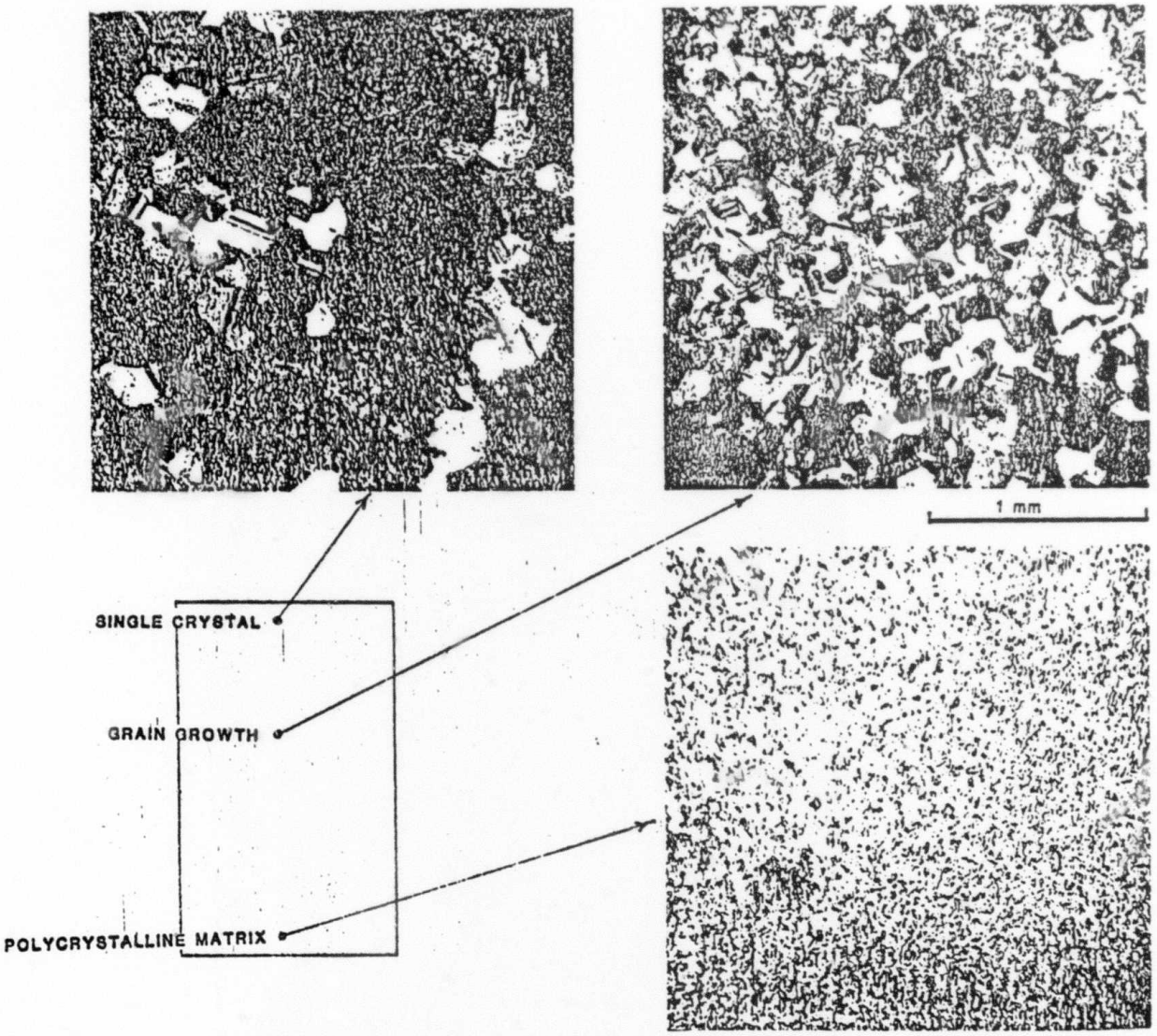

Figure 4. Grain Size Distribution During DR in Alloy X, Sample 5.

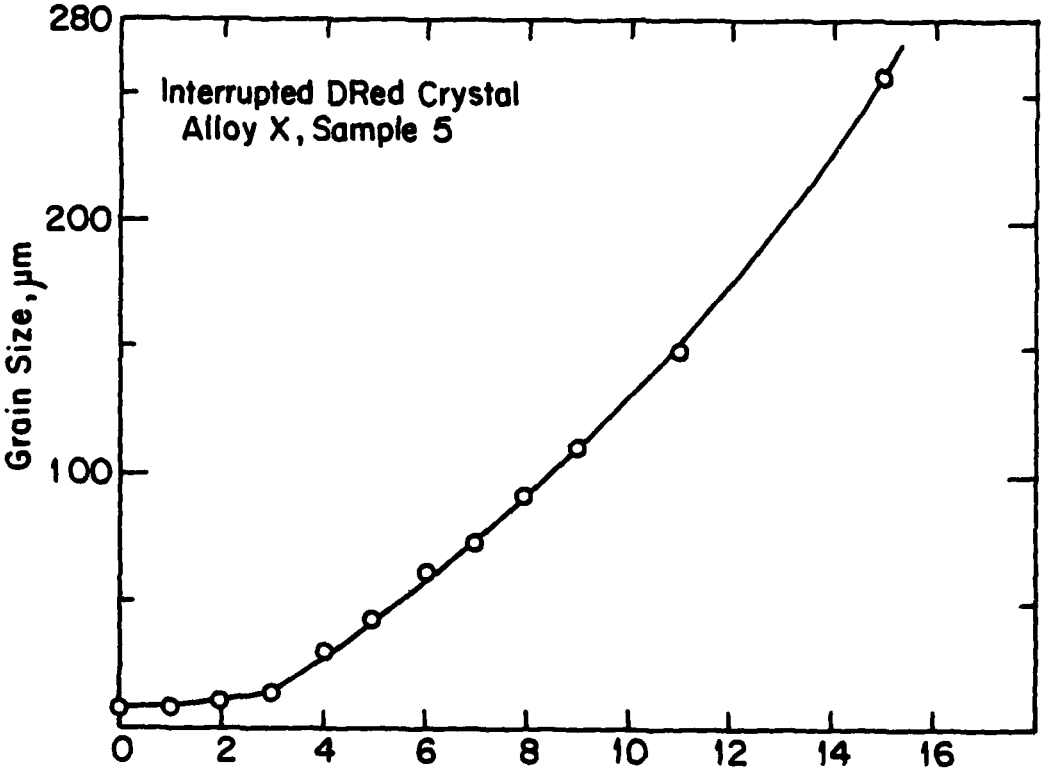

Figure 5. Distance from Polycrystalline Matrix to DR Peak Temperature, mm.

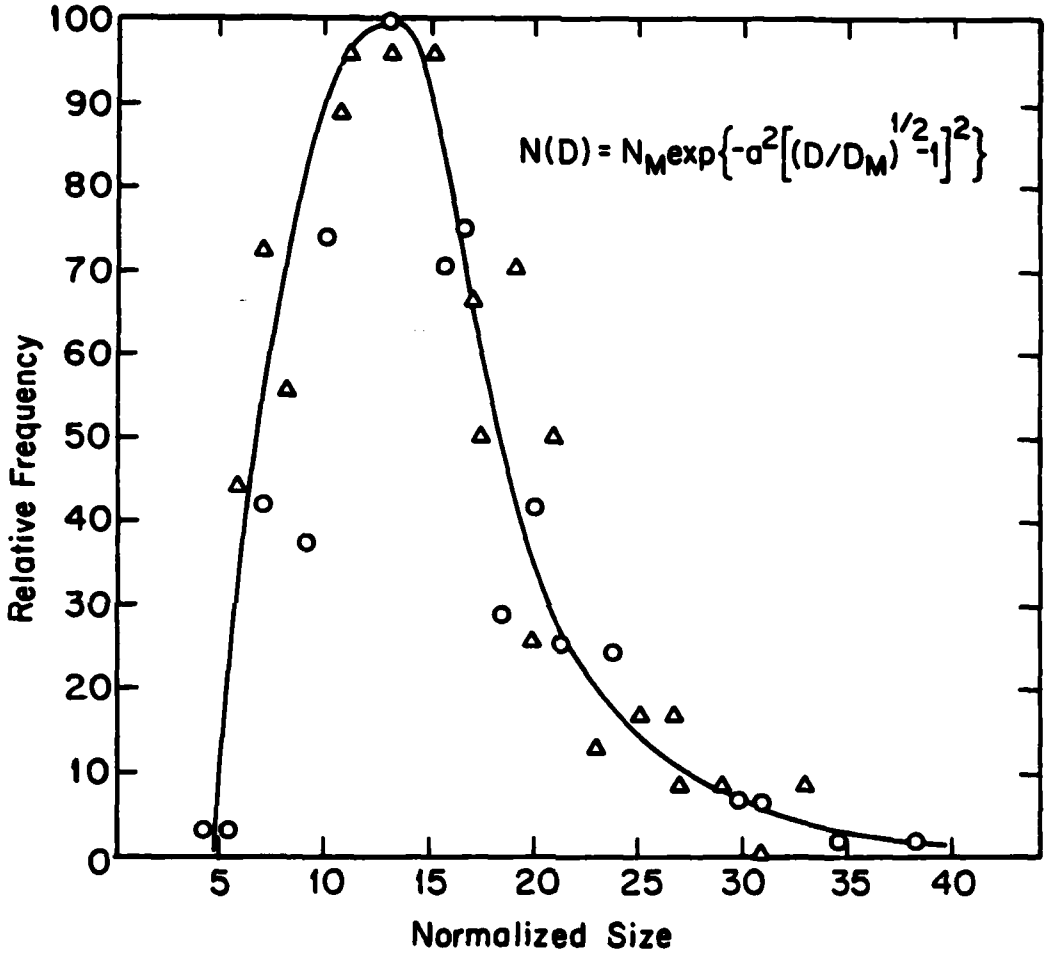

Figure 6. Interrupted DRed Crystal Alloy X, Sample 5.

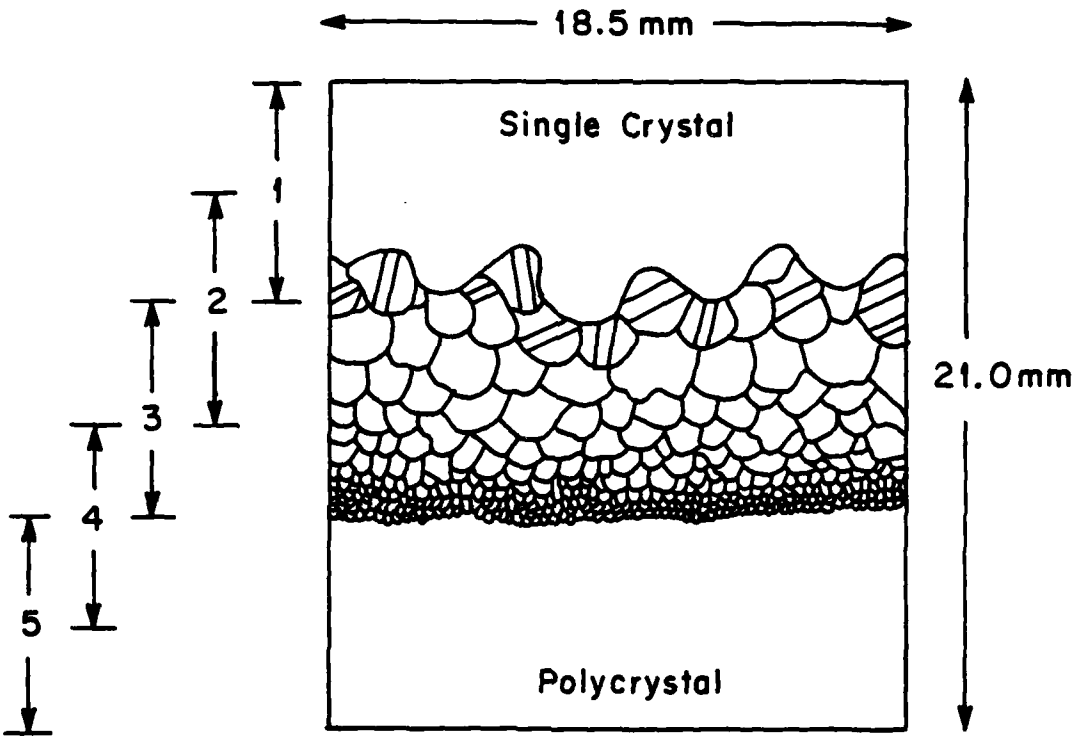

Figure 7. Grain Size Distribution During DR in Alloy X, Sample 5. Showing Regions for Texture Evaluation.

rectionally recrystallized alloy x is shown in Fig. 8. Figure 9 shows (111) pole figure of a directionally recrystallized crystal of alloy 185 with included twins from which the orientation relationship of the included twins in the single crystal of alloy 185 can be ascertained (Fig. 10).

Attempts were then made to observe these twins using scanning electron microscopy, and to determine their orientation relationships using electron channeling patterns. To pinpoint the location of the twins they were marked by a hardness indentor. Figure 11 shows the same region of the directionally recrystallized alloys x, showing twins and the indentation marks. Using such marks, the high magnifications of the twins were finally obtained as shown in Fig. 12. Due to the small width of these twins (2-10 μm) the channeling pattern study of these twins were not very successful.

DISCUSSION

Various mechanisms concerning the formation of annealing twins in f.c.c. metals have been proposed. Essentially, an annealing twin is expected to form whenever such an event will produce a sufficient lowering of the free energy of the grain boundaries.[1]

By such a process a migrating grain boundary of interface can leave behind twins, which initially nucleate at the grain corners. Our observations cannot be accounted for by this

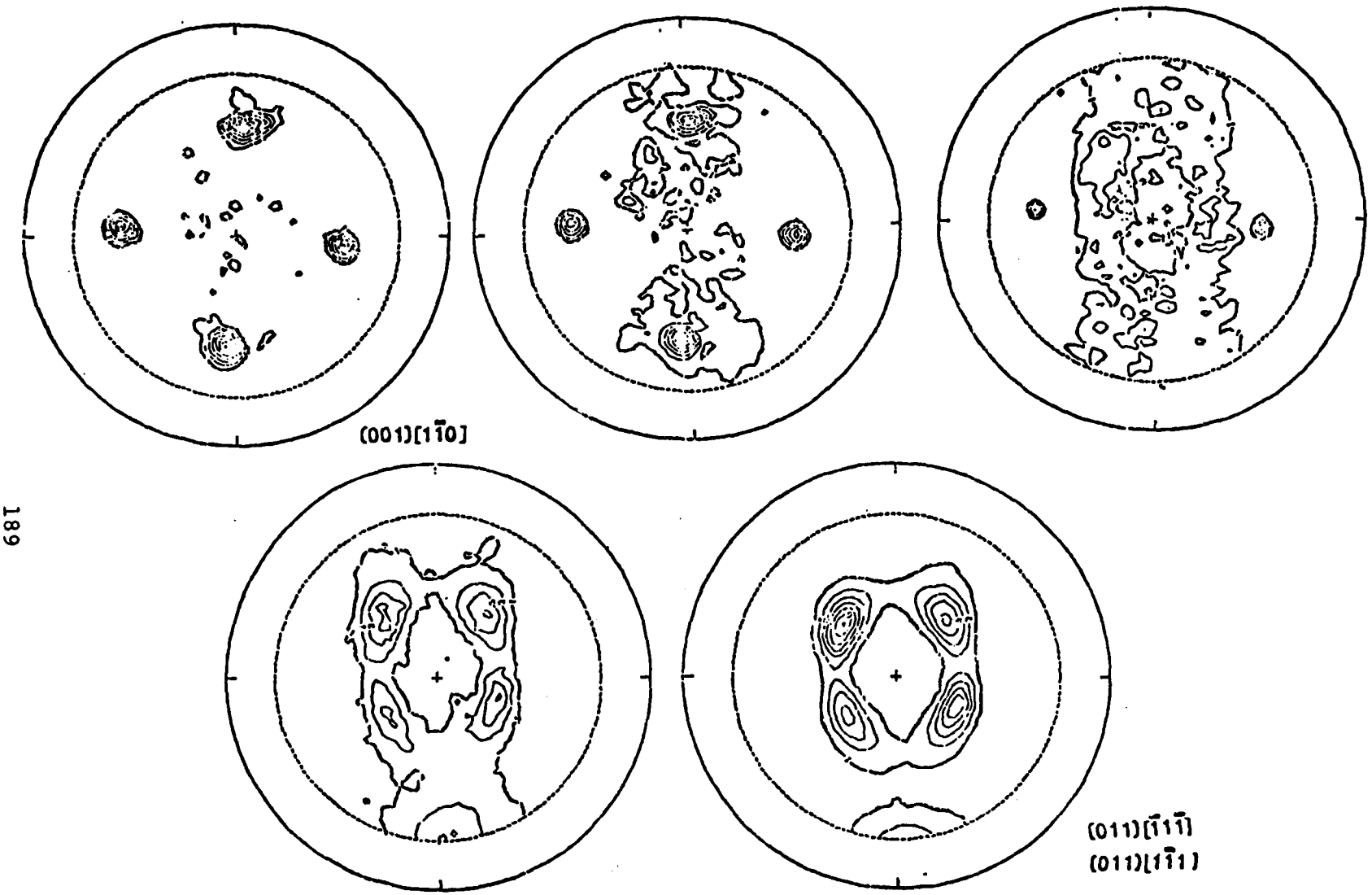

Figure 8. Texture Gradient Along the Growth Direction of an Interrupted DRed Crystal, Alloy X, Sample 5.

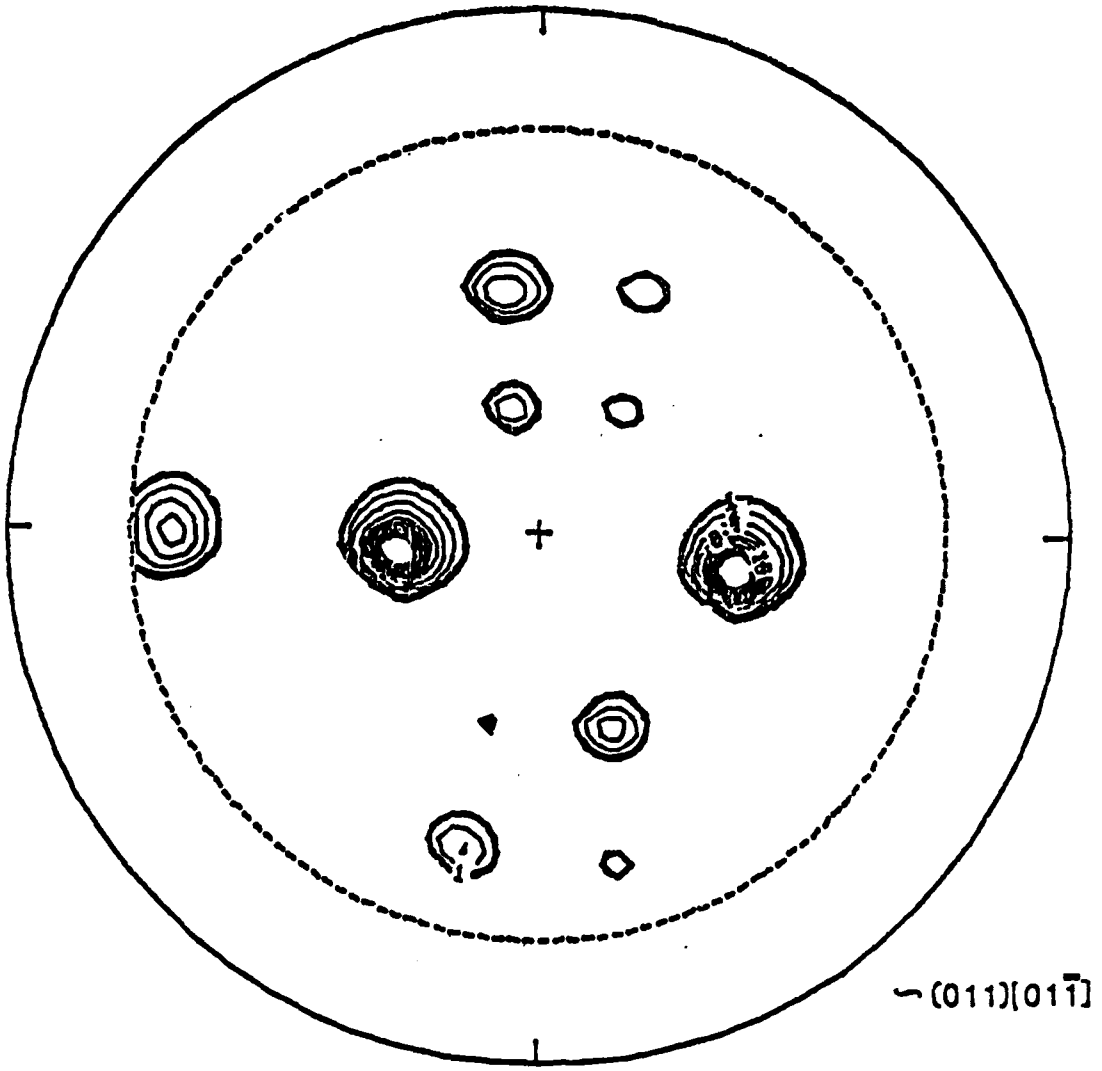

Figure 9. (111) Pole Figure of DRed Crystal of Alloy-O (RSR-185) With Included Twins.

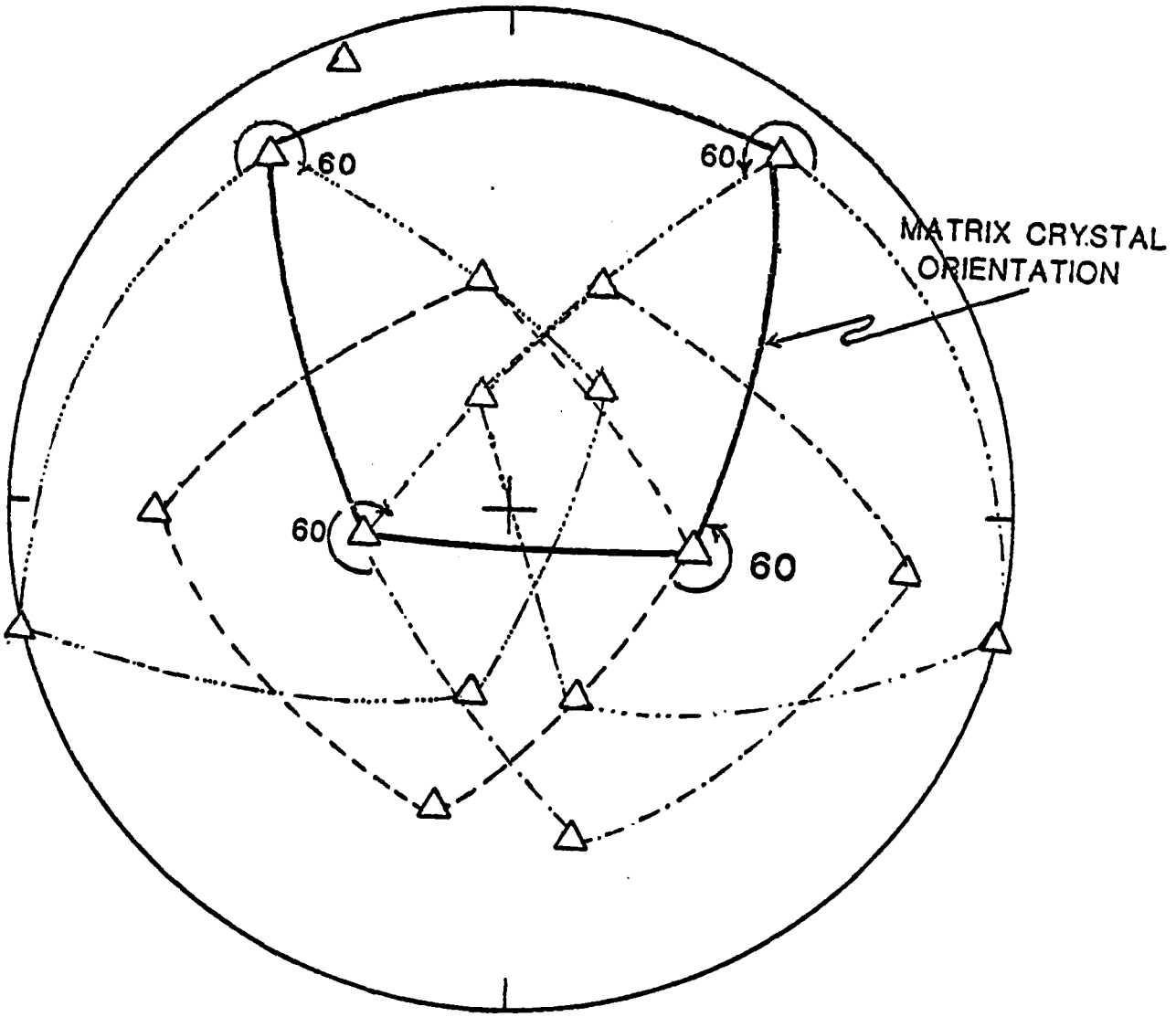

Figure 10. Orientational Relationship of the Included Twins in Single Crystal O, Alloy RSR-185.

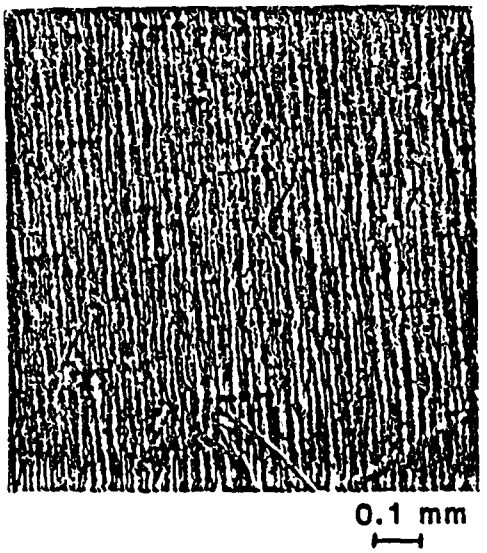

OPTICAL MICROGRAPH

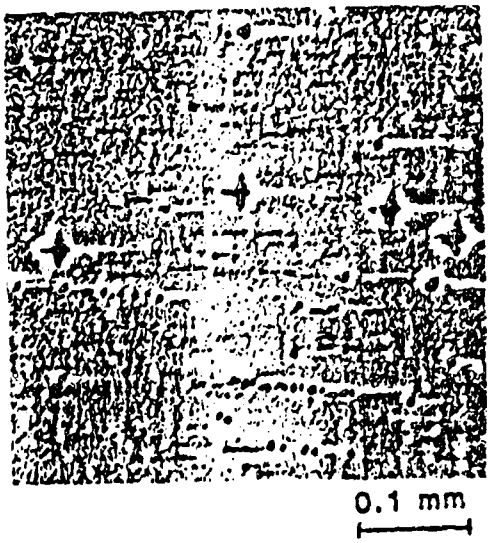

BACK SCATTERED (COMPOSITION)

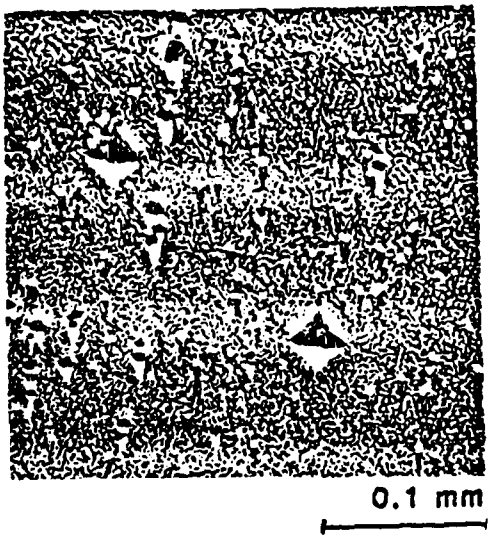

BACK SCATTERED (TOPIGRAPHICAL)

Figure 11. Twins in DRed Crystal, Alloy X.

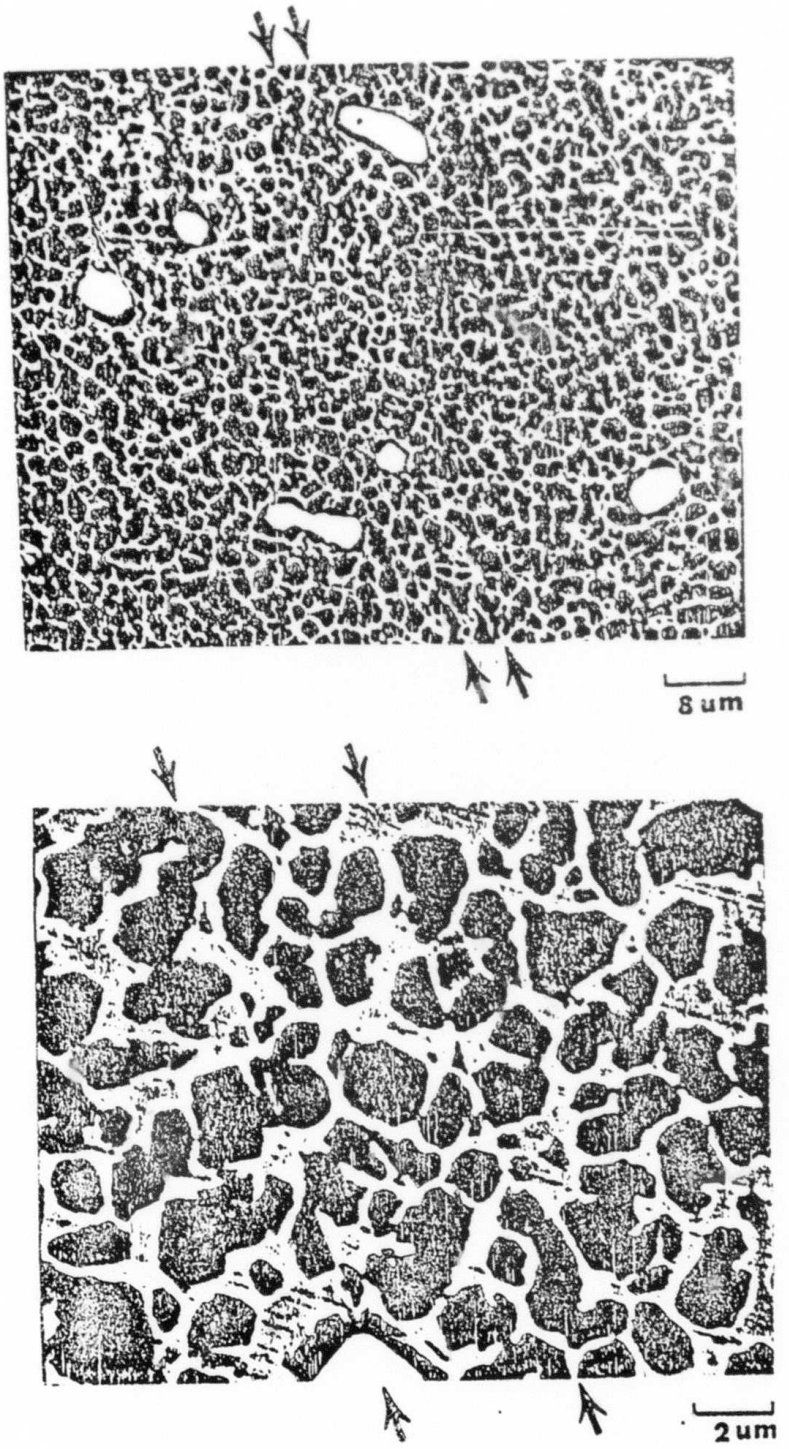

Figure 12. Secondary Scanning Micrographs of Twins.

mechanism alone because their orientations do not indicate that they all formed near grain corners.

Dash and Brown[2] have proposed nucleation of twins by stacking faults and fault packets in migrating grain boundaries and their subsequent growth through motion either of the grain boundary, (which would leave a parallel sided twin) or by the combined motion of the noncoherent twin boundary and the grain boundary. Some of the long thin twins inclined at large angle to the migrating interface, as observed in our interrupted crystals, could be accounted for by this mechanism. However, this process will produce twins of varying thickness in contrast to the observed twins where the majority have nearly the same thickness. Ashby and Harper[3], and Myers and Murr[4] have proposed models in which a twin can be formed by the dissociation of a grain boundary. However, the actual mechanism by which such a dissociation takes place is not specified.

Gleiter[5] has proposed an atomistic model for the formation of annealing twins, according to which the twins formed by a two dimensional nucleation process on the [111] planes of the growing grains of the f.c.c. material. This mechanism would suggest the formation of coherent twin boundaries at the interface. The mechanism also implies the formation of twins and new grains at the same time and under the same conditions by the same process.

Our observations do not always agree with this conclusion. It is thus clear that any single theory of the formation

of annealing twins cannot fully account for all the observation. Detailed transmission electromicroscope studies are therefore required to compare the predictions of the various model and establish the mechanism of the formation of the annealing twins in these superalloys.

SUMMARY

The principal results of this study are briefly summarized below:

1. Extensive grain growth was found to occur ahead of the migrating crystals resulting from a weak temperature gradient.

2. A texture transition was noted between the sharp texture of the matrix and the growing crystal.

3. Grain growth was found to occur over a region of at least 13 mm.

4. All variants of the twins were present in a single crystal, and their frequency was independent of crystal thickness.

5. Twins were found to nucleate at the single and the polycrystal interface during the migration of the interface.

6. Twin frequency was found to be strongly dependent on the processing and metallurgical variables.

REFERENCES

1. R. L. Fullman and J. C. Fisher, J. Appl. Phys. 22, 1350 (1951).

2. S. Dash and N. Brown, Acta Met. 11, 1067 (1963).

3. M. Ashby and E. Harper, Harvard Report, Harvard University, Cambridge, Massachusetts, September 1967.

4. M. A. Meyers and L. E. Murr, Acta Met. 26, 951 (1978).

5. H. Gleiter, Acta Met. 17, 1421 (1969).

SPECIFIC COMMENTS & CONCERNS

A. M. Adair

The Air Force is considering investing resources in titanium RST-one approach that might be done initially is to modify REP(or PREP) processes to have gas cooling added. The concern here remains the cost of the rotating electrode stock and the need for it to be homogeneous. Based on rapid melting of non-homogenous (i.e., source dendritic segregation) alloys, considering the fact that the molten droplets leave the surface quickly in the REP process, the additional concern is that the powder produced may retain inhomogeneties from the rotating electrode barstock. One proposed low cost electrode approach is to use cast electrodes.

The most significant impact of RST on alloys may in fact be on "second tier" properties and broader processing and heat treatment ranges. For example, dispersions in steels which affect grain size control; reduction of second phase size that limits crack initiation sites; and control of minor element contact to effect excellent oxidation resistancen in high molybdenum containing superalloys. It is possible that we should examine various options to broaden the potential application base for all applicable alloy systems.

A problem is that we do not necessarily know how the RST materials have a memory of their genesis that allows homogeneity and control of second phases to be possible after extensive

processing operations. Also, since we tend to apply RST to high strength alloys which are used in highly stressed designs, we really need to address the "short crack problem" and be concerned with ways to increase the defect tolerance of these new materials. Since the Ni-Al-Mo-X alloys are also very strong at temperatures appropriate for turbine disc application, perhaps we should explore this application potential to a greater extent.

I am convinced that we must have all inert production and handling of RST materials, regardless of the alloy base. This affects quality and we must have quality products for DoD application. In general, all the RST materials should be characterized in detail so that we can better understand how the microstructures track through various consolidation and processing steps. Weldability of RST materials seems to be an unknown. Many potential applications are likely to require assembly by welding. A question is whether it has really been demonstrated that the Allied Chemical melt spinning process for "microcrystalline alloys" can be scaled-up to production quantities?

As has been stated in many different ways, we should explore processing windows for RST materials rather than concentrate on specific "cooling rate" effects.

Also, we should not lose sight of the fact we are in the midst of an exciting, aggressive, fast moving, high-risk technology; we shouldn't be discouraged or become "panicky" over failures.

NEEDS FOR FUNDAMENTAL STUDIES

Anthony F. Giamei

In the past three weeks (W. Palm Beach, Gaithersburg and La Jolla) we have been fully debriefed on RST. My impression is that the entire thrust is moving at a rapid pace toward a variety of important potential applications. I am concerned that certain key processing areas in the superalloy PM approach are not receiving sufficient focus from a fundamental point of view. The following areas are critical to the ultimate success of RST:

-control of inclusions

-texture management

-defect control during directional recrystallization

These are discussed (briefly) below:

Inclusions

Critical aerospace applications will require careful control of the size, number density and character of inclusions within the consolidated powder product. I see an ultimate need for ceramic-free melting (skull methods) prior to atomization and inert gas handling. I feel that the RSR remelt stock should be clean to begin with -an improved coupling between DARPA and AFWAL programs could definitely help here. Further studies are also required on the influence of inclusions on LCF (strain controlled) that results. This would help to set standards, in a production situation.

Texture Management

Potential cellular coarsening reactions at grain boundaries in the highest strength alloys dictate a need for tight sheet texture control. Mechanical anisotropy is very high in the alloys of interest, and therefore it is important to have processing flexibility to achieve any one of at least four single crystal orientations: <100>, <110>, <111> or <112>. The fundamental details of how the deformation texture relates to alloy chemistry, working temperature and deformation schedule are incomplete. Also, the relationship between deformation texture and recrystallization texture is still ambiguous.

Directional Recrystallization Defect Control

During DR both the orientation and the defect density must be controlled. A low density of twins and occluded grains may require high gradient processing. The constraints of a low superheat and normal radiation heating and cooling make significant advances in thermal gradient difficult to achieve. The heat flow during DR and the impact of gradient on microstructure must be better understood. A new approach to high gradient DR may be required. Any defects which may form such as twins or sub-boundaries must be well characterized in terms of their thermal stability.

DISCUSSION

M. A. De Crescente

Rapidly Solidified Oxidation Resistant Coatings

Current coatings used in military and commercial gas turbines have reached a high degree of sophistication in terms of composition development and processing. They are extremely oxidation resistant and provide added oxidation protection to airfoil substrates for thousands of hours in many duty cycles. These coatings are aluminide-base and derive their excellent oxidation resistance through the growth of Al_2O_3 which is extremely adherent. As the Al_2O_3 film is lost by erosion in stress-induced spallation it can be quickly reformed by aluminum in the coating diffusing to the surface. Oxidation protection provided by the coating is eventually exhausted as the source of aluminum is depleted. Although remarkable progress has been made to reduce spallation rates, e.g., Y additions which promote "pinning" of the oxide, stress-induced spallation of the Al_2O_3 films is a major mechanism which limits coating life.

Experiments conducted at UTRC indicate that rapid resolidification by laser or electron beams of coatings applied by standard techniques impart added spallation resistance.

Figure 1 is a photo micrograph of a $MCrAl_4$ coating before and after laser surface processing. In order to evaluate the performance of a coating processed in this manner a "burner rig" test was performed for 100 hrs. at 1800°F. on a coated

CONTROLLED DEPTH PROCESSING OF RAPIDLY SOLIDIFIED COATING

As received

20 μm

Laser processed

20 μm

specimen which was laser processed only on one side. Fig. 2 compares the laser processed side with the side which was not laser processed.

After the oxidation test the laser processed side looks identical to what it did before test whereas the side which was not laser processed has a mottled and pitted appearance which is characteristic of repeated spallations.

Metallographic studies indicate that oxidation is proceeding so slowly in the laser processed layer that the low aluminum phase has time to equilibrate with the high Al phase. This does not normally occur, see Figs. 3 & 4.

Work should be performed to quantify the magnitude of the benefit described, to understand the mechanisms responsible, and to define coating compostion which uniquely benefit by the process.

Oxide Dispersion Strengthened RSR Supercelloys

Research has accelerated at UTRC during the last 18 months in support of P&WA's interest in further exploiting the unique characteristics the RSR process offers for the development of advanced superalloys. Analytical studies have indicated that rare earth oxide dispersoids, which would impart significant strengthening to existing RSR alloys, could be formed on a very fine scale during RSR powder atomization and would resist Ostwald ripening during directional recrystallization. In addition, model experiments have been performed at UTRC which have shown that such dispersoids can be introduced during RSR powder

RAPIDLY SOLIDIFIED COATING RESULTS

Conventional process

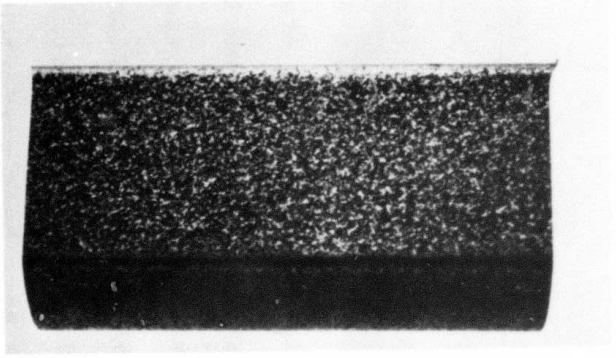

Oxide spalling

RSC process

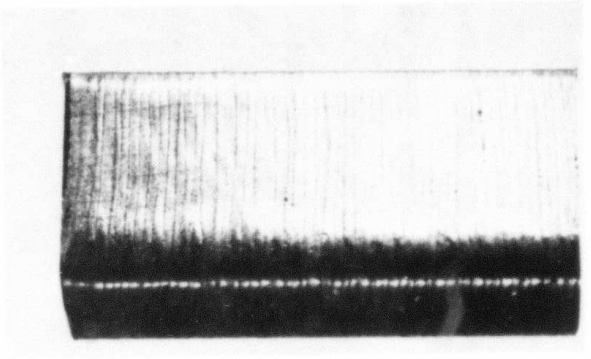

Oxide adhering

1800 F — 100 hrs cycle burner rig tests

MCrAlY COATING SHOWING NORMAL OXIDE SPALLING

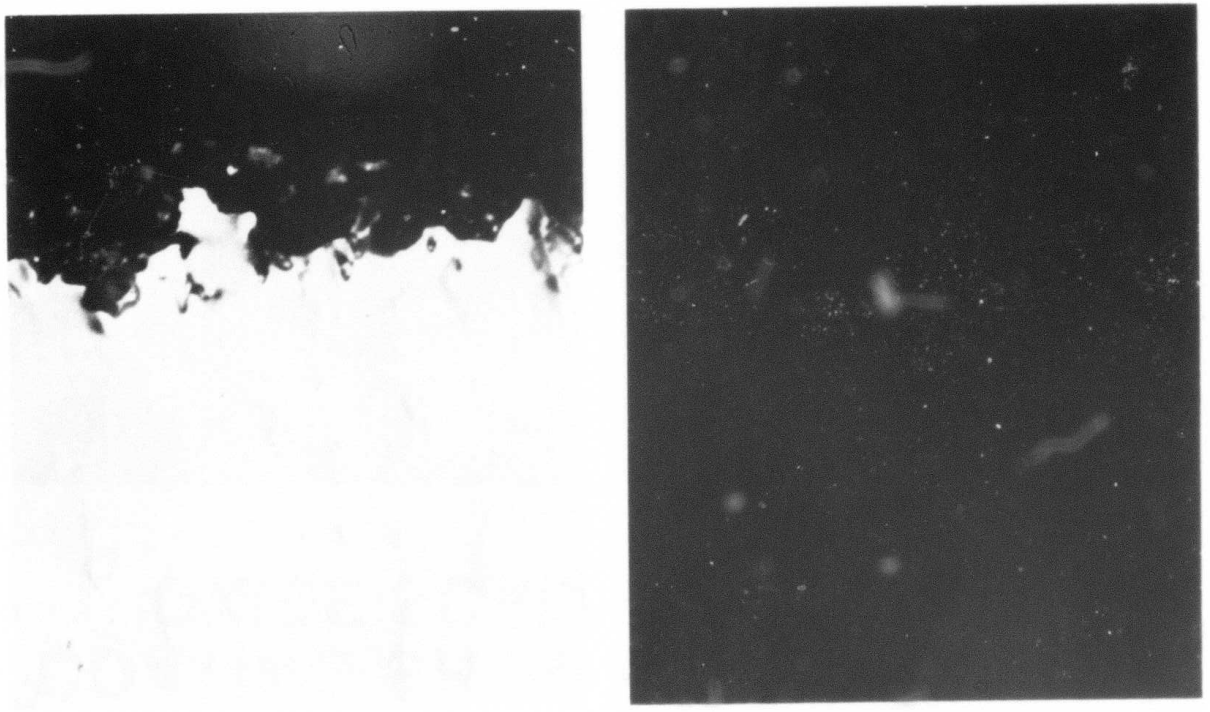

RAPIDLY SOLIDIFIED MCrAlY COATING SHOWING EXCELLENT OXIDE SCALE RETENTION

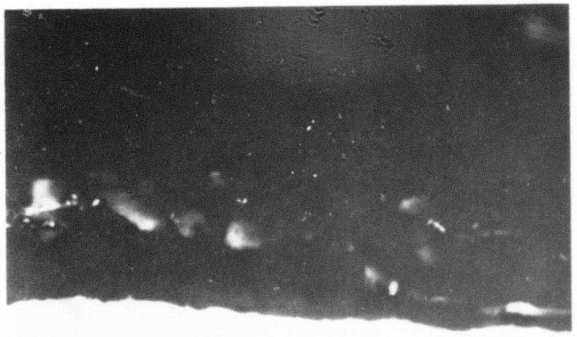

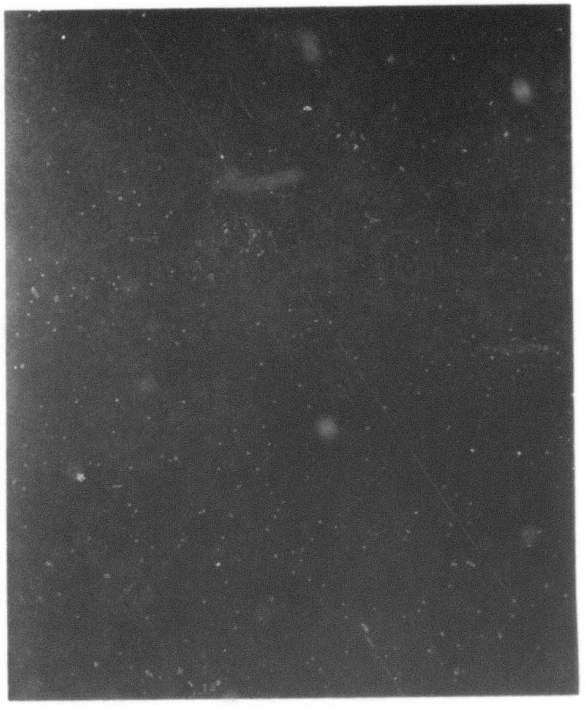

atomization. P&WA is preparing several 35 lb. RSR powder lots with rare earth oxide dispersoids for metallographic and mechanical property evaluations.

MEMORANDUM

E. W. Bloore

The efforts being conducted at the Army Armament and Research and Development Command (ARRADCOM) are in the areas of improved high strength aluminum alloys and improved armament materials.

For years ARRADCOM has supported the development of aluminum alloys and has contributed significantly toward the present thermal mechanical treatment of these alloys and the development of X7090 (CT91) powder metallurgy (P/M) alloys. The present program consists of efforts to:

a. Improve P/M alloys through thermal mechanical treatment.

b. Complete the comparison of P/M and ingot metallurgy alloys.

c. Complete the evaluation of mechanically alloyed materials.

d. Participate in a DARPA program with Rockwell International on superplastic forming of P/M alloys.

e. Initiate product improvement program on alternate alloys for artillery bases and ogives.

The efforts on armament material were initiated this year and include efforts to:

a. Establish the feasibility of consolidating metallic

glass ribbons into metal matrix composites without major degradation occurring to the metallic glass.

b. Investigate the benefits of RST processed AISI-S7 tool steel for penetrator applications.

c. Investigate the consolidation of RST processed Ni-Mo-B alloys powders as a new penetrator material with Allied Corporation.

A basic study is being conducted to examine recrystallization kinetics in amorphous metallic materials. The Cu-Zr system is presently being studied to develop the required techniques. Future effort will include the systems discussed above.

DISCUSSION

Aldo B. Vidoz

Physiochemical characterization of particulates: the characteristics of the particulate surface, changes that may occur during processing prior to consolidation, contamination due to exposure to environment, and effects of all the possible surface phenomena upon subsequent processing as well as resulting properties should be an important concern in our future research planning.

In RST we are dealing with a process in which most of the time the material is in the form of fine particulates. It seems peculiar that the subject of surface phenomena has been presented only superficially during this meeting.

Not much was discussed about directionality of the mechanical properties of RST materials and its relationship with thermomechanical treatment or about characteristics of the oxide film present on the surface of the particulate. These areas need further work.

DEPENDENCE OF FRACTURE TOUGHNESS AND FLOW STRENGTH ON RAPIDLY SOLIDIFIED POWDER DIAMETER

(A possible explanation of why smaller diameter powders lead to reduced fracture toughness despite higher hardness or flow strength.)

D. C. Drucker

Metallic alloys of much higher than usual yield and flow strengths for their composition can be produced by consolidation of rapidly solidified powders and appropriate heat treatment. The smaller the powder diameter, the higher the flow strengths that are possible, a result to be expected from smaller grain size and subgrain size, and from more effective dispersion and solution hardening. The fine structure and strength enhancement can be maintained to an appreciable extent through a suitable thermomechanical treatment employed primarily to eliminate much of the deleterious effect of the contamination of and the segregation at the initial particle surface.

Local microscopic ductility also should be enhanced by the fineness of the distribution of dispersions. However, any increase in tensile ductility on the macroscale tends to be severely limited by necking instability, an overall geometric change that usually occurs after at most a few percent of plastic strain, because of the rather small strain hardening of such strong materials at larger strains.

A similar limitation on total elongation will exist on the microscale if transverse contraction can occur. If it

should be true that the relevant dimensions of the tension ligaments on the microscale are about equal to the initial particle size D, and the flow strength in tension of the alloy is σ_o, then the critical value of energy dissipated per unit area of unstable crack advance through plastic deformation of a laterally unconstrained ductile ligament ahead of the crack is about equal to

$$\frac{1}{2}\,\sigma_o\,D = G_c \qquad (1)$$

A multiplicative constant of the order of unity is needed if the ligament dimensions are a fraction or multiple of D of order unity. With full lateral constraint in any region, the tensile stress ahead of an advancing crack is about $3\sigma_o$ and the separation of material or crack opening displacement is indeterminate. If, however, the memory of the particle boundaries persists and separation is of dimension D then once again

$$G_c = n\,\sigma_o\,D \qquad (2)$$

where n is of order unity.

The critical crack intensity K_c depends upon Young's modulus E and G_c

$$K_c^2 = G_c E = (n\,\sigma_o\,D)E \qquad (3)$$

The flow strength σ_o increases somewhat with decreasing D but even at the extreme of σ_o proportional to $D^{-1/2}$, G_c and K_c will decrease with decreasing D.

Is it reasonable to believe that the tension ligaments are of lateral dimension D and that (2) holds with n not too far from unity? In many metallic alloys of large grain size the dimension is the spacing of large inclusions which fracture or debond from the ductile matrix as the crack advances, Fig. 1. When rapidly solidified powders are the starting point,

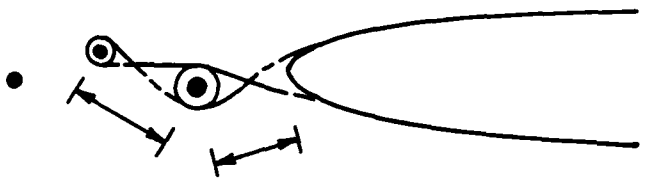

Figure 1.

and subsequent heat treatment and fabrication does not cause precipitates to agglomerate or the material originally at the particle surface to diffuse completely, the grain boundaries are likely sources of crack and void initiation, Fig. 2. The fine particles in the interior of the grains are likely to be strong and well-bonded to the matrix.

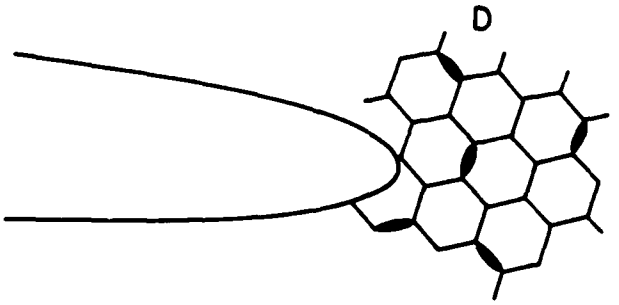

Figure 2.

This pictorial representation and the accompanying words of explanation amount to little more than a statement that the rapidly solidified particle diameter D is the main controlling linear dimension beyond the atomic scale. Perhaps this statement would be viewed as obvious when powder boundaries are evident in the final microstructure, although it is not appropriate in ordinary powder metallurgy for which inclusion or large precipitate spacing in the final product is more significant in fracture toughness.

The high flow strength σ_o of the ductile matrix is associated with solution and dispersion hardening and depends upon the volume fractions of the solutes f_s and the dispersion spacing δ which is normalized by the atomic spacing b. Initial particle diameter D is important because the process of rapid solidification sets the several f_s and the δ on the submicron scale. The smaller D the more rapid the cooling, the higher the f_s, the smaller δ and the higher the flow strength σ_o.

A dimensional analysis is only moderately informative with these variables, but it does bring out the usual dominance of subgrain dimensions δ, rather than grain or particle size D, in the determination of matrix flow strength.

σ_o is a function of the f_s, δ, b, D, E and other crystal structure variables. Consequently, σ_o/E is a function F of the dimensionless variables of the problem.

$$\frac{\sigma_o}{E} = F\left(f_s, \frac{b}{\delta}, \frac{\delta}{D}, \ldots\right) \qquad (4)$$

with δ/D unlikely to be important in the practical range of $\delta/D<<1$.

However, a dimensional analysis translates the simple assumption that the atomic and dispersion structure affects fracture toughness only through σ_o and E into a strong result.

G_c is a function of σ_o, E, and D

Therefore

$$\frac{G_c}{\sigma_o D} \text{ can be a function of } \frac{\sigma_o}{E} \text{ only.} \qquad (5)$$

When the matrix is highly ductile on the microscale, the dependence of G_c on σ_o/E is small so that $G_c/\sigma_o D$ is close to constant as is $K_c^2/\sigma_o ED$. This decrease of fracture toughness with decrease in D discussed earlier, Eqs. (1), (2), and (3), does not depend upon any detailed fracture mechanism in Fig. 2. It requires only that D sets the geometry of fracture in some way.

Of course if the influence of the particle boundaries is almost completely eliminated from the consolidated material through some thermal or thermomechanical treatment which maintains the fine structure of the powder within the grains, then D no longer is relevant. Some other larger dimension such as the spacing of voids in incompletely compacted material or unwanted particles of quite different composition or poor properties will govern instead. If other independent linear dimensions are introduced that are of importance on the scale of D, the particle diameter cannot remain the controlling linear dimension. It seems likely, however, that if the properties of the rapidly

solidified material are maintained on the fine microscale then many of the powder boundaries will become sources of separation.

ACKNOWLEDGEMENT

This paper was written under the auspices of the DARPA Materials Research Council, Contract #MDA903-80-C-0505 with the University of Michigan.

MICROSTRUCTURAL SELECTION FOR FRACTURE RESISTANCE

J. C. Williams and J. P. Hirth

The availability of RSP powders with virtually any composition is cause to re-evaluate t' role of microstructure in monotonic loading fracture resistance. Two cases will be considered; the case of general plasticity such as in a tensile test and the case of local plasticity such as in the case of a sharp propagating crack.

Microstructure has at least two types of influence on fracture behavior. First, it affects the way the material deforms and, second, it fixes the length or scale over which the material is plastically inhomogeneous. The microstructure also fixes the scale over which cracks are initiated and influences the types of sites at which they form. In order to achieve reasonable strength ($\sigma_y \cong G/50$) a relately close spacing of particles needs to be maintained ($\ell \cong 50b$). This leads to a high work hardening rate if the particles are not shearable ($\frac{d\sigma}{d\varepsilon} \propto \frac{1}{\ell}$). In Ashby's treatment of work hardening there is an upper limit to the flow stress which is due to geometrically necessary dislocations. At this limit cross slip occurs at no further increase in flow stress.

It appears that in addition to selection of a dispersoid size and volume fraction which gives $\ell \cong 50b$, the fracture behavior depends in a substantial way on the type of dispersoid, its characteristics of atomic bonding and its characteristics of

bonding to the matrix. The dispersoids can act as fracture initiation sites either by decohering from the matrix or by fracturing themselves, thereby leading to incipient cracks. The preponderant view seems to be that the former case is generally operative although relatively little evidence is available for very small (~ 10nm) particles. Some question exists regarding the critical parameter for particle/matrix decohesion. One view is that decohesion occurs at a critical stress while another view is that the critical stress scales inversely with the square root of the particle size. It would appear that the latter view is in closer agreement with observations, since there are numerous examples of early decohesion of large particles.

Presumably more strongly bonded particles will not decohere at the same stress and size combinations as more weakly bonded ones. In this regard, it is worth commenting that the interfacial strengths are influenced by intrinsic factors such as bonding and structure and by extrinsic factors such as impurity absorption. For small particles a Griffith-type relationship would lead to the square root dependence where the applied stress is magnified by local incompatibility stresses. For large particles the strain distribution is independent of particle size so no size dependence would be expected in a first order sense. However, statistical considerations might suggest that larger particles would be more likely to nucleate voids (e.g. particle spacing, slip distribution effects). If the

square root dependence is correct then the critical stress for deconesion scales linearly with the interfacial bond strength and inversely with the square root of the particle diameter, as shown in Eq. 1, where k is a constant with units of length. If

$$\sigma^{crit}_{applied} = k \frac{\sigma\ bond}{d^{1/2}_{part}} \qquad (1)$$

the critical stress for competing fracture mechanisms such as grain boundary cracking does not strongly depend on the alloy composition or microstructure then below a critical particle size no voids should be formed at particles and fracture should occur intergranularly. However, this stress for grain boundary fracture may depend on the grain size also. Thus, refining the grain size should also be helpful in extending the uniform plastic strain which can be accommodated without the onset of fracture.

An alternate method of strengthening is to combine precipitation hardening with dispersion strengthening. In such a case, the precipitates would be sheared and the slip mode would change from wavy or turbulent to planar. The presence of dispersoids would tend to block the planar slip bands or at least cause them to be more diffuse. This should mitigate the stress concentrations at grain boundaries and minimize the tendency for nucleation of grain boundary cracks. However, the stress concentrations at the intersection of dispersoid particles and planar slip bands may cause interface deconesion. If so, then

the dispersoid size may have to be reduced. One way to minimize such stress concentrations is to introduce a stable substructure which further limits the slip length and helps to make the planar slip bands more diffuse. However, in systems which can undergo precipitation hardening, heterogeneous nucleation and rapid growth of second phases at such substructure is common. In such cases the substructure nucleated phases may act as sites for early void formation. Thus, it appears that combining precipitation hardening with substructure strengthening is not attractive. One way to eliminate this may be to introduce substructure after precipitation as is done in HSLA steels.

It is attractive to contemplate the addition of solid solution hardening additions which raise the modulus, e.g. Li in Al. Such additions can have two potential benefits. First, by increasing the matrix modulus the compatibility with higher modulus dispersoid particles is improved. This may be helpful in minimizing the stress gradient across the interface, therefore reducing the tendency for particle decohesion. Second, increasing the matrix modulus will enhance the strengthening by reducing the flexibility of the dislocations.

Another phenomenon which is affected by the above considerations and which can lead directly to failure is the onset of plastic instability. The factors which stabilize a microstructure against such an instability include high work hardening rate and resistance to void nucleation. In view of the above, dispersoids which increase work hardening and matrix

solutes which increase modulus additions may help in minimizing void nucleation, both factors improving the resistance to plastic instability.

When all of the above considerations are jointly weighed it appears that the best microstructure for combined strength and ductility is one which contains a dispersion of small non-deforming particles. This will give particle strengthening without localized strain, will give high work hardening and will stabilize the substructure. The matrix should also contain solutes which increase the modulus. Precipitation hardening is attractive from a strength standpoint but must be employed with caution because of the potential for inducing early void formation, plastic instability or microstructural instability due to coarsening. The grain size must also be small in order to prevent or minimize grain boundary fracture.

The case of toughness or localized plasticity is somewhat different from the tensile ductility case described above. Here those microstructures which enhance ductility should also enhance toughness by increasing the energy required to extend the crack a unit distance. However, in the case of localized plasticity, such as that associated with a propagating crack, an additional contribution to the toughness can be obtained if the crack turns frequently due to interaction with randomly oriented preferred fracture paths. Thus, the toughness may be improved by introducing a uniform distribution of preferred fracture paths which cause the crack front to be reoriented. Such paths

can be grain boundaries, second phase interfaces, prior powder particle boundaries or other microstructural innomogeneities. It is important to understand the way in which these crack reorienting features operate and what (stress or strain) is the critical parameter for activating them. If they are too weak, then the unit crack propagation energy is reduced. If they are too strong, they are never activated. So the strength of these features needs to be in the intermediate regime. Further, the spacing of these features is important but it is not clear how to calculate an optimum spacing. Finally, it would be useful to attempt a calculation of how much K_{IC} increases due to crack reorientation and to estimate the optimum frequency of such an event.

In summary, with respect to the sharp crack propagation resistance, the microstructure which gives good ductility should be desirable because it should lead to large values for the energy dissipated per unit crack extension. However, in addition to this microstructure a uniform distribution of moderately strong crack reorientation sites should be present. The relative benefits to toughness from these two contributions would be useful to calculate.

Based on the above discussion several suggestions can be offered for further work.

1. The recommended "ideal" microstructures should be made from RSP powder and evaluated.

2. The existence of a size dependence of the propensity for particles to decohere should be examined theoretically or analytically using methods of mechanics or crystal plasticity (or both).
3. The same question posed in #2 should be examined experimentally in monodispersoids of varying sizes. These results should be compared to selected bimodal dispersions.
4. The contribution of crack reorientation to toughness should be examined analytically.
5. Experiments to produce microstructures with varying propensities for crack reorientation should be conducted and toughness variations measured.

ACKNOWLEDGEMENT

This paper was written under the auspices of the DARPA Materials Research Council, Contract #MDA903-80-C-0505 with the University of Michigan.

POSSIBILITIES OF INCREASED CORROSION RESISTANCE OF RST ALLOYS

E. E. Hucke and J. P. Hirth

Corrosion of Mg Alloys

Strategies for improving the corrosion resistance of an alloy involve (i) protective coatings (ii) formation of a passivating film and (iii) addition of a more active constituent which forms a passivating film (e.g. Cr & Fe). The latter method is not applied for Mg alloys since they are at the anodic end of the galvanic series except for alkali metals. Coatings are continuously used for Mg-alloys. MgO is stable and provides passivation in mildly corrosive environments but is susceptible to pitting attack in salt exposures and breaks down in strong acids.

RST has provided enhanced corrosion resistance for alloys in general compared to wrought alloys. This arises in part from a more homogeneous matrix structure, permitting the formation of a uniform passive film and restricting the localization of impurities which can break down the passivity. Improved corrosion is also observed for RST structures containing second phase particles provided they are very fine. It is conceivable that RST magnesium alloys would have improved resistance to breakdown of passivation and pitting because of increased homogeneity and this merits some study. Because of the high reactivity of Mg-alloys, the gain would probably be only incremental, but this could be significant for some DoD appli-

cations (saline fog, brackish water). Any improved passivity would help both for direct corrosion and corrosion under galvanic contact with other alloys.

A more dramatic improvement might be achieved with a glassy film to provide passivation. Here, a more uniform, RST substrate would be expected to improve film adherence and uniformity. A specific example of such a film could be provided for the Mg-Li-B alloys which are considered next.

Mg-Li-B Alloys

Some very attractive mechanical properties were demonstrated in exploratory work on Mg-Li-B alloys by F. Wang while at the Naval Surface Weapon Laboratory. These alloys have very large quantities (~30 at%) of B and are not related to the previously investigated cubic Mg-Li alloys. Several of the alloys showed enough ductility (~10% Elongation) to be useful in engineering applications while at the same time giving attractive tensile properties and Youngs' Modulus above 10^7 psi. Since these alloys are substantially less dense than Mg, the specific properties, especially stiffness, are very promising since they would substantially better those of the Al-Li alloys now under development.

Preliminary salt water corrosion testing showed results more favorable than ordinary Mg alloys which in general are quite unsatisfactory. Small samples made by moderately rapid quench of liquid droplets showed better corrosion resistance.

The alloys were made by solution of B in Li at low temperature with subsequent alloying with Mg in the liquid. They are in a non-equilibrium liquid state which shows irreversible precipitation and solidification upon heating (Mg-Li binary case). The reaction apparently involves precipitation of one or more borides in a very fine dispersion.

RSP may allow even larger quantities of B and/or Li to be used which together with processing optimization might allow retention of all constituents in solution. There is some chance that at the high boron contents used, a protective film not based on MgO could be achieved. Could these alloys be passivated by oxidation at a temperature low enough to preclude the boride precipation while forming a B_2O_3 based glass film? Borate glasses are common and dissolve many metals and metal oxides and are very viscous at modest temperatures (e.g. color bead tests in general chemistry).

Also at the relatively large B and Li contents it may be possible to form a crystalline film of a complex oxide rather than MgO. This approach may be facilitated if additional modest alloying with Si and/or Al is employed. There are several complex oxides in the lithium-aluminum-silicate system.

Improved Oxidation Resistance of Refractory Alloys

As suggested in the question (appended) silicides and other compounds could in principle provide oxidation resistance. Problems with these compounds, as also noted in the question,

involve nonuniformity leading to increased spallation tendency, and the reaction to form other compounds at the interface which can also crack and lead to film breakdown, particularly when nonuniform. An example would be $MoSi_2$ on Mo. The disilicide would have good oxidation resistance but could tend to react by interdiffusion at the interface to form lower silicides such as Mo_3Si.

RST could provide improvements in one of three ways. First, the increased homogeneity in structure would give more uniform films and decreased spallation tendency. Second, increased homogeneity would reduce the nucleation rate of interface phases and this perhaps would increase the stability of more protective films such as $MoSi_2$. Finally, and perhaps most promising, a dispersion of, say, $MoSi_2$ in Mo could be produced without the usual severe embrittlement on the basis of analogous improvements in steels found by M. Cohen and coworkers at M.I.T. If very fine and finely distributed, the particles should not detract from mechanical properties but should pin a fine grain size. With particles on high diffusivity path grain boundaries, a measure of self healing of the films could be provided, analogous to the effects of Al on Al_2O_3 films in Ni-base alloys. Supply of Si from $MoSi_2$ particles along the grain boundaries could produce a protective SiO_2 layer at a break on this spot in the oxide.

Because of the sensitivity of many of the refractory metals to interstitial embrittlement when the interstitials are

absorbed at grain boundaries, developments such as the above would clearly be more difficult than for more forgiving alloys. However, the potential benefits would appear to be such that some studies of this type would be warranted.

ACKNOWLEDGEMENT

This paper was written under the auspices of the DARPA Materials Research Council, Contract #MDA903-80-C-0505 with the University of Michigan.

CAN FAST ENOUGH QUENCHING ALONE PRODUCE AMORPHOUS AND GLASSY PHASES

H. Reiss

The question has been raised as to whether it is possible to quench a melt fast enough to frustrate nucleation of the solid. Although this seems to have been accomplished practically in many cases, the question remains as to whether other factors besides speed of quench are involved. Montroll and Reiss looked into this question in connection with a specialized model of the two dimensional ferromagnet (Glauber's model) and discovered, rigorously, for this case, that only a rapid quench was necessary in order to avoid a transition to the ordered spin phase which is possible in the two dimensional ferromagnet.

The phase transition in this case is of higher order than the first and so may not be directly comparable to a first order transition. On the other hand the free energy of "activation" in the first order case is likely to be larger than that of the higher order transition and so nucleation should be even more avoidable by rapid quench. It is probably safe to draw the conclusion that nothing more than a rapid quench is necessary.

Montroll and Reiss' work appears in the DARPA Material Research Council's Proceedings for 1980 and in the Proceedings of the National Academy, April and May, 1981.

IS THERE A NEED FOR A NONISOTHERMAL THEORY OF NUCLEATION FOR USE IN RST

H. Reiss

A nonisothermal theory of nucleation (from liquid to solid) would only be necessary for RST processes in which the cooling or quenching time was comparable with, or in excess of, the relaxation time to the "steady state" in the corresponding nucleation process. Then, not only would it be necessary to consider a non-steady theory of nucleation, but to also account for rate changes, during nucleation, due to the change of temperature itself.

This question was investigated and the results of investigation, published in the proceedings of the DARPA Materials Research Council for 1977 (Authors, Reiss and Katz).

The method of proceeding involved developing a matrix method for obtaining the time dependent distribution of embryos of the nucleating phase such that the kinetic equation became the analog of the time dependent wave equation of quantum mechanics, and the distribution of embryos, the analog of the wave function. At the same time the relaxation times for the process became the analogy of the reciprocals of the quantized energy levels.

Because of this mathematical isomorphism, a lower bound for the longest relaxation time (to steady state) - the analog of an upper bound to the lowest energy level in the quantal

case - could be obtained using the Ritz Variation Principle. This longest relaxation time provides an estimate of the time required to produce the steady state. Although the result is only a bound there is ample reason to believe that it is of the same order of magnitude as the relaxation time itself.

In order to make use of the theory it is necessary to have an estimate of the self diffusion coefficient in supercooled liquid metals. For this purpose one might either extrapolate an Arrhenius-like temperature dependence, or make use of the Cohen-Turnbull free volume theory of viscosity. It emerged that application of both methods led to about the same result. Ultimately, it turned out that the relaxation times in question were of the order of 10^{-13}-10^{-12} sec for a typical assortment of metals. Thus, insofar as cooling rates of 10^{6}-10^{8} deg sec^{-1} are concerned, the steady state is constantly achieved. Time then enters the nucleation rate only through the temperature in the conventional theory. Furthermore, even this time dependence is trivial since the whole nucleation process will effectively occur at one temperature.

A cautionary note may be necessary. In the case where a multicomponent crystal is to be formed the control of rate may be lodged in the process of arranging the atoms in the crystal nucleus into the equilibrium configuration. In such cases relaxation may be considerably slower. On the other hand if non-equilibrium composition and structures are involved this phenomenon is probably not a factor.

A fully detailed description of the quantum mechanical analog method has recently been published (Schelling and Reiss, Journal of Chemical Physics, 1981) where it has been applied to the vapor liquid transitions.

ACKNOWLEDGEMENT

This paper was written under the auspices of the DARPA Materials Research Council, Contract #MDA903-80-C-0505 with the University of Michigan.

PROGRAM AND LIST OF ATTENDEES

I. Tuesday, 7 July 1981, 8-12 A.M.

Fundamentals: Solidification, Microstructure

Chairman: J. W. Cahn, National Bureau of Standards

Speakers: R. Mehrabian, National Bureau of Standards
"Advances in Our Understanding of Rapid Solidification"

R. J. Patterson, Pratt and Whitney,
"Solidification of Amorphous Powders"

M. Cohen, M.I.T., "Alloy Design Based on Rapid Solidification"

H. L. Fraser, University of Illinois,
"Analytical Electron Microscopy in RSP"

Discussers: J. W. Cahn, National Bureau of Standards,
J. Vander Sande, M.I.T.
H. A. Lipsitt, USAF Mat. Lab.

II. Tuesday, 7 July 1981, 1-3:30 P.M.

Fundamentals: Microstructure, Properties

Chairman: J. P. Hirth, Ohio State University

Speakers: J. Williams, Carnegie-Mellon University,
"Microstructure-Properties Relations in PM Products"

R. E. Lewis and I. Palmer, Lockheed,
"Microstructure-Properties in Rapidly Solidified Powder Aluminum Alloys"

Discussers: A. Lawley, Drexel University,
R. Apelian, Drexel University

Group Discussion: "Needs and Suggestions for Fundamental Research"

III. Wednesday, 8 July 1981, 8-12 A.M.

Applications and Technology

Chairman: M. Cohen, M.I.T.

Speakers: E. van Reuth, DARPA, "Overview of DARPA Program on Rapid Solidification"

C. Adam, Pratt and Whitney, "Development of Naval Alloys Through RST"

R. Ray, Marko, "Microcrystalline Alloys in Bulk Form"

L. Davis, Allied Chemical, "Applications of Metallic Glasses"

T. F. Kearns, IDA, "An Assessment of RST and its DoD Applications"

Discussers: E. J. Dulis, Colt Ind.
P. Domalavage, M.I.T.
J. Moore, Pratt and Whitney

IV. Wednesday, 8 July 1981, 1-3:30 P.M.

Summary Discussions:

Chairman: R. Mehrabian, National Bureau of Standards

Review of the COMAT/RST Meeting,

General Discussion:

M. Cohen, M.I.T.
L. Davis, Allied Chemical
E. J. Dulis, Colt Ind.
L. Jacobson, DARPA
R. Mehrabian, National Bureau of Standards

General Discussion:

"Where Do We Stand and Where Do We Go?" (Including question of supply of rapidly solidified material.)
T. E. Tietz, NMAB

V. Thursday, 9 July 1981, 8-12 A.M.

Informal Discussion

ATTENDEES

John Cahn	Nat. Bur. Stds.
John Hirth	Ohio State Univ.
Morris Cohen	M.I.T.
Jim Williams	Carnegie-Mellon Univ.
Ed vanReuth	DARPA
Ranjan Ray	Marko Materials, Inc.
Jun Millan	Garrett Turbine Engine Co.
H. Reiss	UCLA
Ed Dulis	Crucible Res./Colt Ind.
Tony Evans	U.C. Berkeley
Robert Ware	US Army Meradcom
Tom Tietz	National Materials Advisory Board
Alan Lawley	Drexel Univ.
Diran Apelian	Drexel Univ.
Peter Domalavage	M.I.T.
John Bjeletich	Lockheed Palo Alto
Don Polk	ONR
T. F. Kearns	IDA
Dan Drucker	MRC-Univ. Illinois Urbana
Harry Lipsitt	AFWAL/Materials Lab
Attwell Adair	AFWAL/Materials Lab
Roy Athey	Pratt & Whitney Aircraft
Art Cox	Pratt & Whitney Aircraft
Robert J. Patterson II	Pratt & Whitney Aircraft
Joe Moore	Pratt & Whitney Aircraft
Joseph R. Crisci	David Taylor Naval Ship R&D Center
Colin Adam	Pratt & Whitney Aircraft
Ian Palmer	Lockheed Palo Alto Res. Lab.
Floyd Larson	Garrett-Airesearch Casting Co.
Hamish Fraser	Univ. of Illinois
Bhakta B. Rath	Naval Research Lab
John W. Hutchinson	MRC-Harvard Univ.
Norman M. Tallan	USAF Materials Lab.
Robert E. Green, Jr.	Johns Hopkins Univ.
Loren Jacobson	DARPA
James R. Rice	Brown Univ.
Aldo E. Vidoz	Lockheed Palo Alto Res. Lab
Lance A. Davis	Allied Corp.
Carl F. Cline	Lawrence Liv. Nat. Lab.
Elliott C. Levinthal	DARPA
John B. VanderSande	M.I.T.
Anthony F. Giamei	United Technologies Res. Center
Mike DeCrescente	United Technologies Res. Center
Robert Mehrabian	NBS, Dept. of Commerce
Evert Bloore	U.S. Armament R&D Command
Edward E. Hucke	Univ. of Michigan
Rowland M. Cannon Jr.	M.I.T., Mat. Sci. & Eng.